Grasping the Sampling Behaviour of Event-Triggered Control

Self-Triggered Control, Abstractions and Formal Analysis

Delimpaltadakis, Giannis

DOI
10.4233/uuid:6592cc11-fb2b-4d9c-a8f2-6dd2bb4584be

Publication date
2022

Document Version
Final published version

Citation (APA)
Delimpaltadakis, G. (2022). *Grasping the Sampling Behaviour of Event-Triggered Control: Self-Triggered Control, Abstractions and Formal Analysis*. [Dissertation (TU Delft), Delft University of Technology]. https://doi.org/10.4233/uuid:6592cc11-fb2b-4d9c-a8f2-6dd2bb4584be

Important note
To cite this publication, please use the final published version (if applicable).
Please check the document version above.

GRASPING THE SAMPLING BEHAVIOUR *of* EVENT-TRIGGERED CONTROL

Self-Triggered Control, Abstractions and Formal Analysis

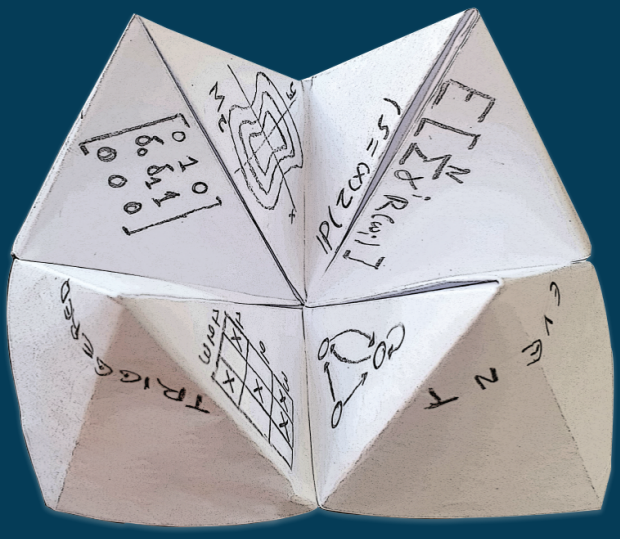

Giannis Delimpaltadakis

Grasping the Sampling Behaviour of Event-Triggered Control

Self-Triggered Control, Abstractions and Formal Analysis

GRASPING THE SAMPLING BEHAVIOUR OF EVENT-TRIGGERED CONTROL

SELF-TRIGGERED CONTROL, ABSTRACTIONS AND FORMAL ANALYSIS

Dissertation

for the purpose of obtaining the degree of doctor
at Delft University of Technology,
by the authority of the Rector Magnificus Prof. dr. ir. T.H.J.J. van der Hagen,
chair of the Board of Doctorates,
to be defended publicly on
Tuesday 28 June 2022 at 10:00 o'clock

by

Giannis DELIMPALTADAKIS

Master of Science in Electrical and Computer Engineering,
National Technical University of Athens, Greece,
born in Veria, Greece.

This dissertation has been approved by the promotors.

Composition of the doctoral committee:

Rector Magnificus	chairperson
Dr. M. Mazo Espinosa	Delft University of Technology, promotor
Dr. P. Mohajerin Esfahani	Delft University of Technology, copromotor
Independent members:	
Prof. dr. ir. B. de Schutter	Delft University of Technology
Prof. dr. P. Tabuada	University of California, Los Angeles, USA
Prof. dr. D. Nesic	University of Melbourne, Australia
Dr. R. Postoyan	CNRS, CRAN UMR 7039, Université de Lorraine, France
Dr. ir. D. G. T. Antunes	TU Eindhoven
Prof. dr. ir. T. Keviczky	Delft University of Technology, reserve member

European Research Council

This work is supported by the European Research Council through the SENTIENT project, Grant No. ERC-2017-STG 755953 (https://cordis.europa.eu/project/id/755953).

This dissertation has been completed in fulfillment of the requirements of the Dutch Institute of Systems and Control (DISC) for graduate studies and the TU Delft Graduate School for the Doctoral Education Program.

Keywords: event-triggered control, self-triggered control, abstraction, nonlinear, stochastic, scheduling, sampling behaviour, networked control systems

Printed by: Print Service Ede

Front & Back: Giannis Delimpaltadakis and Artemis Zografou

ISBN 978-94-6384-346-1

An electronic version of this dissertation is available at http://repository.tudelft.nl/.

To my parents, for they instilled me with the passion for knowledge.

An ounce of action is worth a ton of theory.

Friedrich Engels / Ralph Waldo Emerson

CONTENTS

SUMMARY

Networked Control Systems (NCSs) are control systems, where the different components (sensors, controllers and actuators) communicate through a network, which is usually shared among multiple control systems or other processes. NCSs have become ubiquitous, due to their reduced deployment costs and simpler maintenance. Nevertheless, they, also, pose new challenges. A fundamental challenge is reducing the amount of communications of each system in the network, so that bandwidth and energy are used efficiently.

Towards such a communication reduction, the research community has shifted its focus to Event-Triggered Control (ETC). ETC is a sampling paradigm where communication between the control system's different components takes place only when it is necessary (when a state-dependent *triggering condition* is satisfied). ETC's event-based nature of sampling often results into a big reduction in communications, when compared to the widely adopted periodic-sampling paradigm. On the other hand, communication times (or sampling times) of ETC are unknown beforehand and predictions thereof require intricate mathematical analysis on the system's (perturbed) dynamics. Nonetheless, predicting ETC's sampling is of paramount importance, as it enables:

- *Self-Triggered Control (STC)*: STC is a more economic implementation of ETC. In STC, the controller, at each communication time, decides the next communication time based on the received state-measurement; this removes the need for continuous monitoring of the triggering condition and the intelligent hardware needed to do so, which is necessary for ETC. STC needs 1-step predictions of ETC's sampling to operate; given a state measurement it predicts ETC's next communication time.

- *Traffic Scheduling*: Traffic scheduling is planning bandwidth allocation to each entity using the network. For control applications, it is very important; without it, many systems may access the network at the same time, resulting into network overflow and hindering the systems' stability. For scheduling, a multi-step or infinite-step prediction of communication times is needed, to ensure that there are no unsafe phenomena in the future by a scheduling action taken at the present.

- *Formal Assessment*: Usually, the performance of an ETC design in terms of sampling and control is validated through simulations. However, simulations do not provide definite formal results, but indications. To obtain formal guarantees on the sampling (vs. control) performance of ETC, e.g. by computing associated long-term metrics, knowledge on its communication patterns is needed. Multi-step or infinite-step predictions of ETC's sampling constitute exactly such knowledge.

The present dissertation studies ETC's sampling behaviour and derives predictions thereof in all three aforementioned contexts.

Research on STC for nonlinear systems is relatively scarce. Most existing works are tailored to emulate (i.e., predict the sampling of) a *specific* ETC design, thus providing a specific performance specification (e.g., stability). Moreover, they do not provide a method to trade off sampling performance and online computational load. To address these issues, we propose a novel STC scheme, termed *region-based STC*, for nonlinear systems with bounded disturbances or uncertainties. The system's state-space is partitioned into a finite number of regions, and to each region a uniform STC intersampling time is assigned. To decide the next sampling time, at each sampling time the controller simply checks to which region the measured state belongs. To derive the partition and corresponding intersampling times, such that a given ETC design is emulated, we use approximations of *isochronous manifolds* (sets of points in the state space that correspond to the same ETC intersampling time). To derive the approximations, we address certain theoretical issues of prior works and propose a computational algorithm. Finally, to account for disturbances or uncertainties, we employ differential inclusions.

Regarding traffic scheduling, our work is placed in the recent direction of the so-called *abstraction-based* approach. This approach offers a more versatile alternative to the established controller-scheduler co-design, where, whenever a new system joins the network, the design process has to be applied from scratch. According to the abstraction-based approach, the sampling behaviour of a given ETC system is modelled by a finite-state system (the abstraction), offering an infinite-horizon prediction on ETC's sampling, that can be leveraged for scheduling. Thus far, such abstractions have been constructed only for linear ETC systems. To extend the applicability of abstraction-based scheduling, we construct abstractions of nonlinear ETC systems with bounded disturbances or uncertainties. The system's state-space is partitioned into finitely many regions, representing the abstraction's states. For each region, a timing interval is determined, containing all intersampling times corresponding to states in the region. These intervals serve as the abstraction's output. Finally, the abstraction's transitions, given a starting region, indicate where the system's trajectories end up after an elapsed intersampling time. To determine the timing intervals and the transitions, we propose algorithms based on *reachability analysis*. Regarding state-space partitioning, we propose a partition similar to that of region-based STC, aiming at providing control over the timing intervals and improving their tightness, thus containing the abstraction's non-determinism.

Finally, research on formal analysis and assessment of ETC's sampling behaviour is surprisingly scarce. A recent research direction employs the aforementioned abstractions, to utilize the information they provide on ETC's sampling patterns and compute metrics associated to ETC's sampling. Specifically, a recent work showed how abstractions of linear PETC (periodic ETC; a practical variant of ETC) systems can be used to compute their average intersampling time. However, a generic framework that allows the study of ETC's sampling behaviour through general associated metrics is still missing. Moreover, stochastic systems, which model more accurately processes affected by random noise, remain unaddressed. In fact, for assessment purposes, the probabilistic framework of stochastic systems is naturally less strict than the deterministic one, as it takes into account the disturbances' probability distribution, instead of being bound by the worst case scenario. In this work, we formally analyze the sampling behaviour of stochastic linear PETC systems by computing bounds on associated metrics. Specifically,

we consider functions over sequences of state measurements and intersampling times that can be expressed as average, multiplicative or cumulative rewards, and introduce their expectations as metrics on PETC's sampling behaviour. We compute bounds on these expectations, by constructing appropriate Interval Markov Chains (IMCs) equipped with suitable reward structures, that abstract stochastic PETC's sampling behaviour, and employing *value iteration* over these IMCs.

SAMENVATTING

Networked Control Systems (NCS'en) (Netwerk regelsystemen) zijn regelsystemen, waarbij de verschillende componenten (sensoren, controllers en actuatoren) communiceren via een netwerk, dat meestal wordt gedeeld door meerdere regelsystemen of andere processen. NCS'en zijn overal aanwezig geworden vanwege hun lagere implementatiekosten en eenvoudiger onderhoud. Toch stellen ze ook nieuwe uitdagingen. Een fundamentele uitdaging is het verminderen van de hoeveelheid communicatie van elk systeem in het netwerk, zodat bandbreedte en energie worden bespaard.

Voor een dergelijke communicatievermindering heeft de onderzoeksgemeenschap haar focus verlegd naar *Event-Triggered Control* (ETC) (gebeurtenis-gestuurde regeling). ETC is een bemonsteringsparadigma waarbij communicatie tussen de verschillende componenten van het regelsysteem alleen plaatsvindt wanneer dat nodig is (wanneer aan een toestandsafhankelijke *triggervoorwaarde* is voldaan). De bemonstering basis van gebeurtenissen van ETC resulteert vaak in een grote vermindering van communicatie, in vergelijking met het algemeen aanvaarde paradigma van periodieke bemonstering. Aan de andere kant zijn de communicatietijden (of bemonsteringstijden) van ETC vooraf onbekend en voorspellingen daarvan vereisen een ingewikkelde wiskundige analyse van de (verstoorde) dynamica van het systeem. Desalniettemin is het voorspellen van de bemonstering van ETC van het grootste belang, omdat het het volgende mogelijk maakt:

- *Self-Triggered Control (STC) (zelf-gestuurde regeling)*: STC is een meer economische implementatie van ETC. In STC bepaalt de regelaar op elk communicatietijdstip het volgende communicatietijdstip op basis van de ontvangen toestandsmeting; dit elimineert de noodzaak voor continue monitoring van de triggerconditie en de intelligente hardware die nodig is om dit te doen, wat nodig is voor ETC. STC heeft 1-staps voorspellingen van ETC's bemonstering nodig om te kunnen werken; gegeven een toestandsmeting voorspelt het de volgende communicatietijd van ETC.

- *Verkeersplanning*: Verkeersplanning plant bandbreedtetoewijzing aan elke entiteit die het netwerk gebruikt. Voor regeltoepassingen is dit erg belangrijk; zonder dit kunnen veel systemen tegelijkertijd toegang krijgen tot het netwerk, wat leidt tot een netwerkoverloop en de stabiliteit van de systemen wordt belemmerd. Voor planning is een voorspelling van communicatietijden in meerdere of oneindige stappen nodig, om ervoor te zorgen dat er in de toekomst geen onveilige verschijnselen optreden door een planningsactie die nu wordt ondernomen.

- *Formele toetsing*: Gewoonlijk worden de prestaties van een ETC-ontwerp in termen van bemonstering en regeling gevalideerd door middel van simulaties. Simulaties geven echter geen definitieve formele resultaten, maar indicaties. Om formele garanties te verkrijgen over de bemonstering (versus regeling) prestaties van ETC,

bijvoorbeeld door het berekenen van bijbehorende lange-termijnsmetrieken, is kennis over de communicatiepatronen nodig. Meerdere-stappen of oneindige-stappen-voorspellingen van ETC's bemonstering vormen precies dergelijke kennis.

Dit proefschrift bestudeert het bemonsteringsgedrag van ETC en leidt voorspellingen daarvan af in alle drie de bovengenoemde contexten.

Onderzoek naar STC voor niet-lineaire systemen is relatief schaars. De meeste bestaande werken zijn op maat gemaakt om een *specifiek* ETC-ontwerp na te bootsen (d.w.z. de bemonstering te voorspellen) en zo een specifieke prestatiespecificatie te geven (bijvoorbeeld stabiliteit). Bovendien bieden ze geen methode om de afweging te maken tussen bemonsteringsprestaties en online rekenbelasting. Om deze problemen aan te pakken, stellen we een nieuw STC-schema voor, *region-based STC* (regio gebaseerd STC) genaamd, voor niet-lineaire systemen met begrensde verstoringen of onzekerheden. De toestandsruimte van het systeem is verdeeld in een eindig aantal regio's en aan elk gebied wordt een uniforme STC-interbemonstering-tijd toegewezen. Om het volgende bemonsteringstijdstip te bepalen, controleert de regelaar op elk bemonsteringstijdstip eenvoudig tot welk gebied de gemeten toestand behoort. Om de partitie en bijbehorende interbemonstering-tijden af te leiden, zodat een bepaald ETC-ontwerp wordt geëmuleerd, gebruiken we benaderingen van *isochrone variëteiten* (sets van punten in de toestandsruimte die overeenkomen met dezelfde ETC-interbemonstering-tijd). Om de benaderingen af te leiden, behandelen we bepaalde theoretische problemen van eerdere werken en stellen we een computationeel algoritme voor. Ten slotte gebruiken we differentiële insluitsels om rekening te houden met verstoringen of onzekerheden.

Met betrekking tot verkeersplanning, wordt ons werk geplaatst in de recente richting van de zogenaamde *abstractie-gebaseerde* methode. Deze aanpak biedt een veelzijdiger alternatief voor het gevestigde regelaarplanner co-ontwerp, waarbij, wanneer een nieuw systeem zich bij het netwerk voegt, het ontwerpproces helemaal opnieuw moet worden toegepast. Volgens de op abstractie gebaseerde methode wordt het bemonsteringsgedrag van een bepaald ETC-systeem gemodelleerd door een eindig toestandssysteem (de abstractie), dat een oneindige horizon voorspelling geeft van ETC's bemonstering, die kan worden gebruikt voor planning. Tot dusver zijn dergelijke abstracties alleen geconstrueerd voor lineaire ETC-systemen. Om de toepasbaarheid van op abstractie gebaseerde planning uit te breiden, construeren we abstracties van niet-lineaire ETC-systemen met begrensde storingen of onzekerheden. De toestandsruimte van het systeem is opgedeeld in eindig veel gebieden, die de toestanden van de abstractie vertegenwoordigen. Voor elke regio wordt een timing-interval bepaald, dat alle interbemonstering-tijden bevat die overeenkomen met toestanden in de regio. Deze intervallen dienen als output van de abstractie. Tenslotte worden de overgangen van de abstractie bepaald via *bereikbaarheidsanalyse*. Om de timingsintervallen en de overgangen te bepalen, stellen we algoritmen voor op basis van bereikbaarheidsanalyse. Wat betreft toestandsruimte-partitionering, stellen we een partitie voor die vergelijkbaar is met die van regio gebaseerde STC, met als doel om controle over de timing-intervallen te bieden en hun strakheid te verbeteren, waardoor het niet-determinisme van de abstractie wordt beperkt.

Ten slotte, onderzoek naar formele analyse en beoordeling van het steekproefgedrag van ETC is verrassend schaars. Een recente onderzoeksrichting maakt gebruik van de bovengenoemde abstracties om de informatie te gebruiken die ze geven over de be-

monsteringspatronen van ETC en metrieken te berekenen die verband houden met de bemonstering van ETC. In het bijzonder, een recent werk toonde aan hoe abstracties van lineaire PETC-systemen (periodieke ETC; een praktische variant van ETC) kunnen worden gebruikt om hun gemiddelde interbemonstering-tijd te berekenen. Er ontbreekt echter nog steeds een generiek raamwerk dat het bestuderen van het bemonsteringsgedrag van ETC door middel van algemene bijbehorende metrieken mogelijk maakt. Bovendien blijven stochastische systemen, die nauwkeuriger processen modelleren die worden beïnvloed door willekeurige ruis, ongeadresseerd. Voor beoordelingsdoeleinden is het probabilistische raamwerk van stochastische systemen van nature minder strikt dan het deterministische, omdat het rekening houdt met de kansverdeling van de verstoringen, in plaats van gebonden te zijn aan het worst-case scenario. In dit werk analyseren we formeel het bemonsteringsgedrag van stochastische lineaire PETC-systemen door grenzen te berekenen voor bijbehorende metrieken. In het bijzonder beschouwen we functies over reeksen toestandsmetingen en interbemonstering-tijden die kunnen worden uitgedrukt als gemiddelde, multiplicatieve of cumulatieve beloningen, en introduceren we hun verwachtingen als metrieken voor het bemonsteringsgedrag van PETC. We berekenen grenzen aan deze verwachtingen door geschikte *Interval Markov Chains* (IMCs) (interval Markovketens) te construeren die zijn uitgerust met geschikte beloningsstructuren, die het stochastische PETC-bemonsteringsgedrag abstraheren en *waarde iteratie* over deze IMCs gebruiken.

1

INTRODUCTION

In this chapter, we discuss the motivation surrounding the dissertation, related literature and gaps therein, we present the dissertation's main contributions, and give an outline of the manuscript.

1

1.1. MOTIVATION

Many modern control systems are Networked Control Systems (NCSs). The sensors, the controller and the actuators communicate with each other through a network, which is usually shared among many control systems and other processes. For example, the electrical system of a present-day car includes CAN buses that are used simultaneously by the transmission control loop, ABS, ESP, etc. [1]. Due to this possibility to be shared among many applications, NCSs offer reduced deployment costs and simpler maintenance [2], compared to the old paradigm of dedicated wired point-to-point connections. However, they also come with new challenges.

The fundamental challenge in NCSs is reducing communications to the least amount possible. In NCSs, the available bandwidth is limited, and often scarce, when many processes are using the network. Thus, applications communicating frequently and consuming a lot of bandwidth, hinder the sharing of the network among a big number of different processes, thus defeating its purpose to a certain extent. Furthermore, when the network is wireless, sensors consume a lot of energy to communicate; increased amounts of communication implies more energy usage and even more maintenance (e.g., when sensors run on batteries).

Towards reducing communication in NCSs, in the past two decades, the control systems community has shifted its research focus to Event-Triggered Control (ETC) (see the surveys [3], [4], as well as some notable work, e.g., [5]–[18]). ETC is a sampling paradigm where communication between the different components of the control system takes place only when deemed necessary. The sensors continuously measure the state of the system $\zeta(t)$ and check a so-called *triggering condition* $\phi(\zeta(t)) \geq 0$. When this condition is satisfied, they transmit the measurements to the controller, which uses them to transmit an updated control signal to the actuators; communication takes place only when the triggering condition is satisfied, or, to use the field's terminology, when *events* happen. These events typically imply that desired control performance is about to be compromised, and thus communication takes place in order to update the control signal accordingly. Owing to its event-based nature of sampling, ETC promises to greatly reduce the amount of communications a control system generates, compared to the conventional periodic sampling that is typically used nowadays, thus saving bandwidth and energy in NCSs.

Nonetheless, ETC's communication times - the times when events happen - are unknown beforehand, due to event-based sampling, in contrast to periodic control, where the specified period determines completely the communication times. Since events are determined by the satisfaction of the state-dependent triggering condition $\phi(\zeta(t)) \geq 0$, the sequences of communication times that are generated by the control system directly depend on the trajectory of its state $\zeta(t)$, and thus on the system's dynamics and the disturbances acting on it. Hence, prediction of ETC's communication times or events is far from straightforward and intricate analysis on the (perturbed) dynamics is needed. However, predicting ETC's events is of paramount importance, towards its widespread adoption as the sampling paradigm of the future, as it enables:

- *Self-Triggered Control (STC)*: STC is a more economic and proactive implementation of ETC. In STC, the controller, at each communication time, decides the next communication time based solely on the received state-measurement; this removes

the need for continuous monitoring of the triggering condition and the intelligent hardware needed to do so, which is necessary for ETC. Typically in STC, to decide the next communication time, the controller approximately predicts[1] when ETC would communicate, based on the received state-measurement. Thus, STC needs 1-step predictions of ETC's sampling to operate; given a state measurement it needs to predict the next communication time of ETC.

- *Traffic Scheduling*: Traffic scheduling in a network is planning when to allocate bandwidth to each entity using the network. For many control applications, which are safety-critical, traffic scheduling is very important; without it, there is a possibility that many components access the network at the same time, thus resulting into data packet collisions. In such case, control loops are unable to communicate, which hinders stability of the systems that are controlled. To derive a traffic schedule, in most cases a multi-step or infinite-step prediction of communication times is needed, in order to ensure that there are no unsafe phenomena in the future by a scheduling action taken at the present.

- *Formal Assessment*: Most often, when a new ETC design is proposed, its performance in terms of sampling and control is validated through simulations. However, simulations do not provide definite formal results, but only indications. To obtain formal results and guarantees on the sampling (or sampling vs. control) performance of ETC, e.g. by computing long-term metrics such as the *expected average intersampling time* in a certain horizon, knowledge on its communication patterns is needed. Multi-step or infinite-step predictions of ETC's sampling constitute exactly such knowledge.

The present doctoral dissertation studies ETC's sampling and obtains corresponding predictions in all three above contexts.

1.2. EXISTING WORK

Let us take a dive into the existing related work and some open gaps lying therein.

1.2.1. SELF-TRIGGERED CONTROL

STC has been studied quite extensively during the last 15 years [18]–[31]. The vast majority of works on STC adopts the so-called *emulation approach*: predicting, in a conservative way, when the triggering condition of an underlying ETC scheme would be satisfied. For example, in [26], a condition that enforces an exponential decay on the system's Lyapunov function is emulated, thus guaranteeing exponential stability. In [30], the condition that is emulated guarantees finite-gain $\mathscr{L}_2$-stability.

Despite the relatively big amount of research, STC for nonlinear systems, which model more accurately most controlled processes compared to linear systems, has not been studied thoroughly and the related literature is scarce [18]–[24]. In [18], Liu and Jiang

[1] These predictions are approximate in a safe manner; they predict well enough ETC's next communication time so that certain performance guarantees (e.g. stability), that are enforced by ETC, are retained by an STC implementation. Typically, to achieve that, STC's communication times are lower bounds on ETC's communication times.

design ETC and STC schemes for perturbed input-to-state stable (ISS) systems, following a small-gain theorem approach. In [20], an STC design is proposed that enforces the system's state to remain in a safe set, by employing Taylor approximations of the system's Lyapunov function. Tiberi and Johansson [19] propose an ETC and a corresponding STC scheme to enforce uniform ultimate boundedness for perturbed uncertain systems, while Tolic *et al.* [21] employ a small-gain approach to design STC that guarantees $\mathscr{L}_p$-stability. In [22] an STC design is proposed that copes with actuator delays. Finally, in [23], Anta and Tabuada derive STC formulas for nonlinear systems employing interesting properties of homogeneous systems, while in [24] their results are improved by incorporating the notion of *isochronous manifolds*.

All techniques listed above, except for [23] and [24], suffer from the same limitation: they are tailored to emulating a specific triggering condition and providing a specific performance specification (e.g., stability, safety, etc.). On the other hand, [23], in spite of its interesting results, is conservative w.r.t. other techniques in the literature in terms of sampling performance (it tends to sample more frequently). Regarding [24], there are certain theoretical and practical issues that are thoroughly discussed and addressed in the present dissertation, although it has certainly proven a source of inspiration for a part of the dissertation. What is more, neither [23] nor [24] addresses systems with disturbances and uncertainties. Finally, it is worth noting that, with the exception of [20], none of all aforementioned approaches provides a method to trade off sampling performance and online computational load (i.e., how heavy are the computations that are performed by the controller online to determine the communication times).

The first part of the main body of the present dissertation (Chapters 3 and 4) is occupied with STC and the gaps in the related literature mentioned above.

1.2.2. TRAFFIC SCHEDULING

Traffic scheduling for ETC has not received much attention [32]–[41]. Most proposed methods approach the problem from a controller-sampler-scheduler co-design perspective [32]–[38]. According to them, the controller, the sampling scheme and the scheduler are all designed in a coupled manner, such that network access is performed safely, resource utilization is efficient and certain performance specifications are guaranteed. The co-design nature of these approaches lacks the versatility that is needed in many modern NCSs; for example, when a new control loop joins the network, the whole design process has to be applied from scratch, resulting in different controllers, samplers and schedulers. The same happens when a control loop's performance specification changes: all components have to be redesigned.

Recently, a new set of approaches on scheduling for ETC has emerged [39]–[41], that tackles the versatility problem of the co-design approaches. These new approaches are based on *abstractions*: the sampling behaviour of a given ETC system is modelled by a finite-state system (the abstraction). The abstraction's set of output sequences contains all possible sequences of *intersampling times* that can be exhibited by the ETC system. In this way, an infinite-horizon prediction on the sampling patterns of ETC is obtained, that can be leveraged for traffic scheduling. For example, in [39], ETC-traffic scheduling is performed as follows: 1) abstractions of all ETC systems in the network are created, 2) the abstractions are equipped with scheduling actions, and become semantically

equivalent to *timed game automata* (TGA, see [42]), 3) the network's state (idle, occupied, etc.) is modelled as a TGA, as well, and then all TGA are composed to create a big TGA modelling the whole interconnection, and finally 4) a safety game is solved over the resulting TGA, such that there are no packet collisions (or network-access conflicts) on an infinite horizon. Abstraction-based approaches are more versatile than co-design approaches, as for example the abstraction of each system in the network is computed only once offline, and does not change with the presence of a new system.

Nevertheless, so far, such abstractions have been constructed only for linear systems with a specific type of triggering conditions (with quadratic triggering functions $\phi(\cdot)$). Specifically, [39] and [40] have considered linear ETC systems, while [41] has considered linear PETC (periodic ETC; a more practical variant of ETC, see for example [10]) systems.

The second main part of the present dissertation (Chapter 5) is occupied with constructing abstractions of the sampling behaviour of nonlinear ETC systems with general triggering functions, thus extending the applicability of versatile abstraction-based scheduling to a significantly wider class of systems.

1.2.3. FORMAL ASSESSMENT

The research efforts to study the sampling behaviour of ETC and characterize its sampling (or sampling vs. control) performance are very recent [43]–[46]. One branch of this research is the analytic approaches [44]–[46]. Demirel *et al.* [44] consider stochastic linear PETC systems equipped with deadbeat controllers. Thanks to the particularities of deadbeat control, studying the sampling behaviour simplifies to analyzing a Markov chain, which can be used to compute quantitative metrics on the system's sampling performance. Nevertheless, assuming the presence of a deadbeat controller is admittedly restrictive. Furthermore, in [45] and [46] the asymptotic properties of intersampling times of planar linear ETC systems with quadratic triggering conditions are investigated. Among others, conditions under which the intersampling times converge to a fixed point or a periodic pattern are derived. Despite their interesting insights, these works obey certain limitations: a) only 2-D systems are considered, b) the type of triggering condition considered is key in the whole analysis, and most importantly c) they do not offer quantitative insights on all possible sampling patterns that an ETC system can generate; thus, there is no straightforward way of employing them for computing general metrics on ETC's sampling performance or for predicting its patterns.

The other branch of research leverages the abstractions of ETC's sampling behaviour that were mentioned in the previous section. In particular, [43] employs abstractions for linear PETC systems to compute their infinite-horizon minimum average intersampling time. In fact, arguably, other abstractions could be employed as well in a similar manner for the same purpose, such as the abstractions for nonlinear systems developed here in Chapter 5, thus extending the applicability of the methods in [43]. In contrast to the analytic approaches, with abstraction-based approaches there is no restrictive assumption on the type of controller, on the dimensions of the system (modulo computational complexity) or on the type of triggering condition considered (albeit some minor steps in the abstraction's construction might vary). More importantly, as mentioned earlier, these abstractions offer an infinite-horizon look to all possible sampling patterns of ETC, and thus enable the computation of general metrics on its sampling performance.

However, a generic framework that allows the study of ETC's sampling behaviour through general associated metrics is still missing: [43] is occupied specifically with the average intersampling time, while the rest of the abstraction-based approaches have been written in the context of traffic scheduling. Moreover, stochastic systems, which model more accurately processes affected by random noise, remain unaddressed. In fact, for assessment purposes, the probabilistic framework of stochastic systems is naturally less strict than the deterministic one, as it takes into account the disturbances' probability distribution, instead of being bound by the worst case scenario.

The third and final part of the main body of the dissertation derives a generic framework to study the sampling behaviour of stochastic ETC systems through associated metrics, constructs corresponding abstractions to compute (bounds on) these metrics, and characterizes stochastic ETC's sampling performance.

1.3. ORIGINAL CONTRIBUTIONS

Now that the existing related literature has been discussed and the corresponding gaps have been pointed out, we can proceed to stating the main high-level contributions of the present dissertation:

- We propose an STC method, termed *region-based* STC, for nonlinear systems with bounded disturbances and uncertainties, that provides a unified framework to emulate general triggering conditions and, thus, incorporate a wide range of performance specifications. Moreover, it provides a way to trade off online computational load with sampling performance.
- We abstract the sampling behaviour of nonlinear ETC systems with disturbances, uncertainties, and general triggering functions. That way, we significantly extend the applicability of versatile abstraction-based scheduling of ETC traffic in NCSs.
- We construct a generic framework to study stochastic PETC's sampling behaviour through metrics associated to its sampling (vs. control) performance and sampling patterns. We formally assess the sampling behaviour of linear stochastic PETC systems by computing bounds on such metrics. To that end, we abstract their sampling behaviour via *Interval Markov Chains*, providing probabilistic quantitative information on all possible sampling patterns.

To attain these high-level contributions, we have made several technical contributions in the process. The detailed listing of all contributions takes place in the beginning of each corresponding chapter. Finally, it is worth emphasizing that:

- Most of the theoretical and computational developments of the dissertation have been automated through our Python toolbox ETCetera [47], which is publicly available at `https://gitlab.tudelft.nl/sync-lab/ETCetera`. The experimental results of the dissertation can be reproduced by using ETCetera. The toolbox is subject to ongoing extensions and improvements.

1.4. OUTLINE

The dissertation is structured as follows:

- **Chapter 2** introduces notation and nomenclature used throughout the manuscript, as well as background technical knowledge that is needed to follow its technical developments.
- **Chapter 3** is concerned with developing the region-based STC method for nonlinear systems.
- **Chapter 4** extends the STC method to systems with bounded disturbances and uncertainties.
- **Chapter 5** constructs abstractions of the sampling behaviour of perturbed/uncertain nonlinear ETC systems with general triggering functions, in the context of ETC traffic scheduling.
- **Chapter 6** devises a framework to study the sampling behaviour of stochastic PETC through associated metrics, and computes bounds on such metrics via abstractions. The focus is on linear stochastic PETC systems.
- **Chapter 7** concludes the dissertation with discussion on the aforementioned developments and recommendations for future work.

Finally, all Chapters 3-6 contain several numerical examples that demonstrate the corresponding theoretical results. Moreover, notation, terminology and background knowledge that is employed only in specific chapters, is introduced in the beginning of these chapters, to enhance readability.

2

PRELIMINARIES

In this chapter, we introduce notation and nomenclature that is used throughout the dissertation. Moreover, we present some background technical knowledge on deterministic ETC systems, homogeneous ETC systems and the emulation approach to STC. Notation and background knowledge that are chapter-specific, i.e. that are employed in a specific chapter only, are introduced in their corresponding chapter and not here.

2.1. NOTATION AND NOMENCLATURE

$\mathbb{R}$ stands for the set of real numbers and $\mathbb{R}_{>0}$ (resp. $\mathbb{R}_{\geq 0}$) for the positive (resp. non-negative) reals. $\mathbb{N}$ stands for the set of natural numbers including 0, and $\mathbb{N}_{>0}$ for the naturals without 0. I_n is the n-dimensional identity matrix. We use the symbol $\exists!$, to denote existence and uniqueness. We denote points in $\mathbb{R}^n$ as x and their Euclidean norm as $|x|$. For vectors, we also use the notation $(x_1, x_2) = \begin{bmatrix} x_1^\top & x_2^\top \end{bmatrix}^\top$. For $x, y \in \mathbb{R}^n$, we write $x \preceq y$ if $x_i \leq y_i$ $(i = 1, \ldots, n)$, where the subscript i denotes the i-th component of the corresponding vector. When there is no harm from ambiguity, the subscript i may be, also, used to denote different points $x_i \in \mathbb{R}^n$.

Consider a system of ordinary differential equations (ODE):

$$\dot{\zeta}(t) = f(\zeta(t)), \tag{2.1}$$

where $\zeta : \mathbb{R} \to \mathbb{R}^n$. We denote by $\zeta(t; t_0, \zeta_0)$ the solution of (2.1) with initial condition ζ_0 at initial time t_0. When t_0 (or ζ_0) is clear from the context, then it is omitted, i.e. we write $\zeta(t; \zeta_0)$ (or $\zeta(t)$). Given a set of initial states $\mathscr{I} \subseteq \mathbb{R}^n$, the *reachable set* of (2.1) from $\mathscr{I}$ at time T is $\mathscr{X}_T^f(\mathscr{I}) := \{\zeta(T; \zeta_0) : \zeta_0 \in \mathscr{I}\}$. Likewise, the *reachable flowpipe* of (2.1) in the time interval $[\tau_1, \tau_2]$, with initial set $\mathscr{I}$, is $\mathscr{X}_{[\tau_1,\tau_2]}^f(\mathscr{I}) := \bigcup_{T \in [\tau_1,\tau_2]} \mathscr{X}_T^f(\mathscr{I})$.

2.2. HOMOGENEOUS SYSTEMS

Let us introduce some preliminary concepts on homogeneous systems and their properties, as they play a pivotal role in Chapters 3, 4, and 5. Here, only the classical notion of homogeneity is presented. For the general definition of homogeneity, the reader is referred to [48].

Definition 2.2.1 (Homogeneous Function)**.** *Consider a function $f : \mathbb{R}^n \to \mathbb{R}^m$. We say that f is homogeneous of degree $\alpha \in \mathbb{R}$, if for all $x \in \mathbb{R}^n$ and any $\lambda > 0$: $f(\lambda x) = \lambda^{\alpha+1} f(x)$.*

Definition 2.2.2 (Homogeneous System)**.** *A system (2.1) is called homogeneous of degree $\alpha \in \mathbb{R}$, whenever $f(\cdot)$ is a homogeneous function of the same degree.*

For homogeneous ODEs, the following scaling property of solutions holds:

Proposition 2.2.1 (Scaling Property of Homogeneous ODEs [48])**.** *Let the system of ODEs (2.1) be homogeneous of degree $\alpha \in \mathbb{R}$. Then, for any $\zeta_0 \in \mathbb{R}^n$ and any $\lambda > 0$:*

$$\zeta(t; \lambda\zeta_0) = \lambda\zeta(\lambda^\alpha t; \zeta_0). \tag{2.2}$$

2.3. EVENT-TRIGGERED AND SELF-TRIGGERED CONTROL

2.3.1. DETERMINISTIC EVENT-TRIGGERED CONTROL SYSTEMS

Consider the control system with state-feedback:

$$\dot{\zeta}(t) = f\Big(\zeta(t), \upsilon(\zeta(t))\Big), \tag{2.3}$$

where $\zeta : \mathbb{R} \to \mathbb{R}^n$ is the state, $f : \mathbb{R}^n \times \mathbb{R}^{m_u} \to \mathbb{R}^n$ is the vector field, and $\upsilon : \mathbb{R}^n \to \mathbb{R}^{m_u}$ is the control input. In any sample-and-hold scheme, the control input is updated on *sampling*

times (or communication times) t_i and held constant between consecutive sampling times:

$$\dot{\zeta}(t) = f\Big(\zeta(t), v(\zeta(t_i))\Big), \quad t \in [t_i, t_{i+1}).$$

If we define the *measurement error* as the difference between the last measurement and the present state:

$$\varepsilon_\zeta(t) := \zeta(t_i) - \zeta(t), \quad t \in [t_i, t_{i+1}), \tag{2.4}$$

then the sample-and-hold system can be written as:

$$\dot{\zeta}(t) = f\Big(\zeta(t), v(\zeta(t) + \varepsilon_\zeta(t))\Big), \quad t \in [t_i, t_{i+1}). \tag{2.5}$$

Notice that the error $\varepsilon_\zeta(t)$ resets to zero at each sampling time. In ETC, the sampling times (i.e. the times of events or *event times*) are determined by:

$$t_{i+1} = t_i + \inf\{t > 0 : \phi(\zeta(t; x_i), \varepsilon_\zeta(t)) \geq 0\}, \tag{2.6}$$

and $t_0 = 0$, where $x_i \in \mathbb{R}^n$ is the previously sampled state, $\phi(\cdot,\cdot)$ is the *triggering function*, (2.6) is the *triggering condition* and $t_{i+1} - t_i$ is called *intersampling time*[1]. Each point $x \in \mathbb{R}^n$ corresponds to a specific intersampling time, defined as:

$$\tau(x) := \inf\{t > 0 : \phi(\zeta(t; x), \varepsilon_\zeta(t)) \geq 0\}. \tag{2.7}$$

Between two consecutive sampling times t_i and t_{i+1}, the triggering function starts from a negative value $\phi(\zeta(t_i; x_i), 0) < 0$ (the measurement error is zero at sampling times), and stays negative until t_{i+1}^-, when it becomes zero. Then, at t_{i+1}, the latest state-measurement is sent to the controller which updates the control action, the triggering function resets to a negative value, and the whole process is repeated again. Triggering functions are designed such that the inequality $\phi(\zeta(t; x), \varepsilon_\zeta(t)) \leq 0$ implies certain performance guarantees (e.g. stability). Thus, sampling times are defined in a way (see (2.6)) such that $\phi(\zeta(t), \varepsilon_\zeta(t)) \leq 0$ for all $t \geq 0$, which implies that the performance specifications are met at all time.

Remark 2.3.1. *In practice, to remove the possibility of the system operating open-loop indefinitely, a maximum allowed intersampling time $\tau_{\max}$ is introduced (often called "heartbeat"), such that sampling times are defined as $t_{i+1} = t_i + \min(\tau(x_i), \tau_{\max})$, where x_i denotes the state measurement at t_i. The presence of a heartbeat is, in fact, assumed for some parts of the present work. When it is assumed, it will be clearly stated.*

Finally, by leveraging that $\dot{\varepsilon}_\zeta(t) = -\dot{\zeta}(t)$, we write the dynamics of the *extended ETC system* in a compact form:

$$\dot{\xi}(t) = \begin{bmatrix} f\Big(\zeta(t), v(\zeta(t) + \varepsilon_\zeta(t))\Big) \\ -f\Big(\zeta(t), v(\zeta(t) + \varepsilon_\zeta(t))\Big) \end{bmatrix} = f_e(\xi(t)), \ t \in [t_i, t_{i+1}) \tag{2.8a}$$

$$\xi(t_{i+1}^+) = \begin{bmatrix} \zeta(t_{i+1}^-) \\ 0 \end{bmatrix} \tag{2.8b}$$

[1] Many times, in the literature, it is also referred to as *interevent time*.

where $\xi = (\zeta, \varepsilon_\zeta) \in \mathbb{R}^{2n}$. At each sampling time t_i, the state of (2.8) becomes $\xi_i = (x_i, 0)$. Thus, for brevity and convenience, instead of writing $\xi\Big(t;(x_i,0)\Big)$ (or $\phi\Big(\xi(t;(x_i,0))\Big)$, or $\tau\Big((x_i,0)\Big)$, etc.) for some $t \in [t_i, t_{i+1})$, we abusively write $\xi(t;x_i)$ (or $\phi(\xi(t;x_i))$, or $\tau(x_i)$, etc.).

2

2.3.2. HOMOGENEOUS ETC SYSTEMS AND SCALING OF INTERSAMPLING TIMES

From now on, we say that an ETC system (2.8) is homogeneous of some degree α, whenever its continuous dynamics (2.8a) define a homogeneous system of the same degree. The intersampling times of homogeneous ETC systems with homogeneous triggering functions satisfy certain interesting properties, discovered in [23]. Specifically, along lines passing through the origin (but excluding the origin) the event-triggered intersampling times scale according to the following rule:

Theorem 2.3.1 (Scaling Law [23])**.** *Consider an ETC system (2.5)-(2.6), such that (2.8) is homogeneous of degree α and the triggering function $\phi(\cdot)$ homogeneous of degree θ. For all $x \in \mathbb{R}^n$, the intersampling times $\tau : \mathbb{R}^n \to \mathbb{R}^+ \cup \{+\infty\}$ defined by (2.7) scale as:*

$$\tau(\lambda x) = \lambda^{-\alpha}\tau(x), \quad \lambda > 0. \tag{2.9}$$

In the following, we refer to lines going through the origin as *homogeneous rays*. Notice that the scaling law for the intersampling times (2.9) does not depend on the degree of homogeneity of the triggering function considered. The property derives from the following useful result, which is a direct consequence of the scaling property of homogeneous flows (Proposition 2.2.1):

Lemma 2.3.1 (Time-Scaling Property of the Triggering Function [23])**.** *Consider an ETC system (2.5)-(2.6), such that (2.8) is homogeneous of degree α and the triggering function $\phi(\cdot)$ homogeneous of degree θ. The triggering function satisfies:*

$$\phi(\xi(t;\lambda x)) = \phi(\lambda\xi(\lambda^\alpha t;x)) = \lambda^{\theta+1}\phi(\xi(\lambda^\alpha t;x)), \tag{2.10}$$

where the first equality follows from Proposition 2.2.1.

2.3.3. SELF-TRIGGERED CONTROL: EMULATION APPROACH

According to the emulation approach to STC, an STC strategy dictates the next sampling time according to a function $\tau^\downarrow : \mathbb{R}^n \to \mathbb{R}^+$ lower-bounding the ETC intersampling times:

$$\tau^\downarrow(x) \le \tau(x), \quad \forall x \in \mathbb{R}^n \tag{2.11}$$

Since $\phi(\xi(t;x)) < 0$ for all $t \in [0, \tau(x))$, then it is guaranteed that $\phi(\xi(t;x)) < 0$ for all $t \in [0, \tau^\downarrow(x))$, and the performance specification of the emulated ETC scheme is preserved. Consequently, the STC intersampling times should be no larger than the corresponding ETC times, but as large as possible in order to achieve greater reduction of communications. Finally, $\tau^\downarrow(\cdot)$ should be designed such that $\tau^\downarrow(x) \ge \epsilon > 0$ for all x in the operating region of the system, in order to avoid infinitely-fast sampling (Zeno behaviour).

3

ISOCHRONOUS PARTITIONS AND REGION-BASED SELF-TRIGGERED CONTROL

In this chapter, we develop a region-based *self-triggered control (STC) scheme for nonlinear systems. Region-based STC provides a unified framework to emulate general triggering conditions and, thus, incorporate a wide range of performance specifications. Furthermore, it provides a way to trade off online computational load with sampling performance. The state space is partitioned into a finite number of regions, each of which is associated to a uniform STC intersampling time. The controller, at each sampling time, checks to which region the current state belongs, and correspondingly decides the next sampling time. The bigger the number of regions, the better the sampling performance and the heavier the online computational load, as the controller needs to perform more checks. To derive the regions along with their corresponding intersampling times, we use inner approximations of* isochronous manifolds *(IMs), a notion firstly introduced in [24]. Towards deriving approximations of IMs, we address certain theoretical issues of [24] and propose an effective computational approach to generate them. The efficiency of both our theoretical results and the proposed algorithm are demonstrated through simulation examples.*

This chapter has been published in [49]. Minor changes have been made, to streamline presentation.

3.1. INTRODUCTION

In this chapter, we derive a *region-based* STC scheme for nonlinear systems, adopting an emulation approach. The proposed STC is able to emulate a big class of triggering conditions and ETC schemes, thus providing the ability to consider a wide range of performance specifications. The state space is partitioned into a finite number of regions, and each region is associated to a uniform STC intersampling time, that lower bounds all intersampling times of the region corresponding to the emulated ETC. Thus, at each sampling time, to decide the next sampling time, the controller simply has to check which of the regions contains the received state measurement. The bigger the number of regions is, the less conservative the STC intersampling times are, which implies better sampling performance. On the other hand, more regions imply more set-membership checks performed by the controller, which translates to higher computational load. Thus, by being able to control the number of regions, we control the trade-off between sampling performance and online computations.

In contrast to [29], in which the state space is firstly partitioned and afterwards the corresponding self-triggered intersampling times are computed, we propose to firstly predefine a set of specific intersampling times and afterwards derive the regions that correspond to the selected times. Thus, in our approach the number of regions in the state space is always equal to the number of times. This tames the curse of dimensionality, as the number of regions is independent of the dimensions of the system.

To partition the state space, we employ inner approximations of *isochronous manifolds* (IMs), a notion originally introduced in [24]. IMs are hypersurfaces in the state space, that consist of points associated to the same ETC intersampling time τ, i.e. if the system's state belongs to an IM at a sampling time t_i, then the next sampling time, under a given triggering condition, is $t_{i+1} = t_i + \tau$. In [24], Anta and Tabuada propose a method to approximate these manifolds by upper-bounding the evolution of the triggering function, and then use the approximations to derive an STC formula. Unfortunately, there are some unaddressed theoretical and practical issues therein, which render the approximations, in general, invalid and hinder the application of the corresponding STC scheme. In particular, the bounding lemma [24, Lemma V.2], based on which the upper-bounds of the triggering function are derived, is incorrect. Furthermore, we pinpoint that, even if a valid bound is obtained, the method proposed in [24] approximates the *zero-level sets of the triggering function*, and not the actual IMs. Finally, although the authors in [24] propose the use of SOSTOOLS [50] to derive the approximations, we have found it to be numerically non-robust regarding solving this particular problem. Here, we tackle all aforementioned issues, towards deriving a partition of the state space for nonlinear systems that enables a region-based STC scheme. The biggest part of the chapter focuses on *homogeneous* ETC systems, for clarity. Nevertheless, it is clearly shown how the approach generalizes to nonhomogeneous systems as well, through an extensive discussion in Section 3.7 and a numerical example.

Overall, the contributions of this chapter are the following:

- We present a valid version of the bounding lemma, based on a higher order comparison lemma [51].
- Employing this new lemma, we propose a refined methodology to approximate the

actual IMs of nonlinear ETC systems.

- We adjust a counter-example guided iterative method (see e.g. [52]) combining Linear Programming and SMT (Satisfiability Modulo Theory) solvers (e.g. [53]), to derive an alternative algorithm that effectively computes approximations of IMs.
- We derive a novel region-based STC scheme that provides a generic framework to emulate a wide range of triggering conditions, and the ability to trade-off online computational load with communications.

Finally, it is worth noting that IMs are an inherent characteristic of any system with an output. Thus, as in [24], the study of IMs and the theoretical contribution of deriving approximations thereof might even exceed the context of ETC and STC.

3.2. NOTATION

If $f:\mathbb{R}^n \to \mathbb{R}^m$ is p-times continuously differentiable, we write $f \in \mathscr{C}^p$. Let $X: M \to TM$ be a vector field and $h: M \to \mathbb{R}$ a map. $\mathscr{L}_X h(x)$ denotes the Lie derivative of h at a point x along the flow of X. Similarly, $\mathscr{L}_X^k h(x) = \mathscr{L}_X(\mathscr{L}_X^{k-1} h(x))$ is the k-th Lie derivative with $\mathscr{L}_X^0 h(x) = h(x)$.

3.3. PROBLEM STATEMENT

The following is in the context of the emulation approach to STC: we assume a given ETC system, and we seek to design an STC scheme as the emulation approach dictates. In a region-based STC scheme, the state-space of the original system (2.5) is divided into a finite number of regions $\mathscr{R}_i \subset \mathbb{R}^n$ $(i = 1,2,\dots)$, each of which is associated to a self-triggered intersampling time τ_i such that:

$$\forall x \in \mathscr{R}_i: \quad \tau_i \leq \tau(x), \tag{3.1}$$

where $\tau(x)$ denotes the event-triggered intersampling time associated to x (see (2.7)). The STC scheme operates as follows:

1. Measure the current state x_k.
2. Check to which of the regions $\mathscr{R}_i$ the point x_k belongs.
3. If $x_k \in \mathscr{R}_i$, set the next sampling time to $t_{k+1} = t_k + \tau_i$.

Thus, to enable region-based STC, we have to find regions $\mathscr{R}_i$ and times τ_i such that (3.1) holds. In [29], the state-space is partitioned into regions $\mathscr{R}_i$ *a priori*, and afterwards the times τ_i are computed such that they satisfy (3.1); this suffers from the curse of dimensionality. Here, we propose an alternative approach: firstly a finite set of times $\{\tau_1, \tau_2, \dots \tau_q\}$ is *predefined* (e.g. by the user), which will serve as STC intersampling times, with $\tau_i < \tau_{i+1}$, and then regions $\mathscr{R}_i$ corresponding to times τ_i are derived *a posteriori*, such that (3.1) is satisfied. In this way, the number of regions is equal to the number of times τ_i and the curse of dimensionality is tamed, as the number of regions does not depend on the system's dimensions. The problem statement is as follows:

Problem Statement. *Given an ETC system* (2.5)-(2.6)*, and a finite set of times* $\{\tau_1, \dots \tau_q\}$*, with* $\tau_i < \tau_{i+1}$ *and* $q > 1$*, find* $\mathscr{R}_i \in \mathbb{R}^n$ *that satisfy* (3.1)*.*

Note that Zeno behaviour is ruled out by construction, since the STC intersampling times are lower bounded: $\tau^{\downarrow}(x) \geq \min_i\{\tau_i\} = \tau_1$. The choice of times τ_i and its effect is discussed later in the document.

Assumption 3.3.1. *For the remaining of the chapter, our analysis is based on the following set of assumptions:*

1. *The extended ETC system* (2.8) *is smooth and homogeneous of degree* $\alpha \geq 1$*, with* $r_i = 1$ *for all* i*.*

2. *The triggering function* $\phi(\xi(t;x))$ *is smooth and homogeneous of degree* $\theta \geq 1$*, with* $r_i = 1$ *for all* i*.*

3. $\phi\Big((0,0)\Big) \leq 0$ *and* $\phi\Big((x,0)\Big) < 0$ *for all* $x \in \mathbb{R}^n \setminus \{0\}$*. For any compact set* $K \subset \mathbb{R}^n$ *there exists* $\epsilon_K > 0$ *such that for all* $x_0 \in K \setminus \{0\}$*,* $\phi(\xi(t;x_0)) < 0$ *for all* $t \in [0, \epsilon_K)$*.*

4. *Compact sets* $\mathrm{Z} \subset \mathbb{R}^n$ *and* $\Xi \subset \mathbb{R}^{2n}$*, containing a neighbourhood of the origin, are given, such that for all* $x \in \mathrm{Z}$*:* $\phi(\xi(t;x)) \leq 0 \implies \xi(t;x) \in \Xi$*.*

5. *The system* (2.3) *has the origin as the only equilibrium.*

Regarding items 1 and 2, they serve clarity of presentation issues; the main developments of the present chapter are stated in the context of homogeneous ETC systems and triggering functions. Nevertheless, our results are applicable to general smooth nonlinear systems and triggering functions, by employing the *homogenization procedure* proposed in [24, Lemma IV.4], which renders any smooth function homogeneous, by embedding it to a higher-dimensional space. This is thoroughly discussed in Section 3.7 and showcased in Section 3.8.2 via a numerical example.

Regarding item 4, it only asks that the ETC implementation is known to satisfy a basic boundedness condition. This is satisfied by most well-known ETC schemes in the literature. For example, in many ETC schemes (e.g., [7]), a radially unbounded Lyapunov function $V(x)$ for the system is known, and the triggering function satisfies $\phi(\xi(t;x)) \leq 0 \implies \dot{V}(\zeta(t;x)) \leq 0$. Then, the set Ξ can be constructed as $\Xi = \mathrm{Z} \times \mathrm{E}$, where $\mathrm{Z} = \{x \in \mathbb{R}^n : V(x) \leq c\}$, $\mathrm{E} = \{x_0 - x \in \mathbb{R}^n : x, x_0 \in \mathrm{Z}\}$ and $c > 0$. An alternative and more general way of constructing Z and Ξ, without assuming that they are given (but requiring a different assumption) is demonstrated in Section 3.8.2 and is fully adopted in Chapter 4 (see (4.15)), where we extend the developments of the present chapter to perturbed uncertain systems. The importance of the sets Z and Ξ is discussed right after Theorem 3.5.2.

Finally, item 3 excludes Zeno behaviour, which is satisfied by any well-designed ETC scheme (e.g., Tabuada's triggering function [7], dynamic triggering [8], mixed triggering [18], Lebesgue sampling [6]), and item 5 is a rather standard assumption in the context of ETC, but as discussed in Chapter 7, it might not be needed.

3.4. ISOCHRONOUS MANIFOLDS, TRIGGERING LEVEL SETS AND PARTITION

Here, we recall results from [24] regarding isochronous manifolds, we introduce the notion of *triggering level sets* and describe how isochronous manifolds and triggering level sets are different. Finally, we point out how, given proper approximations of isochronous manifolds, a state-space partition is generated, enabling a region-based STC scheme.

3.4.1. ISOCHRONOUS MANIFOLDS AND TRIGGERING LEVEL SETS

Definition 3.4.1 (Isochronous Manifolds)**.** *Consider an ETC system* (2.5)-(2.6)*. The set* $M_{\tau_\star} = \{x \in \mathbb{R}^n : \tau(x) = \tau_\star\}$*, where* $\tau(x)$ *is defined by* (2.7)*, is called an isochronous manifold (IM) of time* $\tau_\star$*.*

Alternatively, all points $x \in \mathbb{R}^n$ which correspond to intersampling time $\tau_\star$ constitute the IM $M_{\tau_\star}$. IMs are of dimension $n-1$ (proven in [24]).

Definition 3.4.2 (Triggering Level Sets)**.** *We call the set:*

$$L_{\tau_\star} := \{x \in \mathbb{R}^n : \phi(\xi(\tau_\star; x)) = 0\} \tag{3.2}$$

triggering level set of $\phi(\xi(t;x))$ *for time* $\tau_\star$*.*

Triggering level sets are the zero-level sets of the triggering function, for fixed t. Let us now make a crucial observation: *The equation* $\phi(\xi(t;x)) = 0$ *may have multiple solutions with respect to time t for a given* x. In other words, there might exist points $x \in \mathbb{R}^n$ and time instants $\tau_{x,1} < \tau_{x,2} < \ldots < \tau_{x,k}$, with $k > 1$ such that $\phi(\xi(\tau_{x,i}; x)) = 0$ for all $i = 1, 2, \ldots, k$. We briefly present an example with a triggering function exhibiting multiple zero-crossings for given initial conditions:

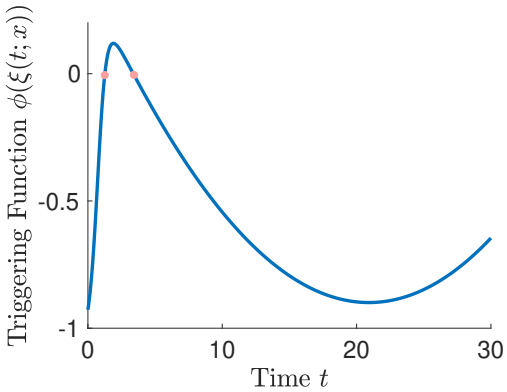

Figure 3.1: The time evolution of $\phi(x;t)$ for initial condition $[-0.5, -1]^\top$. It exhibits multiple zero-crossings.

Example: Consider the jet-engine compressor control system from [54]:

$$\dot{\xi}_1(t) = -\xi_2(t) - \frac{3}{2}\xi_1^2(t) - \frac{1}{2}\xi_1^3(t), \quad \dot{\xi}_2(t) = v(\xi(t)),$$

with control law $v(\xi(t)) = \xi_1(t) - \frac{1}{2}(\xi_1^2(t)+1)(y+\xi_1^2(t)y+\xi_1(t)y^2)+2\xi_1(t)$, where $y = 2\frac{\xi_1^2+\xi_2}{\xi_1^2+1}$. A triggering function that guarantees asymptotic stability is the following [23]:

$$\phi(\xi(t;x)) = |\varepsilon_\zeta|^2 - 0.82\sigma^2|\zeta(t;x)|^2, \qquad \sigma \in (0,1).$$

The evolution of the triggering function $\phi(\xi(t;x))$ for the initial condition $[-0.5\ -1]^\top$ is simulated and illustrated in Fig. 3.1. It is clear from the figure that it exhibits multiple zero-crossings, e.g., for $t = \tau_{x,1} \approx 1.15s$ and $t = \tau_{x,2} \approx 3.22s$. ■

3

Intersampling times are defined as *the first zero-crossing of the triggering function* (see (2.7)), i.e. $\tau(x) = \tau_{x,1}$. IMs are defined with respect to this first zero-crossing, and any point $x \in \mathbb{R}^n \setminus \{0\}$ belongs only to one IM: $M_{\tau_{x,1}}$. However, the same point belongs to all triggering level sets $L_{\tau_{x,i}}$. For instance, in the previous example, the point $x = (-0.5,-1)$ belongs to both triggering level sets $L_{1.15}$ and $L_{3.22}$, whereas it belongs to only one IM, i.e. $M_{1.15}$. In [24], IMs and triggering level sets are treated as if they were identical, which creates problems regarding approximating IMs. This is addressed later in this chapter.

Remark 3.4.1. *If the triggering function $\phi(\xi(t;x))$ has only one zero-crossing for all $x \in \mathbb{R}^n \setminus \{0\}$, then the triggering level sets do coincide with the IMs, i.e. $M_{\tau_\star} = \{x \in \mathbb{R}^n : \tau(x) = \tau_\star\} = \{x \in \mathbb{R}^n : \phi(\xi(\tau_\star;x)) = 0\} = L_{\tau_\star}$.*

In the following, we refer to lines going through the origin as *homogeneous rays*. Owing to the time scaling property (2.10), IMs possess the following properties:

Proposition 3.4.1. *Consider an ETC system (2.5)-(2.6) and let Assumption 3.3.1 hold. Moreover, assume that the intersampling time $\tau(x_0) \in (0,+\infty)$, for all $x_0 \in \mathbb{R}^n \setminus \{0\}$. Then:*

1. *For any time $\tau_\star > 0$, there exists an isochronous manifold $M_{\tau_\star}$.*
2. *Each homogeneous ray intersects an isochronous manifold $M_{\tau_\star}$ only at one point:*

$$\forall \tau_\star > 0 \text{ and } \forall x \in \mathbb{R}^n \setminus \{0\} : \ \exists! \lambda_x > 0 \text{ such that } \lambda_x x \in M_{\tau_\star} \tag{3.3}$$

3. *Given two isochronous manifolds M_{τ_1}, M_{τ_2} with $\tau_1 < \tau_2$, on every homogeneous ray M_{τ_1} is further away from the origin compared to M_{τ_2}, i.e. for all $x \in M_{\tau_1}$:*

$$\exists! \lambda_x \in (0,1) \text{ s.t. } \lambda_x x \in M_{\tau_2} \text{ and } \nexists \kappa_x \geq 1 \text{ s.t. } \kappa_x x \in M_{\tau_2}. \tag{3.4}$$

Proof. Proofs for the above statements appear in [24] and [49]. We include them here, to highlight the importance of the time scaling property (2.10).

- *Proof of properties 1 and 2:* Under Assumption 3.3.1 and the assumption that $\tau(x_0) \in (0,+\infty)$, for all $x_0 \in \mathbb{R}^n \setminus \{0\}$, and according to (2.9) and (2.10), on any homogeneous ray, intersampling times continuously vary from 0 to $+\infty$ as λ_x varies from $+\infty$ to 0. Thus, for any $\tau_\star \in \mathbb{R}^+$ there exists a point x on each ray such that $\tau(x) = \tau_\star$. Hence, for any $\tau_\star \in \mathbb{R}^+$ there exists an IM $M_{\tau_\star}$, which is intersected by any homogeneous ray at least once. What is more, equation (2.9) implies that there do not exist two different points on the same homogeneous ray that correspond to the same intersampling time, hence the IM is intersected only once by the same homogeneous ray.

- *Proof of property 3:* Since each homogeneous ray intersects any IM only at one point, $\exists! \lambda_x > 0$ such that $\lambda_x x \in M_{\tau_2}$, where $x \in M_{\tau_1}$. From the scaling law (2.9) we get:

$$\tau_2 = \tau(\lambda_x x) = \lambda_x^{-\alpha} \tau_1 \implies \lambda_x = \sqrt[\alpha]{(\tfrac{\tau_1}{\tau_2})} < 1,$$

since $\tau_1 < \tau_2$. There can be no other intersection of the homogeneous ray with M_{τ_2}, i.e. $\nexists \kappa_x \geq 1$ s.t. $\kappa_x x \in M_{\tau_2}$.

□

For an illustration of property 3.3, see Fig. 3.2, and for property 3.4, see Fig. 3.3. For the above properties to hold, we have assumed that the intersampling time is finite for all points x_0, except for the origin, which guarantees that $\tau(x)$ varies from 0 to $+\infty$ on every homogeneous ray. Examples of cases where this assumption does not hold are cases of multiple equilibria or cases where the triggering function is designed to not trigger, when the state lies on a stable manifold. In such cases, properties (3.3) and (3.4) do not hold on rays where intersampling times are infinite. Nonetheless, as discussed right after Theorem 3.5.1, the proposed STC scheme does not require such an assumption.

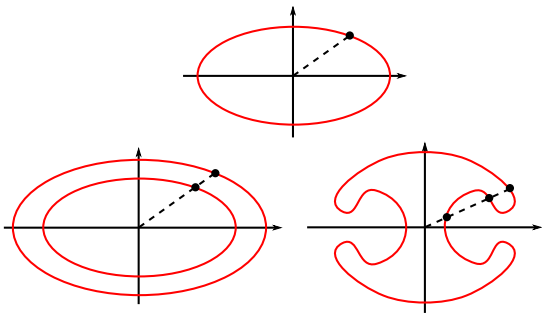

Figure 3.2: The curve on the top is intersected only once by each homogeneous ray, thus it could be an IM of a homogeneous system. The two bottom curves are intersected by some homogeneous rays more than once, thus they cannot be IMs of a homogeneous system.

3.4.2. STATE-SPACE PARTITION AND A SELF-TRIGGERED STRATEGY

For the following, we assume that the system operates in an arbitrarily large compact set $\mathscr{B}$ the whole time. Assume that IMs M_{τ_i} for $\tau_1 < \tau_2 < \tau_3$ are given, as illustrated in Fig. 3.3. We define the regions between manifolds as:

$$R_i = \{x \in \mathbb{R}^n : \exists \kappa_x \geq 1 \text{ s.t. } \kappa_x x \in M_{\tau_i} \wedge \exists \lambda_x \in (0,1) \text{ s.t. } \lambda_x x \in M_{\tau_{i+1}}\} \tag{3.5}$$

for $\tau_i < \tau_{i+1}$, and the region enclosed by the manifold M_{τ_3} as $R_3 = \{x \in \mathbb{R}^n : \exists \kappa_x \geq 1 \text{ s.t. } k_x x \in M_{\tau_3}\}$. Since (3.4) holds, a region R_i is the set with its outer boundary being M_{τ_i} and its inner boundary being $M_{\tau_{i+1}}$. The scaling law (2.9) implies that: $\tau(x) \geq \tau_i$ for all $x \in R_i$. Thus, IMs could be employed for discretizing the state space in regions R_i such that (3.1) is satisfied.

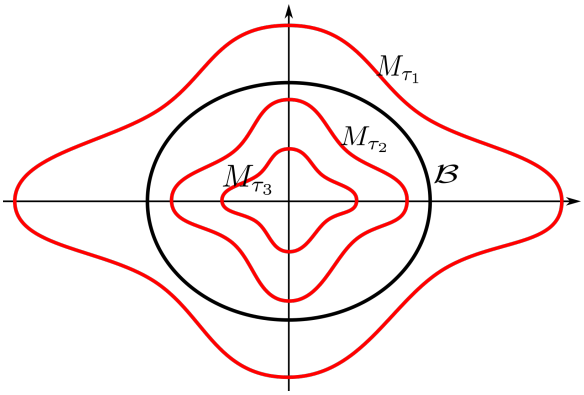

Figure 3.3: IMs M_{τ_1}, M_{τ_2}, M_{τ_3} (red lines) for $\tau_1 < \tau_2 < \tau_3$, and the operating region $\mathscr{B}$ (black line).

3.4.3. INNER-APPROXIMATIONS OF ISOCHRONOUS MANIFOLDS AND PARTITION

Deriving the actual IMs is generally not possible, as nonlinear systems most often do not admit a closed-form analytic solution. Thus, in order to partition the state space and generate a region-based STC scheme, we propose a method to construct inner-approximations of IMs, as shown in Fig. 3.4.

Definition 3.4.3 (Inner-Approximations of Isochronous Manifolds)**.** *Consider an ETC system* (2.5)-(2.6) *and let Assumption 3.3.1 hold. A set* $\underline{M}_{\tau_i}$ *is called inner approximation of an IM* M_{τ_i} *if and only if for all* $x \in \underline{M}_{\tau_i}$*:*

$$\exists \kappa_x \geq 1 \text{ s.t. } \kappa_x x \in M_{\tau_i} \text{ and } \nexists \lambda_x \in (0,1) \text{ s.t. } \lambda_x x \in M_{\tau_i}. \tag{3.6}$$

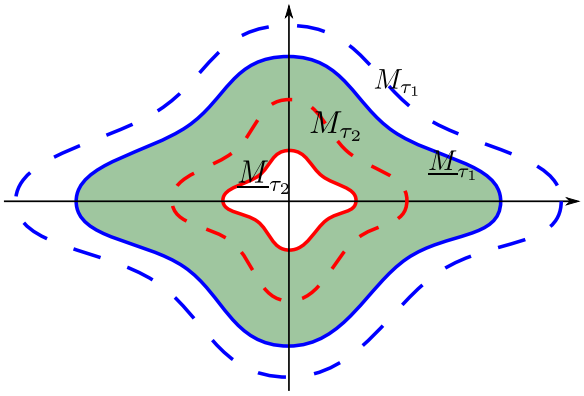

Figure 3.4: IMs M_{τ_i} (dashed lines), and their inner-approximations $\underline{M}_{\tau_i}$ (solid lines). The filled region represents $\mathscr{R}_1$.

In other words, an inner-approximation of an IM is contained inside the region encompassed by the IM. Consider inner-approximations $\underline{M}_{\tau_i}$ of IMs ($\tau_1 < \tau_2 < ...$), that

satisfy the properties listed in Proposition 3.4.1. We consider the regions between sets $\underline{M}_{\tau_i}$:

$$\mathscr{R}_i = \{x \in \mathbb{R}^n : \exists \kappa_x \geq 1 \text{ s.t. } \kappa_x x \in \underline{M}_{\tau_i} \wedge \exists \lambda_x \in (0,1) \text{ s.t. } \lambda_x x \in \underline{M}_{\tau_{i+1}}\}. \tag{3.7}$$

A region $\mathscr{R}_i$ is the set with its outer boundary being $\underline{M}_{\tau_i}$ and its inner boundary being $\underline{M}_{\tau_{i+1}}$ (see Fig. 3.4). For such sets, by (2.9) we get the following result:

Corollary 3.4.1. *Consider an ETC system (2.5)-(2.6) and let Assumption 3.3.1 hold. Consider two inner-approximations $\underline{M}_{\tau_i}$ and $\underline{M}_{\tau_{i+1}}$ of isochronous manifolds, with $\tau_i \leq \tau_{i+1}$. Assume that $\underline{M}_{\tau_i}$ and $\underline{M}_{\tau_{i+1}}$ satisfy the properties listed in Proposition 3.4.1. For the region $\mathscr{R}_i$ defined in (3.7), the following holds:*

$$\forall x \in \mathscr{R}_i : \tau_i \leq \tau(x).$$

Proof. For all $x \in \mathscr{R}_i$, $\exists \kappa_x \geq 1$ s.t. $\kappa_x x \in \underline{M}_{\tau_i}$. Thus, $\exists k_x \geq \kappa_x \geq 1$ s.t. $k_x x \in M_{\tau_i}$. By (2.9), we have $\tau(k_x x) = \tau_i \implies \tau(x) = k_x^{\alpha} \tau_i \geq \tau_i$. □

Thus, given inner-approximations of IMs, that satisfy the properties listed in Proposition 3.4.1, the state space can be partitioned into regions $\mathscr{R}_i$, enabling the region-based STC scheme. Satisfaction of the properties in Proposition 3.4.1 is crucial, as e.g., otherwise, $\mathscr{R}_i$ could potentially intersect with each other and be ill-defined (see Fig. 3.5), or the approximations might not be intersected at all by some homogeneous rays, which would, again, constitute the regions $\mathscr{R}_i$ ill-defined. *Deriving inner-approximations $\underline{M}_{\tau_\star}$ of IMs such that they satisfy the properties in Proposition 3.4.1 constitutes the main theoretical challenge of this chapter.*

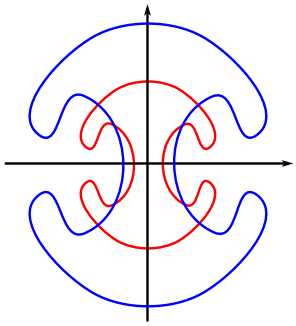

Figure 3.5: If inner-approximations of IMs did not satisfy the properties in Proposition 3.4.1, then the regions $\mathscr{R}_i$ could intersect with each other.

Remark 3.4.2. *As already noted, the number of regions $\mathscr{R}_i$ equals the number q of predefined times τ_i. Given that τ_1 and τ_q are fixed, as the number of times q grows, the areas of regions $\mathscr{R}_i$ become smaller, as the same space is partitioned into more regions. Thus, the STC intersampling times τ_i become more accurate bounds of the actual ETC times $\tau(x)$. However, during the online implementation, the controller in general needs to perform more checks to determine the region of a measured state. Hence, the number q of times τ_i provides a trade-off between computations and conservativeness.*

Remark 3.4.3. *Note that τ_1 has to be selected, such that the operating region $\mathscr{B}$ lies completely inside the region delimited by $\underline{M}_{\tau_1}$ (e.g. see Fig. 3.3). To check this, the approach of [23] or an SMT (Satisfiability Modulo Theory) solver (e.g. [53]) can be used.*

3.5. APPROXIMATIONS OF ISOCHRONOUS MANIFOLDS

Here a refined methodology is presented, which generates inner-approximations of IMs that satisfy the properties in Proposition 3.4.1. First, we show how the method of [24] actually approximates triggering level sets, and then we refine its core idea to derive approximations of IMs.

3.5.1. APPROXIMATIONS OF TRIGGERING LEVEL SETS

The method proposed in [24] is based on bounding the time evolution of the triggering function by another function with linear dynamics: $\psi_1(x,t) \geq \phi(\xi(t;x))$, with $\psi_1(x,0) = \phi(\xi(0;x)) < 0$ for all $x \in \mathbb{R}^n \setminus \{0\}$. The bound is obtained by constructing a linear system according to a bounding lemma [24, Lemma V.2]. Unfortunately, this lemma is invalid and the function that is obtained does not always bound $\phi(\xi(t;x))$. Specifically, a counterexample is given in [55, Example 2, pp.2]. However, later in the document we present a slightly adjusted lemma, that is actually valid. Thus, for this subsection we assume that $\psi_1(x,t)$ is an upper bound of $\phi(\xi(t;x))$.

Since $\psi_1(x,t) \geq \phi(\xi(t;x))$ and $\psi_1(x,0) < 0$, if we define:

$$\tau^{\downarrow}(x) = \inf\{t > 0 : \psi_1(x,t) = 0\},$$

then it is guaranteed that $\phi(\xi(x;t)) \leq 0, \quad \forall t \in [0, \tau^{\downarrow}(x)]$. Hence, the first zero-crossing of $\psi_1(x,t)$ for a given x happens before the first zero-crossing of $\phi(\xi(t;x))$, i.e. the intersampling time of x is lower bounded by $\tau^{\downarrow}(x)$: $\tau(x) \geq \tau^{\downarrow}(x)$.

In [24], under the misconception that IMs and triggering level sets coincide, it is argued that to approximate an IM, it suffices to approximate the set $L_{\tau_\star} := \{x \in \mathbb{R}^n : \phi(\xi(\tau_\star;x)) = 0\}$, i.e. a triggering level set. Thus, the upper bound $\psi_1(x,t)$ of $\phi(\xi(t;x))$ is used to derive the following approximation: $\underline{L}_{\tau_\star} := \{x \in \mathbb{R}^n : \psi_1(x,\tau_\star) = 0\}$. However, as we have already pointed out for the triggering function, $\psi_1(x,t)$ might also have multiple zero-crossings for a given $x \in \mathbb{R}^n$. Thus, the equation $\psi_1(x,t) = 0$ does not only capture the intersampling times of points x, but possibly also more zero-crossings of $\phi(t;x)$. Thus, we can say that the set $\underline{L}_{\tau_\star}$ is an approximation of the triggering level set $L_{\tau_\star}$, and not of the IM $M_{\tau_\star}$. Furthermore, observe that $\psi_1(x,t)$ does not a priori satisfy the time scaling property (2.10). Consequently, there is no formal guarantee that the sets $\underline{L}_{\tau_\star}$ satisfy Proposition 3.4.1. For example, the sets $\underline{L}_{\tau_\star}$ might be intersected by some homogeneous rays more than once, or they may not be intersected at all.

Remark 3.5.1. *In [24], given a fixed time $\tau_\star$, the equation*

$$\psi_1(\tfrac{x_0}{\lambda}, \tau_\star) = 0 \tag{3.8}$$

is solved w.r.t. λ, in order to determine the STC intersampling time of the measured state x_0 as: $\tau^{\downarrow}(x_0) = \lambda^{-\alpha}\tau_\star$. Note that (3.8) finds intersections $\frac{x_0}{\lambda}$ of $\underline{L}_{\tau_\star}$ with the ray passing through x_0. Hence, the above observations imply that (3.8) may not have any real solution, or may admit some solutions λ such that $\tau^{\downarrow}(x_0) = \lambda^{-\alpha}\tau_\star > \tau(x)$, violating (2.11).

3.5.2. INNER-APPROXIMATIONS OF ISOCHRONOUS MANIFOLDS

Although, the method of [24] generates approximations of triggering level sets, which do not necessarily satisfy Proposition 3.4.1, we employ the idea of upper-bounding the triggering function, and we impose additional properties to the upper bound, such that the obtained sets approximate IMs and satisfy the properties in Proposition 3.4.1. Remark 3.4.1 and the proofs of Proposition 3.4.1 indicate that: 1) IMs coincide with triggering level sets, if $\phi(\cdot)$ has only one zero-crossing w.r.t. t, and 2) $\phi(\cdot)$ satisfying (2.10) and assuming that intersampling times are finite on all points $x_0 \in \mathbb{R}^n \setminus \{0\}$ imply that IMs satisfy Proposition 3.4.1. Intuitively, we could construct a function $\mu(x,t)$ that satisfies the same properties and its zero-crossing happens before the one of $\phi(\cdot)$, and use the level sets $\underline{M}_{\tau_\star} = \{x \in \mathbb{R}^n : \mu(x,\tau_\star) = 0\}$ as inner approximations of IMs that satisfy Proposition 3.4.1. The above are summarized in the following theorem:

Theorem 3.5.1. *Consider an ETC system (2.5)-(2.6) and let Assumption 3.3.1 hold. Let $\mu : \mathbb{R}^n \times \mathbb{R}^+ \to \mathbb{R}$ be a function that satisfies:*

$$\mu(x,0) < 0, \quad \forall x \in \mathbb{R}^n \setminus \{0\}, \tag{3.9a}$$

$$\mu(x,t) \geq \phi(\xi(t;x)), \quad \forall t \in [0,\tau(x)] \text{ and } \forall x \in \mathbb{R}^n \setminus \{0\}, \tag{3.9b}$$

$$\mu(\lambda x,t) = \lambda^{\theta+1}\mu(x,\lambda^\alpha t), \quad \forall t,\lambda > 0 \text{ and } \forall x \in \mathbb{R}^n \setminus \{0\}, \tag{3.9c}$$

$$\forall x \in \mathbb{R}^n \setminus \{0\}: \quad \exists! \tau_x \in (0,+\infty) \text{ such that } \mu(x,\tau_x) = 0. \tag{3.9d}$$

The sets $\underline{M}_{\tau_\star} = \{x \in \mathbb{R}^n : \mu(x,\tau_\star) = 0\}$ are inner-approximations of isochronous manifolds $M_{\tau_\star}$ and satisfy the properties listed in Proposition 3.4.1.

Proof. See Appendix 3.A. □

The sets $\underline{M}_{\tau_\star}$ satisfy Proposition 3.4.1, without assuming that the actual manifolds satisfy it, i.e., without assuming that $\tau(x)$ is finite in $\mathbb{R}^n \setminus \{0\}$. That is because, apart from enforcing the scaling property (3.9c) to μ, we have also enforced (3.9d) on $\mu(x,t)$.

Remark 3.5.2. *It is crucial that inequality (3.9b) extends at least until $\tau(x)$, in order for $\mu(x,t)$ to capture the actual intersampling time, i.e. for the minimum time satisfying $\mu(x,t) = 0$ to lower bound the minimum time satisfying $\phi(\xi(t;x)) = 0$.*

3.5.3. CONSTRUCTING THE UPPER BOUND OF THE TRIGGERING FUNCTION

In this subsection, we construct a valid bounding lemma and we employ it in order to derive an upper bound $\mu(x,t)$ of the triggering function $\phi(\xi(t;x))$, that satisfies (3.9).

Lemma 3.5.1. *Consider a system of differential equations $\dot{\xi}(t) = f(\xi(t))$, where $f : \mathbb{R}^n \to \mathbb{R}^n$, a function $\phi : \mathbb{R}^n \to \mathbb{R}$ and a set $\Omega_d = \{x \in \mathbb{R}^n : |x| < d\}$. For every set of coefficients $\delta_0, \delta_1, ..., \delta_p \geq 0$ satisfying:*

$$\mathscr{L}_f^p \phi(z) \leq \sum_{i=0}^{p-1} \delta_i \mathscr{L}_f^i \phi(z) + \delta_p, \quad \forall z \in \Omega_d, \tag{3.10}$$

the following inequality holds for all $\xi_0 \in \Omega_d$:

$$\phi(\xi(t;\xi_0)) \leq \psi_1(y(\xi_0),t) \quad \forall t \in [0, t_e(\xi_0)),$$

where $t_e(\xi_0)$ is defined as:

$$t_e(\xi_0) = \sup\{\tau > 0 : \xi(t;\xi_0) \in \Omega_d, \quad \forall t \in [0,\tau)\} \tag{3.11}$$

and $\psi_1(y(\xi_0),t)$ is the first component of the solution of the following linear dynamical system:

$$\dot{\psi} = \begin{bmatrix} 0 & 1 & 0 & \dots & 0 & 0 \\ 0 & 0 & 1 & \dots & 0 & 0 \\ \vdots & \vdots & & \ddots & \vdots & \vdots \\ 0 & 0 & 0 & \dots & 1 & 0 \\ \delta_0 & \delta_1 & \delta_2 & \dots & \delta_{p-1} & 1 \\ 0 & 0 & 0 & \dots & 0 & 0 \end{bmatrix} \psi = A\psi, \tag{3.12}$$

with initial condition:

$$y(\xi_0) = \begin{bmatrix} \phi(\xi_0) & \mathscr{L}_f\phi(\xi_0) & \dots & \mathscr{L}_f^{p-1}\phi(\xi_0) & \delta_p \end{bmatrix}^\top.$$

Proof. See Appendix 3.A. □

Remark 3.5.3. *The main difference between Lemma 3.5.1 and the bounding lemma in [24] is that in Lemma 3.5.1 the coefficients δ_i are forced to be non-negative. We also include a proof, employing a higher-order comparison lemma, since the comparison lemma arguments used in the proof of [24] are invalid.*

Let us demonstrate how to employ Lemma 3.5.1, to derive upper bounds of the triggering function. Define the open ball:

$$\Omega_d := \{x \in \mathbb{R}^{2n} : |x| < d\}. \tag{3.13}$$

Consider the following feasibility problem:

Problem 1. *Consider an ETC system (2.5)-(2.6) and let Assumption 3.3.1 hold. Find $\delta_0,\dots,\delta_p \in \mathbb{R}$ such that:*

$$\mathscr{L}_{f_e}^p\phi(z) \le \sum_{i=0}^{p-1} \delta_i \mathscr{L}_{f_e}^i\phi(z) + \delta_p, \quad \forall z \in \Omega_d, \tag{3.14a}$$

$$\delta_0\phi\Big((x,0)\Big) + \delta_p \ge \epsilon > 0, \quad \forall x \in \mathrm{Z}, \tag{3.14b}$$

$$\delta_i \ge 0, \quad i = 0,1,\dots,p, \tag{3.14c}$$

where ϵ is an arbitrary predefined positive constant, d is such that $\Xi \subset \Omega_d$, and Z, Ξ and Ω_d are given by Assumption 3.3.1 and (3.13) respectively.

The feasible solutions of (3.14) belong in a subset of the feasible solutions of Lemma 3.5.1, i.e. the solutions of (3.14) determine upper bounds of the triggering function. Moreover, such δ_i always exist, since to satisfy (3.14) it suffices to pick $\delta_p \ge \max\{\epsilon, \sup_{z\in\Omega_d} \mathscr{L}_{f_e}^p\phi(z)\}$ and $\delta_i = 0$ for $i = 0,\dots,p-1$. The following theorem shows how to employ solutions of Problem 1, in order to construct upper bounds that satisfy (3.9).

Theorem 3.5.2. *Consider an ETC system (2.5)-(2.6) and let Assumption 3.3.1 hold. Consider coefficients $\delta_0,\dots,\delta_p$ solving Problem 1. Let $r>0$ be such that $D\subset Z$, where $D=\{x\in\mathbb{R}^n:|x|=r\}$. Define the following function for all $x\in\mathbb{R}^n\setminus\{0\}$:*

$$\mu(x,t):=C(\tfrac{|x|}{r})^{\theta+1}e^{A(\frac{|x|}{r})^{\alpha}t}\begin{bmatrix}\phi\Big((r\frac{x}{|x|},0)\Big)\\ \max\Big(\mathscr{L}_{f_e}\phi\Big((r\frac{x}{|x|},0)\Big),0\Big)\\ \vdots\\ \max\Big(\mathscr{L}_{f_e}^{p-1}\phi\Big((r\frac{x}{|x|},0)\Big),0\Big)\\ \delta_p\end{bmatrix} \tag{3.15}$$

where A is as in (3.12), $C=\begin{bmatrix}1 & 0 & \dots & 0\end{bmatrix}$, and α and θ are the degrees of homogeneity of the system and the triggering function, respectively. The function $\mu(x,t)$ satisfies (3.9).

Proof. See Appendix 3.A. □

Thus, according to Theorem 3.5.1, the sets $\underline{M}_{\tau_\star}=\{x\in\mathbb{R}^n:\mu(x,\tau_\star)=0\}$ are inner-approximations of the actual IMs of the system and satisfy Proposition 3.4.1. The fact that $\mu(x,t)$ satisfies (3.9) directly implies that the region $\mathscr{R}_i$ between two approximations $\underline{M}_{\tau_i}$ and $\underline{M}_{\tau_{i+1}}$ $(\tau_i<\tau_{i+1})$ can be defined as:

$$\mathscr{R}_i:=\{x\in\mathbb{R}^n:\mu(x,\tau_i)\le 0\wedge\mu(x,\tau_{i+1})>0\}. \tag{3.16}$$

To determine online to which region does the measured state belong, the controller checks inequalities like the ones in (3.16).

Remark 3.5.4. *The innermost region $\mathscr{R}_q$ cannot be defined as in (3.16), as there is no τ_{q+1}. For $\mathscr{R}_q$, it suffices that we write:*

$$\mathscr{R}_q:=\{x\in\mathbb{R}^n:\ \mu(x,\tau_q)\le 0\}$$

Let us explain the importance of Z, Ξ from Assumption 3.3.1. By solving Problem 1, an upper bound $\psi(\xi_0,t)$ is determined according to Lemma V.2 that bounds $\phi(\xi(t;\xi_0))$ as follows:

$$\psi(\xi_0,t)\ge\phi(\xi(t;\xi_0)),\quad \forall\xi_0\in\Omega_d \text{ and } \forall\, t\in[0,t_e(\xi_0)),$$

where $t_e(\xi_0)$ is the time when the trajectory $\xi(t;\xi_0)$ leaves Ω_d (see (3.11)). What is needed is to bound $\phi(\xi(t;\xi_0))$ at least until the intersampling time $\tau(\xi_0)$ (see Remark 9), i.e. $\tau(\xi_0)<t_e(\xi_0)$. This is exactly what Assumption 3.3.1 offers: trajectories starting from points $\xi_0\in Z\times\{0\}$ stay in $\Xi\subset\Omega_d$ at least until $\tau(\xi_0)$ (see Figure 3.6). In other words, for all points $\xi_0\in Z\times\{0\}$, we have that $\tau(\xi_0)<t_e(\xi_0)$ (since $\Xi\subset\Omega_d$) and therefore:

$$\psi(\xi_0,t)\ge\phi(\xi(t;\xi_0)),\quad \forall\xi_0\in Z\times\{0\} \text{ and } \forall\, t\in[0,\tau(\xi_0)]. \tag{3.17}$$

Regarding the $\{0\}$-part of $Z\times\{0\}$, note that we only consider initial conditions $\xi_0=(x,0)$, as aforementioned. Finally, transforming $\psi(x,t)$ into $\mu(x,t)$ by incorporating properties (3.9c) and (3.9d), equation (3.17) becomes (3.9b). All these statements are formally proven in Appendix 3.A.

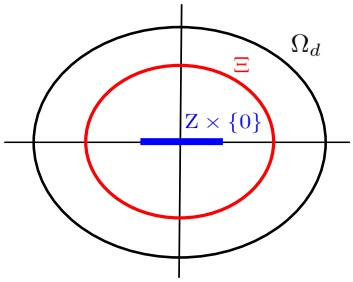

Figure 3.6: The sets $Z \times \{0\} \subset \Xi \subset \Omega_d$.

3.6. AN ALGORITHM THAT COMPUTES THE δ_i-COEFFICIENTS

Although in [24] SOSTOOLS [50] is proposed for deriving the δ_i coefficients that solve Problem 1, our experience indicates that it is numerically non-robust regarding solving this particular problem. We present an alternative approach based on a Counter-Example Guided Iterative Algorithm (see e.g. [52]), which combines Linear Programming and SMT solvers (e.g. dReal [53]), i.e. tools that verify or disprove first-order logic formulas, like (3.14).

Consider the following problem formulation:

Problem. *Find a vector of parameters* Δ *such that:*

$$G(x) \cdot \Delta \leq b(x), \quad \forall x \in \Omega, \tag{3.18}$$

where $\Delta \in \mathbb{R}^p$, $G : \mathbb{R}^n \to \mathbb{R}^{m \times p}$, $b : \mathbb{R}^n \to \mathbb{R}^m$ *and* Ω *is a compact subset of* $\mathbb{R}^n$.

For the initialization of the algorithm, a finite subset $\hat{\Omega}$ consisting of samples x_i from the set Ω is obtained. Notice that the relation: $G(x_i) \cdot \Delta \leq b(x_i), \forall x_i \in \hat{\Omega}$ can be formulated as a linear inequality constraint: $\hat{A} \cdot \Delta \leq \hat{b}$, where $\hat{A} = \begin{bmatrix} G^\top(x_1) & G^\top(x_2) & \dots & G^\top(x_i) & \dots \end{bmatrix}^\top$ and $\hat{b} = \begin{bmatrix} b(x_1) & b(x_2) & \dots & b(x_i) & \dots \end{bmatrix}^\top$, $\forall x_i \in \hat{\Omega}$. Each iteration of the algorithm consists of the following steps:

1. Obtain a candidate solution $\hat{\Delta}$ by solving the following linear program (LP):

$$\text{minimize} \quad \mathbf{c}^\top \Delta, \quad \text{subject to} \quad \hat{\mathbf{A}} \cdot \Delta \leq \hat{\mathbf{b}},$$

   where $\mathbf{c}$ can be freely chosen by the user (we discuss meaningful choices later).

2. Employing an SMT solver, check if the candidate solution $\hat{\Delta}$ satisfies the inequality on the original domain, i.e. if $G(x) \cdot \hat{\Delta} \leq b(x)$, $\forall x \in \Omega$:

   (a) If $\hat{\Delta}$ satisfies (3.18), then the algorithm terminates and returns $\hat{\Delta}$ as the solution.

   (b) If $\hat{\Delta}$ does not satisfy (3.18), the SMT solver returns a point $x_c \in \Omega$ where this inequality is violated, i.e. a counter-example. Add x_c to $\hat{\Omega}$ and update accordingly the matrices $\hat{A}$ and $\hat{b}$. Go to step 1.

Note that in step 2b) a single constraint is added to the LP of the previous step, i.e. $G(x_c)\cdot\Delta \le b(x_c)$, by concatenating $G(x_c)$ and $b(x_c)$ to the $\hat{A}$ and $\hat{b}$ matrices, respectively.

In order to solve Problem 1 in particular, we define $\Delta = \begin{bmatrix}\delta_0 & \delta_1 & \dots & \delta_p\end{bmatrix}^\top$, $b(\cdot) = \begin{bmatrix}-\mathscr{L}_{f_e}^p\phi(z) & -\epsilon & \dots & 0\end{bmatrix}^\top$ and:

$$G(\cdot) = \begin{bmatrix} -\phi(z) & \dots & -\mathscr{L}_{f_e}^{p-1}\phi(z) & -1 \\ -\phi(\xi(0;x_0)) & 0 & \dots & -1 \\ -1 & 0 & \dots & 0 \\ 0 & -1 & \dots & 0 \\ & & \ddots & \\ 0 & 0 & & 0 \\ 0 & 0 & \dots & -1 \end{bmatrix},$$

where $z \in \Omega_d$ and $x_0 \in \mathrm{Z}$, with Ω_d and Z as in (3.13) and Assumption 3.3.1 respectively. Hence, the set $\hat{\Omega}$ consists of points $X_i = (z_i, x_{0_i}) \in \Omega_d \times \mathrm{Z}$, and after solving the corresponding LP, the SMT solver checks if $G(X)\cdot\hat{\Delta} \le b(X)$, $\forall X \in \Omega_d \times \mathrm{Z}$. Finally, intuitively, tighter estimates of $\mathscr{L}_{f_e}^p\phi(z)$ could be obtained by minimizing δ_p, and using the other $\mathscr{L}_{f_e}^i\phi(z)$ terms in the right hand side of (3.10). Hence, $\mathbf{c} = \begin{bmatrix}0 & \dots & 0 & 1\end{bmatrix}$ constitutes a wise choice for the LP. In the following section, numerical examples demonstrate the algorithm's efficiency, alongside the validity of our theoretical results.

Remark 3.6.1. *It is recommended that the parameter d, which determines the size of Ω_d, is chosen relatively small, in order to help the algorithm terminate faster. Moreover, our experiments indicate that just 2 initial samples $x_i \in \hat{\Omega}$ are sufficient for the algorithm to terminate relatively quickly. Intuitively, this is because letting the algorithm determine most of the samples itself (by finding the counter-example points) is more efficient than dictating samples a priori. Finally, p should be chosen large enough so that the obtained bound $\mu(\cdot,\cdot)$ is tight, but also small enough so that the dimensionality of the feasibility problem remains small. According to our experience, a choice of $2 \le p \le 4$ leads to satisfactory results and quick termination of the algorithm, in most cases.*

Remark 3.6.2. *To guarantee that the algorithm terminates in a finite number of iterations, every newly added counter-example inequality can be made stricter by subtracting a positive constant s from the right-hand side: $G(x_c)\cdot\Delta \le b(x_c) - s$. Under certain boundedness and continuity assumptions, this guarantees that, in the next iteration, the solution $\hat{\Delta}$ will satisfy the inequality $G(x)\cdot\Delta \le b(x)$ not only on x_c but for every point in a neighbourhood containing x_c. Thus, with a finite number of iterations, the union of these neighbourhoods will contain the whole compact set Ω and the algorithm will terminate.*

3.7. NONHOMOGENEOUS SYSTEMS AND REGION-BASED STC

As mentioned earlier, in [24] a *homogenization procedure* is proposed that renders homogeneous of degree $\alpha > 0$ any ETC system (2.8), by embedding it into $\mathbb{R}^{2n+1}$ and adding a dummy variable w:

$$\begin{bmatrix}\dot{\xi}\\ \dot{w}\end{bmatrix} = \begin{bmatrix} w^{\alpha+1} f_e(w^{-1}\xi) \\ 0 \end{bmatrix} = \tilde{f}_e(\xi, w) \tag{3.19}$$

An example of the use of the homogenization procedure is demonstrated in Section 3.8. The same can be done for nonhomogeneous triggering functions $\tilde{\phi}(\xi, w) = w^{\theta+1}\phi(w^{-1}\xi)$. Notice that the trajectories of the original ETC system (2.8) with initial condition $(x_0, e_0) \in \mathbb{R}^{2n}$ coincide with the trajectories of the homogenized one (3.19) with initial condition $(x_0, e_0, 1) \in \mathbb{R}^{2n+1}$, projected to the ξ-variables. The same holds for a homogenized triggering function. Thus, the intersampling times $\tau(x_0)$ of system (2.8) with triggering function $\phi(\cdot)$ coincide with the intersampling times $\tau\Big((x_0, 1)\Big)$ of (3.19) with triggering function $\tilde{\phi}(\cdot)$.

Consequently, if the original system (or the triggering function) is nonhomogeneous, then first it is rendered homogeneous via the homogenization procedure (3.19). Afterwards, inner-approximations of isochronous manifolds for the homogenized system (3.19) are derived. Since trajectories of the original system are mapped to trajectories on the $w = 1$-plane of the homogenized one (i.e. the state-space of the original system is mapped to the $w = 1$-plane), to determine the intersampling time τ_i of a state $x_0 \in \mathbb{R}^n$, one has to check to which region $\mathscr{R}_i \subset \mathbb{R}^{n+1}$ the point $(x_0, 1)$ belongs. For an illustration, see Figure 3.7: e.g. given a state $x_0 \in \mathbb{R}^n$, if $(x_0, 1) \in \mathbb{R}^{n+1}$ lies on the cyan segment (i.e. it is contained in $\mathscr{R}_1$), then the STC intersampling time that is assigned to x_0 is $\tau^{\downarrow}(x_0) = \tau_1$. Note that, here, it suffices to inner-approximate the isochronous manifolds of (3.19) only in the subspace $w > 0$, since we only care about determining regions $\mathscr{R}_i$ for points $(x_0, 1) \in \mathbb{R}^{2n}$. Thus, the conditions of Theorem 3.5.1 can be relaxed so that they hold only in the subspace $w > 0$, i.e. for all $(x, w) \in (\mathbb{R}^n \setminus \{0\}) \times \mathbb{R}_{>0}$. A thorough treatment of nonhomogeneous systems takes place in Chapter 4, where any given perturbed system (even if the nominal system is homogeneous) is homogenized. In this chapter, we demonstrate our results' applicability to nonhomogeneous systems in Section 3.8.2, through a numerical example.

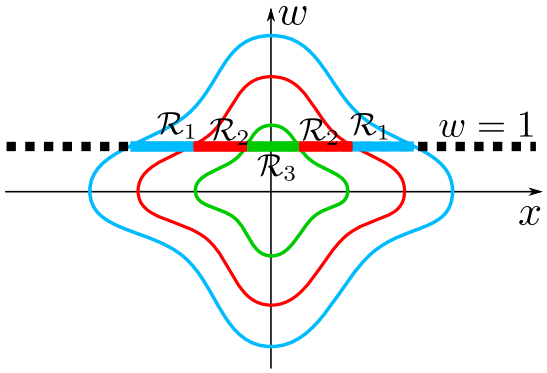

Figure 3.7: Inner-approximations of isochronous manifolds (coloured curves) for a homogenized system (3.19) and the regions $\mathscr{R}_i$ between them. The coloured segments on the $w = 1$-plane represent the subsets of the hyperplane $w = 1$ (i.e. the subsets of the original state space) that are contained in the regions $\mathscr{R}_i$ and are associated to the corresponding intersampling times τ_i.

3.7.1. NONHOMOGENEOUS SYSTEMS AND TABUADA'S TRIGGERING FUNCTION

In the case of nonhomogeneous systems in combination with Tabuada's triggering function [7], a technical detail arises that needs to be discussed. The triggering function of [7] is of the form $\phi(\xi(t)) = |\varepsilon_\zeta(t)|^2 - \sigma|\zeta(t)|^2$ (it is already homogeneous), where $\sigma > 0$. Deriving the function $\mu\Big((x,w),t\Big)$ as in Theorem 3.5.2 for the homogenized system (3.19), for all points $(0,w) \in \mathbb{R}^{n+1} \setminus \{0\}$ on the w-axis:

$$\mu\Big((0,w),t\Big) = C(\tfrac{|w|}{r})^{\theta+1} e^{A(\frac{|w|}{r})^\alpha t} \begin{bmatrix} 0 \\ \max\Big(\mathscr{L}_{f_e}\phi(0),0\Big) \\ \vdots \\ \max\Big(\mathscr{L}_{f_e}^{p-1}\phi(0),0\Big) \\ \delta_p \end{bmatrix}$$

Since $\phi(0) = 0$, then for all these points: $\mu\Big((0,w),t\Big) > 0$ for all $t > 0$. Hence, the w-axis does not belong to any inner-approximation $\underline{M}_{\tau_\star} = \{(x,w) \in \mathbb{R}^{n+1} : \mu\Big((x,w),\tau_\star\Big) = 0\}$ of IMs. In other words, all inner-approximations $\underline{M}_{\tau_\star}$ are punctured by the w-axis and obtain a singularity at the origin, as shown in Fig. 3.8. Consequently, given a finite set

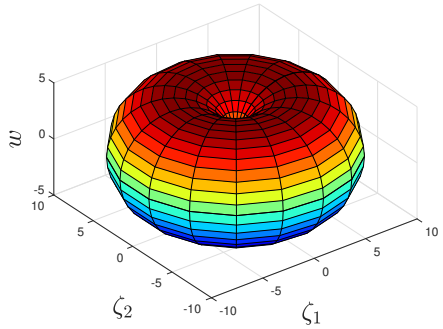

Figure 3.8: Inner-approximation $\underline{M}_{\tau_\star}$ of IMs of a homogenized ETC system with Tabuada's triggering function.

of times $\{\tau_1,\ldots,\tau_q\}$, discretizing the state-space of the extended system into regions $\mathscr{R}_i$ delimited by inner-approximations $\underline{M}_{\tau_i}$, will always result in a neighbourhood around the w-axis not belonging to any region $\mathscr{R}_i$, as depicted in Fig. 3.9. This implies that a neighbourhood around the origin of the original system (2.5), which is mapped to a subset of the hyperplane $w = 1$ around the w-axis in the augmented space $\mathbb{R}^{n+1}$, is not contained to any region $\mathscr{R}_i$. Thus, no STC intersampling time can be assigned to the points of this neighbourhood. Nonetheless, this neighbourhood can be made arbitrarily small, by selecting a sufficiently small time τ_1 for the outermost inner-approximation $\underline{M}_{\tau_1}$. Thus, in order to apply the region-based STC scheme in practice, first we make this neighbourhood arbitrarily small, and then we treat it differently by associating it to an

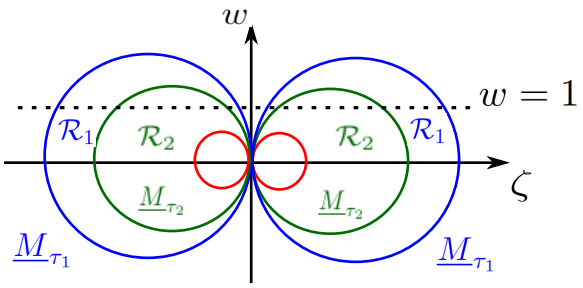

Figure 3.9: Partition of the state space of a homogenized system into regions $\mathscr{R}_i$ delimited by inner-approximations $\underline{M}_{\tau_i}$ (coloured lines) of IMs.

intersampling time that can be designed e.g. according to periodic sampling techniques that guarantee stability (e.g. [56]). Finally, in the numerical example of Section 3.8.2, we completely neglect this region, as it is so small that it is not even reached during the simulation.

Remark 3.7.1. *Note that, as the w-axis acts as a singularity for both the IMs $M_{\tau_\star}$ (the actual intersampling times there are technically 0, and in practice they could be anything) and their inner-approximations $\underline{M}_{\tau_\star}$, the inner-approximations might look very different than the actual manifolds near the w-axis.*

Remark 3.7.2. *These singularities do not arise in cases where $\phi(0) \neq 0$. Such an example is the well-known mixed-triggering function $\phi(\xi(t)) = |\varepsilon_\zeta(t)|^2 - \sigma|\zeta(t)|^2 - \epsilon^2$ (e.g. [18]), where $\sigma > 0$ is appropriately chosen and $\epsilon > 0$. In fact, triggering functions such that $\phi(0) < 0$ are preferred in practice, since when $\phi(0) = 0$ the ETC system exhibits Zeno behaviour around the origin under disturbances. This is briefly discussed right after Assumption 4.3.1 in Chapter 4.*

3.8. NUMERICAL EXAMPLES

In the following numerical examples, SOSTOOLS failed to derive upper bounds, as it mistakenly reasoned that Problem 1 is infeasible. The upper bounds were derived by the algorithm proposed above.

3.8.1. HOMOGENEOUS SYSTEM

In this example, we compare the region-based STC with the STC technique of [23] (which is also computationally light) and with ETC (which constitutes the ideal scenario). Consider the following homogeneous control system:

$$\dot{\zeta}_1 = -\zeta_1^3 + \zeta_1\zeta_2^2, \quad \dot{\zeta}_2 = \zeta_1\zeta_2^2 - \zeta_1^2\zeta_2 + v, \tag{3.20}$$

with $v(\zeta) = -\zeta_2^3 - \zeta_1\zeta_2^2$. A homogeneous triggering function for an asymptotically stable ETC implementation is:

$$\phi(\xi(t;x)) = |\varepsilon_\zeta(t;x)|^2 - 0.0127^2\sigma^2|\zeta(t;x)|^2, \quad \sigma \in (0,1),$$

where $\xi(\cdot)$ denotes the trajectories of the corresponding extended system (2.8), $\varepsilon_\zeta(\cdot)$ is the measurement error (2.4), and x is the previously sampled state. As in [24], we select $\sigma = 0.3$.

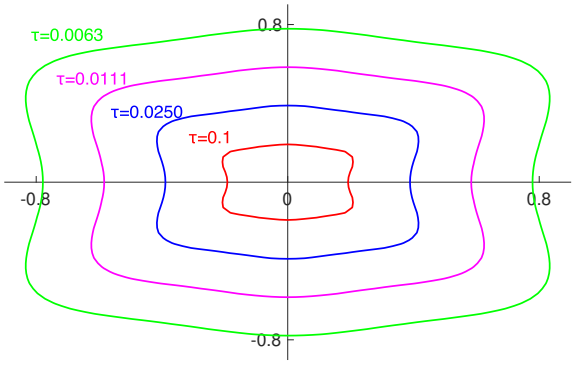

Figure 3.10: Approximations of IMs of the ETC implementation of (3.20).

In order to test the proposed region-based STC scheme, Problem 1 is solved by employing the algorithm presented in the previous section. In particular, we set $p = 3$, $\Omega_d = \{x \in \mathbb{R}^4 : |x| < 0.9\}$ and $\Xi = Z \times E$, where $Z = \{x \in \mathbb{R}^2 : V(x) \leq 0.1\}$, $E = \{x_0 - x \in \mathbb{R}^2 : x, x_0 \in Z\}$ and $V(x) = \frac{1}{2}x_1^2 + \frac{1}{2}x_2^2$ is a Lyapunov function for the system. Observe that $\Xi \subset \Omega_d$. The coefficients found are $\delta_0 = 0$, $\delta_1 = 0.1272$, $\delta_2 = 0$ and $\delta_3 = 0.0191$. In order to construct $\mu(x,t)$ according to (3.15), we fix $r = 0.29$ and the set $D = \{x \in \mathbb{R}^2 : |x| = r\}$ indeed lies in the interior of Z. The state space is partitioned into 348 regions $\mathscr{R}_i$ with corresponding self-triggered intersampling times $\tau_{348} = 0.1s$ and $\tau_i = 1.01^{-2}\tau_{i+1}$. Indicatively, 4 derived approximations of IMs are shown in Fig. 3.10. Observe that the approximations satisfy the properties listed in Proposition 3.4.1.

The system is initiated at $x = [1,1]^\top$ and the simulation lasts for 5s. Fig. 3.11 compares the time evolution of the intersampling times of the region-based STC, the STC proposed in [23] and ETC. In total, ETC triggered 383 times, the region-based STC triggered 554 times, whereas the STC of [23] triggered 2082 times. Given Fig. 3.11 and the number of total updates for each technique we can conclude that: 1) the region-based STC scheme highly outperforms the STC of [23] and 2) the performance of the region-based STC scheme follows closely the ideal performance of ETC, while reducing the computational load in the controller.

3.8.2. NONHOMOGENEOUS SYSTEM

Consider the forced Van der Pol oscillator:

$$\dot{\zeta}_1(t) = \zeta_2(t), \quad \dot{\zeta}_2(t) = (1-\zeta_1^2(t))\zeta_2(t) - \zeta_1(t) + \upsilon(t), \tag{3.21}$$

with $\upsilon(t) = -\zeta_2(t) - (1-\zeta_1^2(t))\zeta_2(t)$. Assuming an ETC implementation, and homogenizing the system with an auxiliary variable w, according to the homogenization procedure

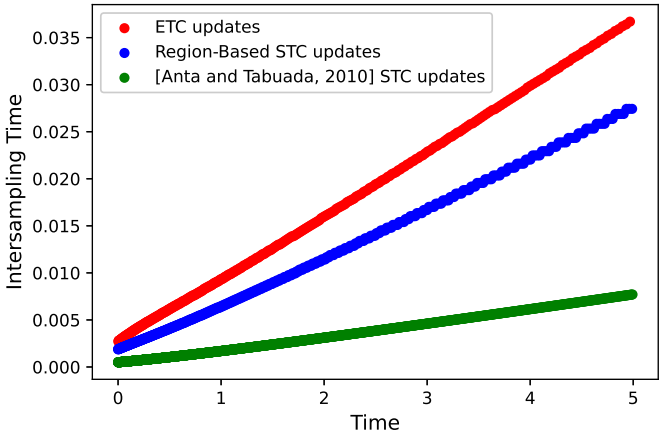

Figure 3.11: The time evolution of region-based STC, STC of [23] and ETC intersampling times along a simulated trajectory of (3.20).

(3.19), the extended system (2.8) becomes:

$$\begin{bmatrix} \dot{\xi} \\ \dot{w} \end{bmatrix} = \begin{bmatrix} \xi_2 w^2 \\ (w^2-\xi_1^2)\xi_2 - \xi_1 w^2 - \epsilon_2 w^2 - (w^2-\epsilon_1^2)\epsilon_2 \\ -\xi_2 w^2 \\ -(w^2-\xi_1^2)\xi_2 + \xi_1 w^2 + \epsilon_2 w^2 + (w^2-\epsilon_1^2)\epsilon_2 \\ 0 \end{bmatrix} \tag{3.22}$$

where $\xi = [\zeta_1, \zeta_2, \varepsilon_{\zeta_1}, \varepsilon_{\zeta_2}]^\top$, $\epsilon_i = \xi_i + \varepsilon_{\zeta_i}$ and ε_ζ is the measurement error (2.4). The homogeneity degree of the extended system is $\alpha = 2$. A triggering function based on the approach of [7] has been obtained in [12]:

$$\phi(\zeta, \varepsilon_\zeta) = W(\varepsilon_\zeta) - V(\zeta),$$

where $W(\varepsilon_\zeta) = 2.222(\varepsilon_{\zeta_1}^2 + \varepsilon_{\zeta_2}^2)$ and $V(\zeta) = 0.0058679\zeta_1^2 + 0.0040791\zeta_1\zeta_2 + 0.0063682\zeta_2^2$ is a Lyapunov function for the original system. Note, that $\phi(\zeta, \varepsilon_\zeta)$ is already homogeneous of degree 1. We fix $\mathrm{Z} = [-0.01, 0.01]^3$ and define the following sets:

$$\begin{aligned} \Phi &= \bigcup_{x_0 \in [-0.01,0.01]^2} \{x \in \mathbb{R}^2 : W(x_0 - x) - V(x) \le 0\}, \\ \mathrm{E} &= \{x_0 - x \in \mathbb{R}^2 : \ x_0 \in [-0.01, 0.01]^2, \ x \in \Phi\}, \\ \Xi &= \Phi \times [-0.01, 0.01] \times \mathrm{E} \times \{0\}. \end{aligned}$$

Notice that Φ is exactly such that for all $x_0 \in [-0.01, 0.01]^2$: $\phi(\xi(t; x_0, w_0)) \le 0 \implies \zeta(t; x_0) \in \Phi$. Then, from the definition of E and the observation that w remains constant at all time, it is easily verified that Z and Ξ are compact, contain the origin and satisfy the requirement of Assumption 3.3.1.

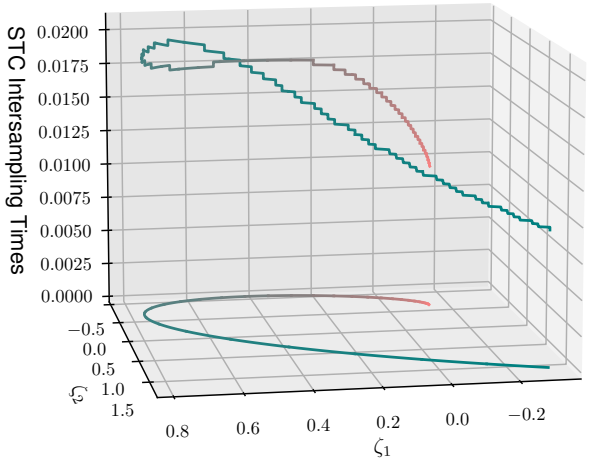

Figure 3.12: The evolution of region-based STC intersampling times along the trajectory of the forced Van der Pol oscillator.

Let us compare the region-based STC to the ideal performance of ETC. Solving Problem 1 for $p = 3$, we obtain $\delta_0 \approx 4.3 \cdot 10^{-4}$, $\delta_1 = 0$ and $\delta_2 \approx 2.1 \cdot 10^{-2}$ and $\delta_3 \approx 4 \cdot 10^{-6}$. To obtain $\mu\Big((x,w),t\Big)$ as in (3.15), we fix $r = 0.009$ and $D = \{x \in \mathbb{R}^3 : |x| = r\}$ indeed lies in the interior of Z. The state space is partitioned into 267 regions $\mathscr{R}_i$, with $\tau_{126} = 0.1$s and $\tau_i = 1.01^{-2} \cdot \tau_{i+1}$. The system is initiated at $x = [-0.3, 1.7]^\top$, and the simulation duration is 5s. In total, the ETC implementation triggered 114 times, whereas the region-based STC implementation triggered 320 times. This is a much better result than the one presented in the published version [49], where region-based STC triggered 1448 times. In [49], it was conjectured that the conservatism of region-based STC in this case was due to homogenization and lifting in higher dimensions, but it appears that it was more a matter of finding a better set of parameters δ.

Figures 3.12 and 3.13 demonstrate the evolution of the intersampling times of region-based STC and ETC, respectively, along the trajectory. In particular, the curve on the $\zeta_1 - \zeta_2$ plane is the trajectory of the system, while the 3D curve above is the evolution of intersampling times along the trajectory. The direction of the trajectory is from the blue-coloured points to the red-coloured points. In Fig. 3.12 the intervals for which the intersampling time remains constant correspond to segments of the trajectory in which the state vector lies inside one particular region $\mathscr{R}_i$. First, note that in contrast to the previous example, the intersampling times do not increase as the system approaches the origin, since the system is not homogeneous and the time-scaling property (2.10) does

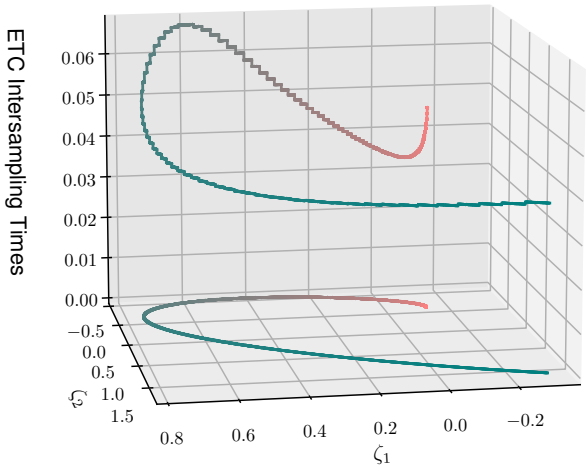

Figure 3.13: The evolution of ETC intersampling times along the trajectory of the forced Van der Pol oscillator.

not apply here. In fact, as stated in [24], the scaling law that applies is :

$$\phi(\xi(t;\lambda x,\lambda w)) = \lambda^{\theta+1}\phi(\xi(\lambda^{\alpha}t;x,w)). \tag{3.23}$$

Moreover, the similarity of the two figures indicates that the intersampling times of the region-based STC approximately follow the trend of the ETC intersampling times. This indicates that the approximations of IMs determined by $\mu\Big((x,w),t\Big)$ preserve the spatial characteristics of the actual IMs of (3.21). Intuitively, the preservation of the spatial characteristics could be attributed to the fact that $\mu\Big((x,w),t\Big)$ also satisfies (3.23), which determines the scaling of the IMs of the homogenized system (3.22) along its homogeneous rays. Besides, note that the IMs of the original system (3.21) are the intersections of the IMs of (3.22) with the $w = 1$-plane.

Remark 3.8.1. *This simulation demonstrates that the results presented in this work are transferable to nonhomogeneous systems, as well.*

3.9. CONCLUSION

We have developed a region-based STC policy that is able to provide different performance guarantees, by introducing a generic framework to emulate a wide range of ETC triggering functions. Moreover, it enables a trade-off between online computations and updates. The scheme employs a state-space partition dictated by inner-approximations

of isochronous manifolds of nonlinear ETC systems. To derive such approximations, theoretical issues of [24] have been addressed and a computational algorithm has been proposed. Finally, simulation results have demonstrated the effectiveness of region-based STC. In the next chapter, the scheme is extended to systems with bounded disturbances or uncertainties.

3.A. TECHNICAL PROOFS AND ASSOCIATED PRELIMINARIES

To conduct the proofs of the previously presented lemmata and theorems, we first introduce some preliminary concepts.

3.A.1. HIGHER ORDER DIFFERENTIAL INEQUALITIES

Definition 3.A.1 (Type W^* functions [51]). *The function $g:\mathbb{R}^n\to\mathbb{R}$ is said to be of type W^* on a set $S\subseteq\mathbb{R}^n$ if $g(x)\le g(y)$ for all $x,y\in S$ such that $x_n=y_n$, $x_i\le y_i$ $(i=1,2,...,n-1)$, where x_i, y_i denote the i-th component of the x and y vector respectively.*

Definition 3.A.2 (Right maximal solution [51]). *Consider the p-th order differential equation:*

$$u^{(p)}(t)=g(t,u(t),\dot{u}(t),\dots,u^{(p-1)}(t)), \tag{3.24}$$

where $u:\mathbb{R}^+\to\mathbb{R}$ and $g(\cdot)$ is continuous on $[0,T]\times\mathbb{R}^p$. A solution $u_m(t;t_0,U_m)$, where t_0 is the initial time instant and $U_m\in\mathbb{R}^p$ is the vector of initial conditions, is called a right maximal solution of (3.24) on an interval $[t_0,\alpha)\subset[0,T]$ if

$$u^{(i)}(t;t_0,U_0)\le u_m^{(i)}(t;t_0,U_m),\quad t\in[t_0,\alpha)\cap[t_0,\alpha^*),$$

for any other solution $u(t;t_0,U_0)$ with initial condition $U_0\le U_m$ defined on $[t_0,\alpha^*)$, for all $i=0,1,2,\dots,m-1$.

Lemma 3.A.1 (Higher Order Comparison Lemma [51]). *Consider a system of first order differential equations:*

$$\dot{\zeta}(t)=f(t,\zeta(t)). \tag{3.25}$$

Let $v:D_r\to\mathbb{R}$ and let $v\in\mathscr{C}^p$, $f\in\mathscr{C}^{p-1}$ on D_r, where $D_r=\{(t,x)|0\le t\le T<+\infty,|x|<r\}$. Let $g(\cdot)$ of (3.24) be of type W^* on $S\subseteq\mathbb{R}^{p+1}$ for each t, where

$$S=\left\{\left(t,v(t,\zeta(t)),\dot{v}(t,\zeta(t)),\dots,v^{(p-1)}(t,\zeta(t))\right):(t,\zeta(t))\in D_r\right\}$$

and

$$v^{(i)}(t,\zeta(t))=\frac{\partial v^{(i-1)}(t,\zeta(t))}{\partial t}+\frac{\partial v^{(i-1)}(t,\zeta(t))}{\partial\zeta(t)}\cdot f(t,\zeta(t)).$$

Assume that:

$$v^{(p)}(t,\zeta(t))\le g(t,v(t,\zeta(t)),\dot{v}(t,\zeta(t)),\dots,v^{(p-1)}(t,\zeta(t))),$$

for all $(t,\zeta(t))\in D_r$. Let J denote the maximal interval of existence of the right maximal solution $u_m(t;0,U_m)$ of (3.24). If $v^{(i)}(0,\zeta_0)=u_m^{(i)}(0;0,U_m)$ $(i=0,1,2,\dots,p-1)$, where $u_m^{(i)}(0;0,U_m)$ are the components of the initial condition U_m of $u_m(t;0,U_m)$, then:

$$v^{(i)}(t,\zeta(t;0,\zeta_0))\le u_m^{(i)}(t;0,U_m),\quad t\in J\cap[0,T],$$

for all $i=0,1,2,\dots,p-1$.

3.A.2. MONOTONE SYSTEMS

Definition 3.A.3 (Monotone System[57]). *Consider a system:*

$$\dot{\zeta}(t) = f(\zeta(t)). \tag{3.26}$$

The system (3.26) *is called monotone if:*

$$\zeta_0 \preceq \zeta_1 \implies \zeta(t; t_0, \zeta_0) \preceq \zeta(t; t_0, \zeta_1).$$

Proposition 3.A.1 ([57]). *Consider the system* (3.26). *If the off-diagonal entries of the Jacobian* $\frac{\partial f}{\partial \zeta}$ *are non-negative, then the system* (3.26) *is monotone.*

3.A.3. TECHNICAL PROOFS

Proof of Theorem 3.5.1. Define $\tau^{\downarrow}(x) = \inf\{t > 0 : \mu(x,t) = 0\}$. (3.9d) implies that $\mu(x, \tau^{\downarrow}(x)) = 0$ is the only zero-crossing of $\mu(x,t)$ w.r.t. t for any given x. Hence:

$$\underline{M}_{\tau_\star} = \{x \in \mathbb{R}^n : \mu(x, \tau_\star) = 0\} = \{x \in \mathbb{R}^n : \tau^{\downarrow}(x) = \tau_\star\},$$

By employing equations (3.9c) and (3.9d) and invoking similar arguments to the ones of the proof of Proposition 3.4.1, we have that $\underline{M}_{\tau_\star}$ satisfies the properties in Proposition 3.4.1.

It is left to prove that $\underline{M}_{\tau_\star}$ is an inner approximation of $M_{\tau_\star}$. Notice that $\phi(\xi(\tau(x); x)) = 0$ together with (3.9b) and (3.9a), imply that the first zero-crossing of $\mu(x,t)$ happens before the one of the triggering function:

$$\tau^{\downarrow}(x) \leq \tau(x). \tag{3.27}$$

Furthermore, (3.9c) implies that $\tau_{\downarrow}(x)$ also satisfies the scaling law (2.9) (the proof for this argument is the exact same to the one derived in [23] for the scaling laws of intersampling times.) The fact that both $\tau_{\downarrow}(x)$ and $\tau(x)$ satisfy (2.9), i.e. they are strictly decreasing functions along homogeneous rays, alongside (3.27) implies that: $\tau(x_1) = \tau^{\downarrow}(x_2) = \tau_\star \implies |x_1| \geq |x_2|$, for all x_1, x_2 on a homogeneous ray. Thus, since $\underline{M}_{\tau_\star}$ satisfies (3.3), we get that for all $x \in \underline{M}_{\tau_\star}$:

$$\exists! \kappa_x \geq 1 \text{ s.t. } \kappa_x x \in M_{\tau_i} \text{ and } \nexists \lambda_x \in (0,1) \text{ s.t. } \lambda_x x \in M_{\tau_i}.$$

The proof is now complete. □

Proof of Lemma 3.5.1. Introduce the following linear system:

$$\dot{\chi} = \begin{bmatrix} 0 & 1 & 0 & \dots & 0 & 0 \\ 0 & 0 & 1 & \dots & 0 & 0 \\ \vdots & \vdots & & \ddots & \vdots & \vdots \\ 0 & 0 & 0 & \dots & 1 & 0 \\ 0 & 0 & 0 & \dots & 0 & 1 \\ \delta_0 & \delta_1 & \delta_2 & \dots & \delta_{p-2} & \delta_{p-1} \end{bmatrix} \chi + \begin{bmatrix} 0 \\ \vdots \\ 0 \\ \delta_p \end{bmatrix}. \tag{3.28}$$

Notice that (3.28) represents the p-th order differential equation $\chi^{(p)} = \sum_{i=0}^{p-1} \delta_i \chi^{(i)} + \delta_p$. The proof makes use of Lemma 3.A.1. Using the notation of Lemma 3.A.1, we identify:

$$\begin{aligned} v(t,\xi(t)) &\equiv \phi(\xi(t)), \quad \forall \xi(t) \in \Omega_d, \\ f(t,\xi(t)) &\equiv f(\xi(t)), \quad \forall \xi(t) \in \Omega_d, \\ g(t,v,v',...,v^{(p-1)}) &\equiv \sum_{i=0}^{p-1} \delta_i v^{(i)} + \delta_p. \end{aligned}$$

For $t > t_e(\xi_0)$, $\xi(t;\xi_0)$ may not belong to Ω_d. Thus, $v(\cdot)$ is well-defined only in the interval $[0, t_e(\xi_0))$. Since $\delta_i \geq 0$ for all i, g is of type W^* in $\mathbb{R}^+ \times \mathbb{R}^p$. Moreover, it is clear that $v \in C^p$ and $f \in C^{p-1}$ on $[0, t_e(\xi_0)) \times \Omega_d$. Inequality (3.10) translates to $v^{(p)}(t,z) \leq g(t,v,v',...,v^{(p-1)})$ for $(t,z) \in [0, t_e(\xi_0)) \times \Omega_d$.

Furthermore, according to Proposition 3.A.1, the linear system (3.28) is monotone, since all off-diagonal entries of its jacobian are non-negative ($\delta_i \geq 0$ for all i). This implies that any solution of (3.28) is a right maximal solution, and its maximal interval of existence is $J = [0, +\infty)$. Consider the solution $\chi(t; X(\xi_0))$, where

$$X(\xi_0) = \begin{bmatrix} \phi(\xi_0) & \mathscr{L}_f \phi(\xi_0) & \dots & \mathscr{L}_f^{p-1} \phi(\xi_0) \end{bmatrix}^\top$$

Observe that the components of the initial condition $X(\xi_0)$ and $\mathscr{L}_f^i \phi(z)$ ($i = 0, 1, 2, \dots, p-1$) are equal. All conditions of Lemma (3.A.1) are satisfied. Thus, we can conclude that for all $\xi_0 \in \Omega_d$:

$$\phi(\xi(t;\xi_0)) \leq \chi_1(t; X(\xi_0)), \quad \forall t \in [0, t_e(\xi_0)).$$

Notice that $\psi_1(y(\xi_0), t) = \chi_1(t; X(\xi_0))$ for all t. Hence $\phi(\xi(t;\xi_0)) \leq \psi_1(y(\xi_0), t), \quad \forall t \in [0, t_e(\xi_0))$. □

To prove Theorem 3.5.2, we first derive the following results.

Proposition 3.A.2. *Consider coefficients δ_i ($i = 0, 1, ..., p$) solving Problem 1, and define an upper-bound $\psi_1(x,t)$ of the triggering function $\phi(\xi(t;x))$ as dictated in Lemma 3.5.1. Let:*

$$\eta_1(x,t) := C e^{At} \eta(x,0), \tag{3.29}$$

where A is as in (3.12), $C = \begin{bmatrix} 1 & 0 & \dots & 0 \end{bmatrix}$ and:

$$\eta(x,0) := \begin{bmatrix} \phi\Big((x,0)\Big) \\ \max\Big(\mathscr{L}_f \phi\Big((x,0)\Big), 0\Big) \\ \vdots \\ \max\Big(\mathscr{L}_f^{p-1} \phi\Big((x,0)\Big), 0\Big) \\ \delta_p \end{bmatrix}. \tag{3.30}$$

The function $\eta_1(x,t)$ satisfies:

$$\eta_1(x,t) \geq \phi(\xi(t;x)), \quad \forall t \in [0, \tau(x)] \text{ and } \forall x \in \mathrm{Z}. \tag{3.31}$$

Proof. Notice that η_1 is the first component of the solution $\eta(x,t)$ to the same linear dynamical system (3.12) as ψ, with initial condition: $\psi(x,0) \preceq \eta(x,0)$. Since the system (3.12) is monotone, according to Proposition 3.A.1, the following holds:

$$\eta_1(x,t) \geq \psi_1(x,t) \geq \phi(\xi(t;x)), \quad \forall t \in [0, t_e(\xi_0)) \text{ and } \forall x \in Z,$$

since $x \in Z \implies \xi_0 = (x,0) \in \Xi \subset \Omega_d$. By the definition of Ξ in Assumption 3.3.1, $\xi(t;x) \in \Xi$ for all $t \in [0, \tau(x)]$. But $t_e(\xi_0)$ is defined in (3.11) as the escape time of $\xi(t;x)$ from Ω_d, and $\Xi \subset \Omega_d$; i.e. $\tau(x) < t_e(\xi_0)$. Thus (3.31) is satisfied. □

3

Proposition 3.A.3. *For all $x \in \mathbb{R}^n \setminus \{0\}$, $\exists! \tau_x \in (0, +\infty)$ such that $\eta_1(x, \tau_x) = 0$.*

Proof. In the following $\eta_1^{(i)}(x,t)$ denotes the i-th derivative of $\eta_1(x,t)$ w.r.t. t. At $t = 0$, initial condition (3.30) implies that $\eta_1^{(i)}(x,0) \geq 0$ for all $i = 1, \ldots, p-1$. For $\eta_1^{(p)}(x,0)$:

$$\eta_1^{(p)}(x,0) = \sum_{i=0}^{p-1} \delta_i \eta_{i+1}(x,0) + \delta_p \geq \delta_0 \phi\Big((x,0)\Big) + \delta_p > 0,$$

since $\eta_{i+1}(x,0) \geq 0$ for all $i = 0, \ldots, p-1$, and (3.14b) and (3.14c) hold. Differentiating $\eta_1^{(p)}$ w.r.t. t, we get:

$$\eta_1^{(p+1)}(x,0) = \sum_{i=0}^{p-1} \delta_i \eta_1^{(i+1)}(x,0) \geq 0.$$

Similarly, $\eta_1^{(i)}(x,0) \geq 0$, for all i. Hence $\eta_1^{(i)}(x,0) \geq 0$ for all $i \in \mathbb{N} \setminus \{0\}$, and in particular $\eta_1^{(p)}(x,0) > 0$. This implies that $\eta_1^{(1)}(x,0) \geq 0$ and that $\eta_1^{(1)}(x,\cdot)$ is strictly increasing in $(0, +\infty)$. Moreover, $\eta_1(x,\cdot)$ is strictly increasing, as well.

Uniqueness of τ_x is proven by the fact that $\eta_1(x,\cdot)$ is strictly increasing. We will now prove existence of τ_x, similarly to what is done in [58]. If $\eta_1(x,1) \geq 0$, then $\tau_x \in (0,1]$, from the intermediate value theorem. Otherwise, then, from strict monotonicity of $\eta_1^{(1)}(x,\cdot)$, we have that $\eta_1^{(1)}(x,1) \geq \epsilon$, for some $\epsilon > 0$. Then, from the mean value theorem, we have that $\eta_1(x, 1 + \frac{k}{\epsilon}) \geq \eta_1(x,1) + k$, for any $k \geq 0$. By picking k, such that $\eta_1(x,1) + k = 0$, we have that $\eta_1(x, 1 + \frac{k}{\epsilon}) \geq 0$, and so, $\tau_x \in (1, 1 + \frac{k}{\epsilon}]$. □

We are ready to prove Theorem 3.5.2.

Proof of Theorem 3.5.2. First, notice that $\mu(x,t)$ satisfies (3.9a) and (3.9c), by construction. Notice that for $x \in D$: $\mu(x,t) = \eta(x,t)$. Thus, according to Proposition 3.A.2 :

$$\mu(x,t) = \eta_1(x,t) \geq \phi(\xi(t;x)), \quad \forall t \in [0, \tau(x)] \text{ and } \forall x \in D. \tag{3.32}$$

Consider now any $x_0 \in \mathbb{R}^n \setminus \{0\}$ and a $\lambda > 0$ such that $x_D = \lambda x_0 \in D$. Employing (3.9c), (2.10) and (3.32) we get:

$$\mu(x_D, t) \geq \phi(\xi(t; x_D)), \ \forall t \in [0, \tau(x_D)] \iff \mu(x_0, \lambda^\alpha t) \geq \phi(\xi(\lambda^\alpha t; x_0)), \ \forall t \in [0, \tau(x_D)] \iff$$
$$\mu(x_0, t) \geq \phi(\xi(t; x_0)), \quad \forall x_0 \in \mathbb{R}^n \setminus \{0\} \text{ and } t \in [0, \tau(x_0)],$$

since $\lambda^\alpha \tau(x_D) = \tau(x_0)$. Thus, $\mu(x,t)$ satisfies (3.9b).

It remains to be shown that $\mu(x,t)$ satisfies (3.9d). Since $\mu(x,t) = \eta(x,t)$ for $x \in D$, then, according to Proposition 3.A.3, $\mu(x,t)$ satisfies (3.9d) for all $x \in D$. Finally, incorporating (3.9c), we get that $\mu(x,t)$ satisfies (3.9d) everywhere in $\mathbb{R}^n \setminus \{0\}$. □

4

Region-Based Self-Triggered Control for Perturbed Uncertain Nonlinear Systems

In this chapter, we extend the region-based STC scheme to systems with bounded disturbances and uncertainties. To deal with disturbances and uncertainties, we employ differential inclusions (DIs). Specifically, we extend certain notions and results on ETC/STC to perturbed uncertain systems, through the DI-framework. Given these results, and adapting the methodology developed earlier, we derive inner-approximations of IMs of perturbed uncertain ETC systems, thus enabling region-based STC. A numerical example is provided, that showcases our theoretical results and compares region-based STC to a state-of-the-art STC method, indicating competitive performance of region-based STC.

This chapter has been published in [59]. Some changes have been made to streamline presentation.

4.1. INTRODUCTION

Here, we extend the region-based STC developed in Chapter 3 to systems with disturbances and uncertainties, which greatly facilitates the applicability of region-based STC in practice. To deal with disturbances and uncertainties in a unified way, we abstract perturbed uncertain systems by differential inclusions (DIs). We introduce ETC notions, such as the intersampling time, to the DI-framework. Within the DI-framework, by employing the notion of homogeneous DIs (see [60]), we extend the scaling law of intersampling times [23] and the homogenization procedure [24] to perturbed uncertain systems. Based on these renewed results, and adapting the tools developed in Chapter 3, we construct approximations of IMs of perturbed uncertain ETC systems, thus extending region-based STC to perturbed uncertain systems. We showcase our theoretical results via simulations and comparisons with other approaches, which indicate that the proposed STC scheme shows competitive performance, while simultaneously achieving greater generality.

4.2. NOTATION AND PRELIMINARIES

4.2.1. NOTATION

Given a set $S \subseteq \mathbb{R}^n$, $\mathrm{cl}(S)$ denotes its closure, $\mathrm{int}(S)$ its interior, $\mathrm{conv}(S)$ its convex hull, and for any $\lambda \in \mathbb{R}$ we denote $\lambda S = \{\lambda x \in \mathbb{R}^n : \ x \in S\}$.

4.2.2. HOMOGENEOUS DIFFERENTIAL INCLUSIONS

Consider the differential inclusion (DI):

$$\dot{\zeta}(t) \in F(\zeta(t)), \tag{4.1}$$

where $\zeta : \mathbb{R} \to \mathbb{R}^n$ and $F : \mathbb{R}^n \to 2^{\mathbb{R}^n}$ is a set-valued map. In contrast to ODEs, which under mild assumptions obtain unique solutions given an initial condition, DIs generally obtain multiple solutions for each initial condition. We denote by $\zeta(t;\zeta_0)$ any solution of (4.1) with initial condition ζ_0. Moreover, $S_F([0,T];\mathscr{I})$ denotes the set of all solutions of (4.1) with initial conditions in $\mathscr{I} \subseteq \mathbb{R}^n$, which are defined on $[0,T]$. Thus, the *reachable set* from $\mathscr{I} \subseteq \mathbb{R}^n$ of (4.1) at time $T \geq 0$ is defined as:

$$\mathscr{X}_T^F(\mathscr{I}) = \{\xi(T;\xi_0) : \ \xi(\cdot;\xi_0) \in S_F([0,T];\mathscr{I})\}.$$

Likewise, the *reachable flowpipe* from $\mathscr{I} \subseteq \mathbb{R}^n$ of (4.1) in the interval $[\tau_1,\tau_2]$ is $\mathscr{X}_{[\tau_1,\tau_2]}^F(\mathscr{I}) = \bigcup_{t\in[\tau_1,\tau_2]} \mathscr{X}_t^F(\mathscr{I})$

Again, we focus on the classical notion of homogeneity. For more information on homogeneous DIs the reader is referred to [60].

Definition 4.2.1 (Homogeneous set-valued maps)**.** *Consider a set-valued map $F : \mathbb{R}^n \to 2^{\mathbb{R}^m}$. We say that F is homogeneous of degree $\alpha \in \mathbb{R}$, if for all $x \in \mathbb{R}^n$ and any $\lambda > 0$: $F(\lambda x) = \lambda^{\alpha+1} F(x)$.*

Correspondingly, a DI (4.1) is called homogeneous of degree $\alpha \in \mathbb{R}$ if the corresponding set-valued map is homogeneous of the same degree. For homogeneous DIs, similarly to homogeneous ODEs, the following scaling property of solutions holds:

Proposition 4.2.1 (Scaling Property [60]). *Let DI (4.1) be homogeneous of degree $\alpha \in \mathbb{R}$. Then, for any $\mathscr{I} \subseteq \mathbb{R}^n$ and any $\lambda > 0$:*

$$\mathscr{X}_t^F(\lambda \mathscr{I}) = \lambda \mathscr{X}_{\lambda^\alpha t}^F(\mathscr{I}). \tag{4.2}$$

4.3. PROBLEM STATEMENT

We aim at extending the region-based STC technique, developed in Chapter 3, to systems with disturbances and uncertainties. Thus, we consider perturbed uncertain ETC systems, written in the compact form:

$$\dot{\xi}(t) = \begin{bmatrix} f\Big(\zeta(t), v(\zeta(t)+\varepsilon_\zeta(t)), d(t)\Big) \\ -f\Big(\zeta(t), v(\zeta(t)+\varepsilon_\zeta(t)), d(t)\Big) \end{bmatrix} = f_e(\xi(t), d(t)), \tag{4.3}$$

where $d : \mathbb{R} \to \mathbb{R}^{m_d}$ is an unknown signal (e.g. disturbance, model uncertainty, etc.), and assume that a triggering function $\phi(\xi(t))$ is given. System 4.3 is the perturbed version of extended ETC system (2.8). Then, the problem statement is similar to the one of Chapter 3:

Problem Statement. *Given an ETC system (4.3), a triggering function $\phi(\cdot)$ and a predefined finite set of times $\{\tau_1 \ldots, \tau_q\}$ (with $\tau_i < \tau_{i+1}$), derive regions $\mathscr{R}_i \subset \mathbb{R}^n$ that satisfy (3.1).*

Assumption 4.3.1. *For the remainder of the chapter we assume the following:*

1. *The nominal (when $d(t) = 0$) continuous-time system (2.3), i.e. $\dot{\zeta}(t) = f\Big(\zeta(t), v(\zeta(t))\Big)$, has the origin as the only equilibrium.*
2. *The function $f_e(\cdot,\cdot)$ is locally bounded and continuous w.r.t. all of its arguments.*
3. *The function $\phi(\cdot)$ is continuously differentiable.*
4. *For all $t \geq 0$: $d(t) \in \Delta$, where $\Delta \subset \mathbb{R}^{m_d}$ is convex, compact and non-empty.*
5. *For all $\xi_0 = (x_0, 0) \in \mathbb{R}^{2n}$: $\phi(\xi_0) < 0$. For any compact set $K \subset \mathbb{R}^n$ there exists $\epsilon_K > 0$ such that for all $x_0 \in K$ and any $d(t) \in \Delta$, $\phi(\xi(t;\xi_0)) < 0$ for all $t \in [0, \epsilon_K)$.*

Item 1 is a rather standard assumption. Items 2 and 4 of Assumption 4.3.1 impose the standard assumptions of differential inclusions on the DIs that we construct later (see (4.4)). These assumptions ensure existence of solutions for all initial conditions (see [60] and [61] for more details). Note that assuming convexity of Δ is not restrictive, since in the case of a non-convex Δ we can consider the closure of its convex hull and write $d(t) \in \mathrm{cl}\Big(\mathrm{conv}(\Delta)\Big)$ for all $t \geq 0$. Finally, item 3 is employed in the proof of Lemma 4.5.1, while item 5 ensures that the emulated ETC does not exhibit Zeno behaviour.

Remark 4.3.1. *The triggering function should be chosen to be robust to disturbances and uncertainties, such that the emulated ETC does not exhibit Zeno behaviour. Examples of such robust triggering functions are the well-known:*

- *Lebesgue sampling (e.g. [5], [62]): $\phi(\xi(t)) = |\varepsilon_\zeta(t)|^2 - \epsilon^2$, where $\epsilon > 0$.*

- *Mixed-Triggering (e.g. [18]):* $\phi(\xi(t)) = |\varepsilon_\zeta(t)|^2 - \sigma|\zeta(t)|^2 - \epsilon^2$, *where* $\sigma > 0$ *is appropriately chosen and* $\epsilon > 0$.

Remark 4.3.2. *In contrast to Chapter 3, here we only assume continuity of* $f_e(\cdot,\cdot)$ *and differentiability of* $\phi(\cdot)$ *(instead of smoothness), since we only make use of the first-order Lie derivative of* $\phi(\cdot)$ *(see Lemma 4.5.1), due to the presence of the unknown (and possibly non-differentiable) signal* $d(t)$. *Moreover, as discussed right after Assumption 3.3.1 in Chapter 3, here we adopt a constructive approach to the sets* Z, Ξ *(which was already demonstrated in Section 3.8.2), and thus we do not assume they are given.*

4.4. PERTURBED UNCERTAIN ETC SYSTEMS AS DIFFERENTIAL INCLUSIONS

In this section, we show how a general perturbed uncertain nonlinear system (4.3), satisfying Assumption 4.3.1, can be abstracted by a homogeneous DI. Moreover, we extend the notion of intersampling times in the context of DIs and show that scaling law (2.9) holds for intersampling times of homogeneous DIs. These results are used afterwards in Section 4.5, to derive inner-approximations of IMs of perturbed uncertain systems (4.3), and thus enable the region-based STC scheme.

4.4.1. ABSTRACTIONS BY DIFFERENTIAL INCLUSIONS

Notice that, since system (4.3) is a time-varying system, many notions that we introduced before for time-invariant systems are now ill-defined. For example, depending on the realization of the unknown signal $d(t)$, a sampled state $x \in \mathbb{R}^n$ can correspond to different intersampling times, i.e. definition (2.7) is ill-posed. However, employing item 4 of Assumption 4.3.1 and the notion of differential inclusions, we can abstract the behaviour of the family of systems (4.3) and remove such dependencies. In particular, system (4.3) can be abstracted by the following differential inclusion:

$$\dot{\xi}(t) \in F(\xi(t)) := \{f_e(\xi(t), d(t)) : \ d(t) \in \Delta\}. \tag{4.4}$$

For DI (4.4) (i.e. for the family of systems (4.3)), the intersampling time $\tau(x)$ of a point $x \in \mathbb{R}^n$ can now be defined as the worst-case possible intersampling time of x, under any possible signal $d(t)$ satisfying Assumption 4.3.1:

Definition 4.4.1 (Intersampling Times of DI)**.** *Consider the family of systems (4.3), the DI (4.4) abstracting them, and a triggering function* $\phi : \mathbb{R}^{2n} \to \mathbb{R}$. *Let Assumption 4.3.1 hold. For any point* $x \in \mathbb{R}^n$, *we define its intersampling time as:*

$$\tau(x) := \inf\left\{t > 0 : \ \sup\left\{\phi\left(\mathscr{X}_t^F((x,0))\right)\right\} \geq 0\right\}, \tag{4.5}$$

Note that we have already emphasized that we consider initial conditions $(x,0) \in \mathbb{R}^{2n}$, since at any sampling time the measurement error $\varepsilon_\zeta = 0$. Finally, now that intersampling times of systems (4.3) abstracted by DIs are well-defined, we can accordingly re-define IMs for families of such systems as: $M_{\tau_\star} = \{x \in \mathbb{R}^n : \tau(x) = \tau_\star\}$, where $\tau(x)$ is defined in (4.5).

4.4.2. HOMOGENIZATION OF DIFFERENTIAL INCLUSIONS AND SCALING OF INTERSAMPLING TIMES

The scaling law of intersampling times (2.9) for homogeneous ETC systems has been employed in developing region-based STC in Chapter 3. Here, we show that a similar result can be derived for intersampling times (4.5) of DIs. First, observe that DI (4.4) can be rendered homogeneous of degree $\alpha > 0$, by slightly adapting the homogenization procedure (3.19) as follows:

$$\begin{bmatrix} \dot{\xi} \\ \dot{w} \end{bmatrix} \in \tilde{F}(\xi, w) := \begin{bmatrix} \{w^{\alpha+1} f_e(w^{-1}\xi, d(t)) : \ d(t) \in \Delta\} \\ \{0\} \end{bmatrix} \tag{4.6}$$

Indeed, $\tilde{F}(\cdot,\cdot)$ is homogeneous of degree α. Recall that the same can be done for a non-homogeneous triggering function, to render it homogeneous of degree $\theta > 0$:

$$\tilde{\phi}(\xi, w) = w^{\theta+1}\phi(w^{-1}\xi). \tag{4.7}$$

Again, trajectories and flowpipes of (4.4) with initial condition $(x_0, e_0) \in \mathbb{R}^{2n}$ coincide with the projection to the ξ-variables of trajectories of (4.6) with initial condition $(x_0, e_0, 1) \in \mathbb{R}^{2n+1}$. This implies that the intersampling time $\tau(x_0)$ for DI (4.4) with triggering function $\phi(\cdot)$, defined as in (4.5), is the same as the intersampling time $\tau\Big((x_0, 1)\Big)$ for DI (4.6) with triggering function $\tilde{\phi}(\cdot)$.

Given the above, by employing the scaling property (4.2) of flowpipes of homogeneous DIs, we can prove that the scaling law (2.9) holds for intersampling times of DIs (4.6):

Theorem 4.4.1. *Consider DI (4.6), the triggering function $\tilde{\phi}(\cdot)$ from (4.7), and let Assumption 4.3.1 hold. The intersampling time $\tau\Big((x, w)\Big)$, where $(x, w) \in \mathbb{R}^{n+1}$, scales for any $\lambda > 0$ as:*

$$\tau\Big(\lambda(x, w)\Big) = \lambda^{-\alpha}\tau\Big((x, w)\Big), \tag{4.8}$$

where $\tau(\cdot)$ is defined in (4.5).

Proof. See Appendix 4.A. □

For an example of how DIs and triggering functions are homogenized, the reader is referred to Section 4.6.

4.5. REGION-BASED STC FOR PERTURBED UNCERTAIN SYSTEMS

In this section, we use the previous derivations about differential inclusions and adapt the method developed in Chapter 3, to inner-approximate IMs of perturbed uncertain systems. Using the derived inner-approximations, the state-space partitioning into regions $\mathscr{R}_i$ is generated. Finally, we show that the applicability of region-based STC for perturbed uncertain systems is semiglobal.

4.5.1. APPROXIMATIONS OF IMS OF PERTURBED UNCERTAIN ETC SYSTEMS

Similarly to Chapter 3, we upper-bound the time evolution of the (homogenized) triggering function $\tilde{\phi}(\xi(t; x), w(t))$ along the trajectories of DI (4.6) with a function $\mu\Big((x, w), t\Big)$ in

analytic form that satisfies (3.9). For this purpose, first we adapt Lemma 3.5.1, to derive upper-bounds with linear dynamics of functions evolving along flowpipes of differential inclusions:

Lemma 4.5.1. *Consider a system of ODEs:*

$$\dot{\xi}(t) = f(\xi(t), d(t)), \tag{4.9}$$

where $\xi(t) \in \mathbb{R}^n$, $d(t) \in \mathbb{R}^{m_d}$, $f : \mathbb{R}^n \times \mathbb{R}^{m_d} \to \mathbb{R}^n$ *and the function* $\phi : \mathbb{R}^n \to \mathbb{R}$. *Let* f, d *and* ϕ *satisfy Assumption 4.3.1. Consider the DI abstracting the family of ODEs (4.9):*

$$\dot{\xi}(t) \in F(\xi(t)) := \{f(\xi(t), d(t)) : \ d(t) \in \Delta\}. \tag{4.10}$$

Consider a compact set $\Xi \subseteq \mathbb{R}^n$. *For coefficients* $\delta_0, \delta_1 \in \mathbb{R}$ *satisfying:*

$$\frac{\partial \phi}{\partial z}(z) f(z,u) \leq \delta_0 \phi(z) + \delta_1, \quad \forall z \in \Xi \text{ and } \forall u \in \Delta, \tag{4.11}$$

the following inequality holds for all $\xi_0 \in \Xi$*:*

$$\sup\left\{\phi\left(\mathscr{X}_t^F(\xi_0)\right)\right\} \leq \psi(y(\xi_0), t) \quad \forall t \in [0, t_e(\xi_0)],$$

where $t_e(\xi_0)$ *is defined as the escape time:*

$$t_e(\xi_0) = \inf\{t > 0 : \mathscr{X}_t^F(\xi_0) \not\subseteq \Xi\}, \tag{4.12}$$

and $\psi(y(\xi_0), t)$ *is:*

$$\psi(y(\xi_0), t) = \begin{bmatrix} 1 & 0 \end{bmatrix} e^{At} y(\xi_0), \tag{4.13}$$

where:

$$A = \begin{bmatrix} \delta_0 & 1 \\ 0 & 0 \end{bmatrix}, \quad y(\xi_0) = \begin{bmatrix} \phi(\xi_0) \\ \delta_1 \end{bmatrix}. \tag{4.14}$$

Proof. See Appendix 4.A. □

Observe that, in contrast to Lemma 3.5.1 where the coefficients δ_i are required to be positive, here $\delta_i \in \mathbb{R}$. This is because here, due to lack of knowledge on the derivative (or even on the differentiability) of the unknown signal $d(t)$, we consider only the first-order time-derivative of ϕ (first-order comparison), in contrast to Chapter 3 where higher-order derivatives of ϕ are considered (higher-order comparison).

Now, we employ Lemma 4.5.1, in order to construct an upper-bound $\mu\Big((x,w),t\Big)$ of the triggering function $\tilde{\phi}(\xi(t;x), w(t))$ that satisfies conditions (3.9) (in the subspace $w > 0$, as mentioned in Section 3.7), which in turn implies that the zero-level sets of $\mu\Big((x,w),t\Big)$ are inner-approximations of IMs of DI (4.6) and satisfy the properties in Proposition 3.4.1. First, consider a compact connected set $\mathrm{Z} \subset \mathbb{R}^n$ with $0 \in \mathrm{int}(\mathrm{Z})$, and the set $\mathrm{W} = [\underline{w}, \overline{w}]$, where $\overline{w} > \underline{w} > 0$. Define the following sets:

$$\begin{aligned} \Phi &:= \bigcup_{x_0 \in \mathrm{Z}} \{x \in \mathbb{R}^n : e = x_0 - x, w \in \mathrm{W}, \tilde{\phi}\Big((x,e,w)\Big) \leq 0\}, \\ \mathrm{E} &:= \{x_0 - x \in \mathbb{R}^n : x_0 \in \mathrm{Z}, \ x \in \Phi\}, \\ \Xi &:= \Phi \times \mathrm{E} \times \mathrm{W}. \end{aligned} \tag{4.15}$$

We assume the following:

Assumption 4.5.1. *The set $\Phi \subset \mathbb{R}^n$ is compact.*

Assumption 4.5.1 is satisfied by most triggering functions $\phi(\cdot)$ in the literature (e.g. Lebesgue sampling [6], and most cases of Mixed Triggering from Remark 4.3.1, the triggering function of [8], etc.). Moreover, since Φ is assumed compact, then E is compact as well, which implies that Ξ is compact. The following theorem shows how the bound $\mu\Big((x,w),t\Big)$ is constructed:

Theorem 4.5.1. *Consider the family of ETC systems (4.3), the DI (4.6) abstracting them, a homogenized triggering function $\tilde{\phi}(\xi(t;x),w(t))$, the sets $\mathrm{Z},\mathrm{W},\Phi,\mathrm{E},\Xi$ defined in (4.15) and let Assumptions 4.3.1 and 4.5.1 hold. Let $\delta_0 \geq 0$ and $\delta_1 > 0$ be such that:*

$$\forall (z,w,u) \in \Xi \times \Delta: \quad \frac{\partial \tilde{\phi}}{\partial z}(z,w)\, w^{\alpha+1} f_e(w^{-1}z,u) \leq \delta_0 \tilde{\phi}(z,w) + \delta_1, \tag{4.16a}$$

$$\forall (z,w) \in \Big(\mathrm{Z} \times \{0\}\Big) \times \mathrm{W}: \quad \delta_0 \tilde{\phi}(z,w) + \delta_1 \geq \varepsilon_\delta > 0, \tag{4.16b}$$

where ε_δ an arbitrary positive constant. Let $r > \underline{w}$ be such that $D_r := \{(x,w) \in \mathbb{R}^{n+1} : |(x,w)| = r,\ w \in \mathrm{W}\} \subset \mathrm{Z} \times \mathrm{W}$. For all $(x,w) \in \mathbb{R}^{n+1} \setminus \{0\}$ define the function:

$$\mu\Big((x,w),t\Big) := \Big(\tfrac{|(x,w)|}{r}\Big)^{\theta+1} \begin{bmatrix} 1 & 0 \end{bmatrix} e^{A\Big(\frac{|(x,w)|}{r}\Big)^{\alpha} t}\, y(x,w), \tag{4.17}$$

where A is as in (4.14) and:

$$y(x,w) = \begin{bmatrix} \tilde{\phi}\Big((r\frac{x}{|(x,w)|}, 0, r\frac{w}{|(x,w)|})\Big) \\ \delta_1 \end{bmatrix}.$$

The function $\mu\Big((x,w),t\Big)$ satisfies (3.9a), (3.9c), (3.9d) for all $(x,w) \in (\mathbb{R}^n \times \mathbb{R}_{>0}) \setminus \{0\}$, but condition (3.9b) is satisfied only in the cone

$$\mathscr{C} = \{(x,w) \in \mathbb{R}^n \times \mathbb{R}_{>0} : |x|^2 + w^2 \leq \frac{w^2}{\underline{w}^2} r^2\} \setminus \{0\} \tag{4.18}$$

and $\forall\, t \in [0, \tau\Big((x,w)\Big)]$.

Proof. See Appendix 4.A. □

Remark 4.5.1. *Observe that, under Assumptions 4.3.1 and 4.5.1, the term $\frac{\partial \tilde{\phi}}{\partial z}(z,w)\, w^{\alpha+1} \cdot \cdot f_e(w^{-1}z,u)$ is bounded for all $(z,w,u) \in \Xi \times \Delta$, since f_e is locally bounded, ϕ is continuously differentiable (implying that $\tilde{\phi}$ is also continuously differentiable for $w \neq 0$), $\tilde{\phi}(z,w)$ is bounded for all $(z,w) \in (\mathrm{Z} \times \{0\}) \times \mathrm{W}$ and $\Xi \times \Delta$ is compact and does not contain any point $(z,0,u)$. Thus, coefficients $\delta_0 \geq 0$ and $\delta_1 > 0$ satisfying (4.16) always exist; e.g. $\delta_0 = 0$ and $\delta_1 > \max\Big\{\epsilon_\delta, \sup_{(z,w,u)\in\Xi\times\Delta} \frac{\partial \tilde{\phi}}{\partial z}(z,w)\, w^{\alpha+1} f_e(w^{-1}z,u)\Big\}$. To compute the coefficients δ_i, we could employ the algorithm described in Section 3.6.*

The intuition behind Theorem 4.5.1 is the same as in Theorem 3.5.2. Equation (3.9b) is satisfied only in the cone $\mathscr{C}$, due to the fact that $0 \notin \text{int}(\mathrm{W})$. Note that W is chosen such that it is guaranteed that (4.16) is well-defined everywhere in $\Xi \times \Delta$. The fact that (3.9b) is satisfied only in the cone $\mathscr{C}$ has the following implication:

Corollary 4.5.1 (to Theorem 3.5.1)**.** *Consider the family of ETC systems* (4.3)*, the DI* (4.6) *abstracting them, a (homogenized) triggering function* $\tilde{\phi}(\xi(t;x), w(t))$ *and let Assumptions 4.3.1 and 4.5.1 hold. Consider the function* $\mu\Big((x,w),t\Big)$ *from* (4.17)*. The sets* $\underline{M}_{\tau_\star} = \{(x,w) \in \mathbb{R}^{n+1} : \mu\Big((x,w),\tau_\star\Big) = 0\}$ *inner-approximate IMs* $M_{\tau_\star}$ *of DI* (4.6) *inside the cone* $\mathscr{C}$*, i.e. for all* $(x,w) \in \underline{M}_{\tau_\star} \cap \mathscr{C}$*:*

- $\exists! \kappa_{(x,w)} \geq 1$ *s.t.* $\kappa_{(x,w)}(x,w) \in M_{\tau_\star}$
- $\nexists \lambda_{(x,w)} \in (0,1)$ *s.t.* $\lambda_{(x,w)}(x,w) \in M_{\tau_\star}$.

Moreover, the sets $\underline{M}_{\tau_\star}$ *satisfy the properties listed in Proposition 3.4.1.*

Proof. It follows identical arguments to the proof of Theorem 3.5.1 in Chapter 3. The only difference is that the arguments are now made for all $(x,w) \in \mathscr{C}$ and not for all $(x,w) \in \mathbb{R}^{n+1}$. □

The implications of the above corollary are depicted in Figure 4.1. Since the zero-level sets $\underline{M}_{\tau_i}$ of $\mu\Big((x,w),t\Big)$ inner-approximate IMs inside $\mathscr{C}$, for the regions $\mathscr{R}_i$ that are delimited by consecutive approximations $\underline{M}_{\tau_i}$ and the cone $\mathscr{C}$ (see Figure 4.1) it holds that: $\tau_i \leq \tau\Big((x,w)\Big)$ for all $(x,w) \in \underline{M}_{\tau_i} \cap \mathscr{C}$. Thus, given the set of times $\{\tau_1, \ldots, \tau_q\}$, the

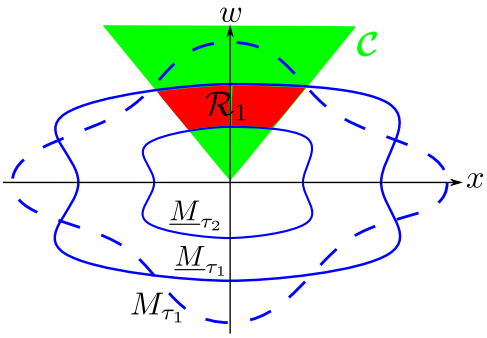

Figure 4.1: IM M_{τ_1} (dashed line) and approximations of IMs $\underline{M}_{\tau_1}, \underline{M}_{\tau_2}$ (solid lines). The set $\underline{M}_{\tau_1}$ inner-approximates M_{τ_1} only inside the cone $\mathscr{C}$. The red region $\mathscr{R}_1$ contained between $\underline{M}_{\tau_1}, \underline{M}_{\tau_2}$ and the cone $\mathscr{C}$ satisfies (3.1).

regions $\mathscr{R}_i$ are defined as the regions between consecutive approximations $\underline{M}_{\tau_i}$ and the cone $\mathscr{C}$:

$$\mathscr{R}_i := \Big\{(x,w) \in \mathscr{C} : \mu\Big((x,w),\tau_i\Big) \leq 0,\ \mu\Big((x,w),\tau_{i+1}\Big) \geq 0\Big\}. \tag{4.19}$$

With regions $\mathscr{R}_i$ defined, region-based STC is enabled.

Remark 4.5.2. *As mentioned in Remark 3.5.4, the innermost region $\mathscr{R}_q$ cannot be defined as in (4.19), as there is no τ_{q+1}. For $\mathscr{R}_q$, it suffices that we write:*

$$\mathscr{R}_q := \Big\{(x,w) \in \mathscr{C} : \mu\Big((x,w),\tau_q\Big) \leq 0\Big\}$$

Remark 4.5.3. *Only the first-order derivative of the triggering function has been used, as there is no assumption on differentiability of the unknown disturbance $d(t)$, which might result into conservatism for the proposed STC scheme. Nonetheless, in certain cases, the disturbance may be known to be differentiable and its derivatives to be bounded in some set. Such a knowledge may be leveraged to use higher-order derivatives of the triggering function, like in Chapter 3, so that conservatism is relaxed.*

4

4.5.2. SEMIGLOBAL NATURE OF REGION-BASED STC

It is obvious that the regions $\mathscr{R}_i$ do not cover the whole $w = 1$-hyperplane (which is where the state space of the original system is mapped), i.e. there exist states $x \in \mathbb{R}^n$ such that the point $(x,1) \in \mathbb{R}^{n+1}$ does not belong to any region $\mathscr{R}_i$, and thus no STC intersampling time can be assigned to x. Let us demonstrate which set $\mathscr{B} \subseteq \mathbb{R}^n$ is covered by the partition created and show that it can be made arbitrarily large.

The set $\mathscr{B}$ is composed of all points $x \in \mathbb{R}^n$ such that $(x,1)$ belongs to some region $\mathscr{R}_i$, i.e.:

$$\mathscr{B} := \{x \in \mathbb{R}^n : (x,1) \in \bigcup_i \mathscr{R}_i\}.$$

From the definition (4.19) of regions $\mathscr{R}_i$ and the scaling property (3.9c) of $\mu(\cdot)$, it follows that $\bigcup_i \mathscr{R}_i = \mathscr{C} \cap \{(x,w) \in \mathbb{R}^n \times \mathbb{R}_{>0} : \mu\Big((x,w),\tau_1\Big) \leq 0\}$. By fixing $w = 1$ in the expression (4.18) of $\mathscr{C}$ and in $\{(x,w) \in \mathbb{R}^n \times \mathbb{R}_{>0} : \mu\Big((x,w),\tau_1\Big) \leq 0\}$, we get:

$$\bullet\ (x,1) \in \mathscr{C} \iff x \in \{x \in \mathbb{R}^n : |x|^2 \leq \frac{r^2 - \underline{w}^2}{\underline{w}^2}\} =: B_1, \tag{4.20}$$

$$\bullet\ (x,1) \in \{(x,w) \in \mathbb{R}^n \times \mathbb{R}_{>0} : \mu\Big((x,w),\tau_1\Big) \leq 0\} \iff x \in \{x \in \mathbb{R}^n : \mu\Big((x,1),\tau_1\Big) \leq 0\} =: B_2 \tag{4.21}$$

Thus, we can write the set $\mathscr{B}$ as:

$$\mathscr{B} := \{x \in \mathbb{R}^n : x \in B_1, x \in B_2\} = B_1 \cap B_2. \tag{4.22}$$

The set B_1 is depicted in Figure 4.5 in Appendix 4.A. Since $r > \underline{w}$, B_1 is non-empty. Moreover, we can choose $\underline{w} > 0$ to be arbitrarily small without changing r, therefore we can make the set B_1 arbitrarily large. Finally, B_2 is non-empty (as it is the set delimited by $\underline{M}_{\tau_1}$ and $\mathscr{C}$) and, owing to the scaling property (3.9c) of $\mu(\cdot)$, it can be made arbitrarily large by selecting a sufficiently small τ_1. Consequently, $\mathscr{B}$ is non-empty, and can be made arbitrarily large. Hence, region-based STC is applicable semiglobally in $\mathbb{R}^n$.

4.6. NUMERICAL EXAMPLE

Let us demonstrate how the proposed STC is applied to a perturbed uncertain system, and compare its performance to the STC of [18]. Consider the ETC system from [18]:

$$\dot{\zeta}_1 = \zeta_2 + g_1(\zeta_1, d_1), \quad \dot{\zeta}_2 = u(\zeta, \varepsilon_\zeta) + g_2(\zeta_2), \tag{4.23}$$

where g_1, g_2 are uncertain and such that $|g_1(\zeta_1, d_1)| \leq 0.1|\zeta_1| + 0.1|d_1|$ and $|g_2(\zeta_2)| \leq 0.2|\zeta_2|^2$, and $d_1(t)$ is an unknown bounded disturbance with $|d_1(t)| \leq 4$. The ETC feedback u is $u(\zeta, \varepsilon_\zeta) = -(7.02|\zeta_2 + \varepsilon_{\zeta_2} - p_1| - 25.515)(\zeta_2 + \varepsilon_{\zeta_2} - p_1)$, where $p_1 = -2.1(\zeta_1 + \varepsilon_{\zeta_1})$. The triggering function from [18], that is to be emulated, is:

$$\phi(\zeta, \varepsilon_\zeta) = |\varepsilon_\zeta(t)|^2 - 0.0049|\zeta(t)|^2 - 16, \tag{4.24}$$

which guarantees convergence to a ball (practical stability). First, we bring (4.23) to the form of (4.3), by writing:

$$\dot{\xi}(t) = \begin{bmatrix} \dot{\zeta}_1 \\ \dot{\zeta}_2 \\ \dot{\varepsilon}_{\zeta_1} \\ \dot{\varepsilon}_{\zeta_2} \end{bmatrix} = \begin{bmatrix} \zeta_2 + 0.1 d_2 \zeta_1 + 0.1 d_1 \\ u(\zeta, \varepsilon_\zeta) + 0.2 d_3 \zeta_2^2 \\ -\zeta_2 - 0.1 d_2 \zeta_1 - 0.1 d_1 \\ -u(\zeta, \varepsilon_\zeta) - 0.2 d_3 \zeta_2^2 \end{bmatrix} = f_e(\xi(t), d(t)) \tag{4.25}$$

where $d(t) = (d_1(t), d_2(t), d_3(t)) \in [-4,4] \times [-1,1]^2$, i.e. $\Delta = [-4,4] \times [-1,1]^2$. Observe that Assumption 4.3.1 is satisfied. Then, we construct the homogeneous DI abstracting (4.25) according to (4.6):

$$\begin{pmatrix} \dot{\xi}(t) \\ \dot{w}(t) \end{pmatrix} = \begin{bmatrix} \{w^2 f_e(w^{-1}\xi, d(t)) : \ d(t) \in \Delta\} \\ 0 \end{bmatrix}, \tag{4.26}$$

and homogenize the triggering function as follows:

$$\tilde{\phi}(\xi(t), w(t)) = |\varepsilon_\zeta(t)|^2 - 0.0049|\zeta(t)|^2 - 16 w^2(t). \tag{4.27}$$

The degree of homogeneity for both (4.26) and (4.27) is 1.

Next, we derive the δ_i coefficients according to Theorem 4.5.1, to determine the regions $\mathscr{R}_i$. We fix $\mathrm{Z} = [-0.1, 0.1]^2$, $\mathrm{W} = [10^{-6}, 0.1]$ and define the sets Φ, E, Ξ as in (4.15), where Φ is indeed compact. By employing the computational algorithm of Chapter 3, $\delta_0 \approx 0.0353$ and $\delta_1 \approx 0.3440$ are obtained. We choose $r = 0.099$ such that $D_r \subset \mathrm{Z} \times \mathrm{W}$, and define $\mu\Big((x, w), t\Big)$ as in (4.17). Finally, the state space of DI (4.26) is partitioned into 434 regions $\mathscr{R}_i$ with $\tau_1 \approx 63 \cdot 10^{-5}$ and $\tau_{i+1} = 1.01\tau_i$.

We ran a number of simulations to compare our approach to the approach of [18] and to the ideal performance of the emulated ETC (4.24). More specifically, we simulated the system for 100 different initial conditions uniformly distributed in a ball of radius 2. The simulations' duration is 5s. As in [18], we fix: $g_1(\zeta_1, d_1) = 0.1\zeta_1 \sin(\zeta_1) + 0.1 d_1$, $d_1 = 4\sin(2\pi t)$ and $g_2(\zeta_2) = 0.2\zeta_2^2 \sin(\zeta_2)$. The self-triggered sampler of [18] determines sampling times as follows: $t_{i+1} = t_i + \frac{1.54}{28(|x_i|+4)+29}$, where x_i is the state measured at t_i. The total number of samplings for each simulation of all three schemes is depicted in Fig. 4.2. The average number of samplings per simulation was: 200.71 for region-based STC, 482.32 for STC [18] and 38.81 for ETC. We observe that region-based STC is in general less

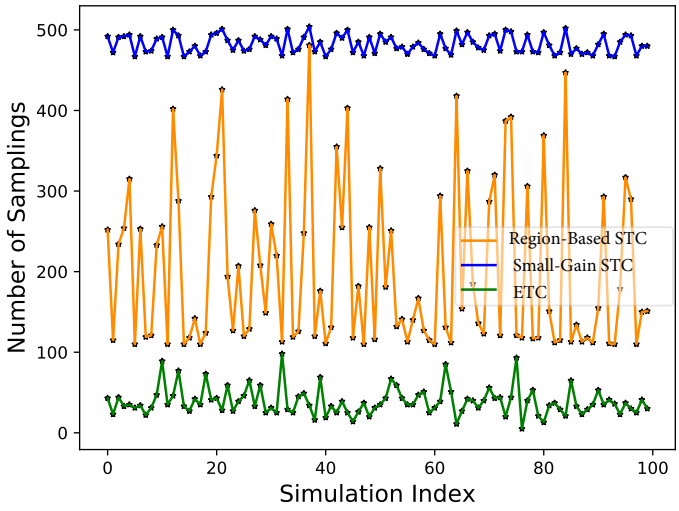

Figure 4.2: Number of samplings for each simulation of region-based STC (orange), STC of [18] (blue) and ETC (4.24) (green).

conservative than the STC of [18], while being more versatile as well. Recall that the main advantage of our approach is its versatility compared to the rest of the approaches, in terms of its ability to handle different performance specifications and different types of system's dynamics, provided that an appropriate triggering function is given. For example, [18] is constrained to ISS systems, while our approach does not obey such a restriction. Finally, as expected, ETC leads to a smaller amount of samplings compared to both STC schemes.

We, also, present illustrative results for one particular simulation with initial condition $(-1,-1)$. Figure 4.3 shows the trajectories of the system when controlled via region-based STC and the STC from [18], while Figure 4.4 shows the time-evolution of intersampling times for the two schemes. Region-based STC led to 166 samplings, whereas the STC of [18] led to 483. We observe that, while the performance of both schemes is the same (the trajectories are almost identical in Figure 4.3), region-based STC leads to a smaller amount of samplings, i.e. less communication. Moreover, from Figure 4.4 we observe that, especially during the steady-state response, region-based STC performs considerably better, in terms of sampling. However, there is a small period of time in the beginning of the simulation, when the trajectories overshoot far away from the origin and region-based STC gives faster sampling.

4.7. CONCLUSION

Building on Chapter 3, we have extended region-based STC to nonlinear systems with disturbances and uncertainties. By employing a framework based on DIs and introducing

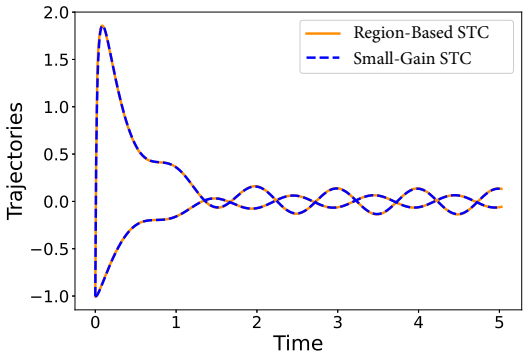

Figure 4.3: Trajectories of system (4.23) with initial condition $(-1,-1)$, under region-based STC (orange lines) and the STC of [18] (dashed blue lines).

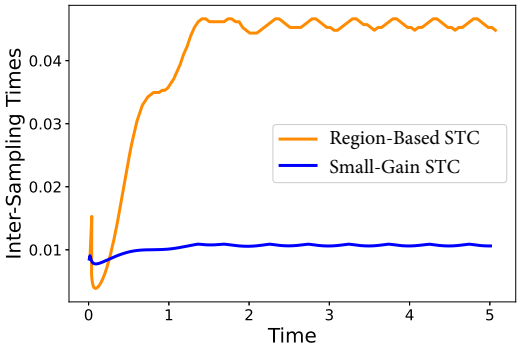

Figure 4.4: Evolution of intersampling times during a simulation with initial condition $(-1,-1)$, for region-based STC (orange line) and the STC of [18] (blue line).

ETC notions therein, we have extended significant results on ETC/STC to perturbed uncertain systems. Employing the renewed results, we have constructed approximations of IMs of perturbed uncertain systems, enabling region-based STC. The provided numerical simulations indicate that our approach, while being more versatile, is competitive with respect to other state-of-the-art approaches as well, in terms of intersampling times.

4.A. TECHNICAL PROOFS

Proof of Theorem 4.4.1. According to the definition of intersampling times (4.5), for $\tau\Big(\lambda(x,w)\Big)$ we have:

$$\tau\Big(\lambda(x,w)\Big) = \inf\Big\{t>0 : \sup\Big\{\tilde{\phi}\Big(\mathscr{X}_t^{\tilde{F}}(\lambda(x,0,w))\Big)\Big\} \geq 0\Big\}$$

Employing the scaling property (4.2) and the fact that $\tilde{\phi}$ is homogeneous of degree θ, we can write $\tau\Big(\lambda(x,w)\Big)$ as:

$$\begin{aligned}
&\inf\Big\{t>0 : \sup\Big\{\tilde{\phi}\Big(\lambda \mathscr{X}^{\tilde{F}}_{\lambda^{\alpha} t}((x,0,w))\Big)\Big\} \geq 0\Big\} = \\
&\inf\Big\{t>0 : \sup\Big\{\lambda^{\theta+1}\tilde{\phi}\Big(\mathscr{X}^{\tilde{F}}_{\lambda^{\alpha} t}((x,0,w))\Big)\Big\} \geq 0\Big\} = \\
&\inf\Big\{\lambda^{-\alpha} t>0 : \sup\Big\{\tilde{\phi}\Big(\mathscr{X}^{\tilde{F}}_{t}((x,0,w))\Big)\Big\} \geq 0\Big\} = \\
&\lambda^{-\alpha}\tau\Big((x,w)\Big)
\end{aligned}$$

□

Proof of Lemma 4.5.1. Consider the restriction of ODE (4.9) to the set Ξ:

$$\dot{\xi}(t) = f(\xi(t), d(t)), \quad \xi(t) \in \Xi. \tag{4.28}$$

Any solution of (4.28) is also a solution of (4.9) (possibly not a maximal one). Note that (4.11) is equivalent to:

$$\dot{\phi}(\xi(t;\xi_0)) \leq \delta_0 \phi(\xi(t;\xi_0)) + \delta_1, \tag{4.29}$$

where $\xi(t;\xi_0)$ is any solution of (4.28), with $\xi_0 \in \Xi$. Observe that $\psi(y(\xi_0), t)$ is the solution to the scalar differential equation $\dot{\psi} = \delta_0\psi + \delta_1$ with initial condition $\psi_0 = \phi(\xi_0)$:

$$\psi(y(\xi_0), t) = \begin{bmatrix} 1 & 0 \end{bmatrix} e^{At} y(\xi_0) = e^{\delta_0 t}\phi(\xi_0) + \frac{e^{\delta_0 t} - 1}{\delta_0}\delta_1.$$

Thus, by employing the comparison lemma (see [63], pp. 102-103), from (4.29) we get that for any $d_\star(t)$ satisfying Assumption 4.3.1 and all $\xi_0 \in \Xi$:

$$\phi(\xi(t;\xi_0)) \leq \psi(y(\xi_0), t), \quad \forall\, t \in [0, t_{e,d_\star}(\xi_0)), \tag{4.30}$$

where $[0, t_{e,d_\star}(\xi_0))$ is the maximal interval of existence of solution $\xi(t;\xi_0)$ to ODE (4.28) under the realization $d(t) = d_\star(t)$. The time $t_{e,d_\star}(\xi_0)$ is defined as the time when $\xi(t;\xi_0)$, under the realization $d(t) = d_\star(t)$, leaves the set Ξ:

$$t_{e,d_\star}(\xi_0) = \sup\{\tau > 0 : d(t) = d_\star(t), \xi(t;\xi_0) \in \Xi\ \forall\, t \in [0,\tau)\}$$

Since (4.30) holds for all $d_\star(t)$ satisfying Assumption 4.3.1, we can conclude that $\psi(y(\xi_0), t)$ bounds all solutions of DI (4.10) starting from $\xi_0 \in \Xi$ as follows:

$$\sup\Big\{\phi\Big(\mathscr{X}^{F}_{t}(\xi_0)\Big)\Big\} \leq \psi(y(\xi_0), t), \quad \forall\, t \in [0, \inf_{d_\star} t_{e,d_\star}(\xi_0)).$$

Finally, note that $\inf\limits_{d_\star} t_{e,d_\star}(\xi_0)$ represents the smallest possible Ξ-escape time among all trajectories generated by DI (4.10), i.e. $\inf\limits_{d_\star} t_{e,d_\star}(\xi_0) = \inf\{t > 0 : \mathscr{X}^{F}_{t}(\xi_0) \notin \Xi\} = t_e(\xi_0)$. Hence, we can conclude that:

$$\sup\Big\{\phi\Big(\mathscr{X}^{F}_{t}(\xi_0)\Big)\Big\} \leq \psi(y(\xi_0), t), \quad \forall\, t \in [0, t_e(\xi_0)).$$

□

Proof of Theorem 4.5.1. First notice that, under item 5 of Assumption 4.3.1, (3.9a) holds: $\mu\Big((x,w),0\Big) = \Big(\frac{|(x,w)|}{r}\Big)^{\theta+1}\tilde{\phi}\Big((r\frac{x}{|(x,w)|},0,r\frac{w}{|(x,w)|})\Big) < 0$ for all $(x,w)\in\mathbb{R}^{n+1}\setminus\{0\}$. Moreover, observe that $\mu(\cdot,\cdot)$ satisfies the time-scaling property (3.9c) by construction. It remains to prove that $\mu(\cdot,\cdot)$ satisfies (3.9b) and (3.9d).

In order to prove that $\mu(\cdot,\cdot)$ satisfies (3.9b), as already explained in Section 4.5.1, we follow the following steps: 1) we show that the coefficients δ_0,δ_1 satisfying (4.16a) determine a function $\psi(y((x,0,w_\star)),t)$ satisfying (4.31), 2) using the sets Z, W, E, Φ, Ξ we show that $\psi(y((x,0,w_\star)),t)$ satisfies (4.32), and finally 3) observing that μ is obtained by a projection of ψ to D_r, we show that μ satisfies (3.9b) (see (4.36)).

Let us formally prove it. Assumption 4.3.1 implies that $\tilde{F}(\xi,w)\subseteq\mathbb{R}^{2n+1}$ is non-empty, compact and convex for any $(\xi,w)\in\mathbb{R}^{2n+1}\setminus\{0\}$ and outer-semicontinuous. These conditions ensure existence and extendability of solutions for each initial condition [61]. According to Lemma 4.5.1 and since Ξ is compact, the coefficients δ_0,δ_1 satisfying (4.16a), determine a function $\psi(y((x,e,w_\star)),t)$ such that for all $(x,e,w)\in\Xi$: $\psi(y((x,e,w)),t)\geq\sup\Big\{\phi\Big(\mathscr{X}_t^{\tilde{F}}((x,e,w))\Big)\Big\}$, $\forall\, t\in[0,t_e\Big((x,e,w)\Big)]$, where $t_e\Big((x,e,w)\Big)$ is defined in (4.12) as the time when $\mathscr{X}_t^{\tilde{F}}((x,e,w))$ leaves the set Ξ. Since we are only interested in initial conditions with the measurement error component being 0, we write:

$$\psi(y((x,0,w)),t)\geq\sup\Big\{\phi\Big(\mathscr{X}_t^{\tilde{F}}((x,0,w))\Big)\Big\},\quad \forall(x,0,w)\in\Xi \text{ and } \forall\, t\in[0,t_e\Big((x,0,w)\Big)]. \tag{4.31}$$

Observe that for all initial conditions $(x,0,w)\in\mathrm{Z}\times\mathrm{E}\times\mathrm{W}$, the sets Φ and E are exactly such that $\xi(t;(x,0))\notin\Phi\times\mathrm{E}\implies\phi(\xi(t;(x,0)))>0$, where $\xi(\cdot)$ represents the ξ-component of solutions of DI (4.6) (since $w(t)$ remains constant along solutions of DI (4.6), we neglect it). Thus, all trajectories that start from any initial condition $(x,0,w)\in\mathrm{Z}\times\mathrm{E}\times\mathrm{W}$ reach the boundary of $\Xi=\Phi\times\mathrm{E}\times\mathrm{W}$ after (or at) the intersampling time $\tau\Big((x,w)\Big)$, i.e. $\tau\Big((x,w)\Big)\leq t_e\Big((x,e,w)\Big)$ for all $(x,w)\in\mathrm{Z}\times\mathrm{W}$. Thus, employing (4.31) we write:

$$\psi(y((x,0,w)),t)\geq\sup\Big\{\phi\Big(\mathscr{X}_t^{\tilde{F}}((x,0,w))\Big)\Big\},\quad \forall(x,w)\in\mathrm{Z}\times\mathrm{W} \text{ and } \forall\, t\in[0,\tau\Big((x,w)\Big)]. \tag{4.32}$$

Now, consider any point $(x_0,w_0)\in D_r\subseteq\mathrm{Z}\times\mathrm{W}$. Observe that $\mu\Big((x_0,w_0),t\Big)=\psi(y((x_0,0,w_0)),t)$. Thus, since $D_r\subseteq\mathrm{Z}\times\mathrm{W}$, from (4.32) we get:

$$\mu\Big((x_0,w_0),t\Big)\geq\sup\Big\{\phi\Big(\mathscr{X}_t^{\tilde{F}}((x_0,0,w_0))\Big)\Big\},\forall(x_0,w_0)\in D_r \text{ and } \forall\, t\in[0,\tau\Big((x_0,w_0)\Big)]. \tag{4.33}$$

To prove that $\mu(\cdot)$ satisfies (3.9b) in the cone $\mathscr{C}$ from (4.18), we have to show that (4.33) holds for all $(x,w)\in\mathscr{C}$. First, observe that $\mathscr{C}$ is defined as the cone stemming from the origin with its extreme vertices being all points in the intersection $D_r\cap\mathrm{Z}\times\mathrm{W}$ (see Figure 4.5). Thus, since D_r is a spherical segment, for any point $(x,w)\in\mathscr{C}$ there always exists a $\lambda>0$ and a point $(x_0,w_0)\in D_r$ such that $(x,w)=\lambda(x_0,w_0)$. If we interchange (x_0,w_0) with $\lambda^{-1}(x,w)$ in (4.33), we get:

$$\mu\Big(\lambda^{-1}(x,w),t\Big)\geq\sup\Big\{\phi\Big(\mathscr{X}_t^{\tilde{F}}(\lambda^{-1}(x,0,w))\Big)\Big\},\forall(x,w)\in\mathscr{C} \text{ and } \forall\, t\in[0,\tau\Big(\lambda^{-1}(x,w)\Big)]. \tag{4.34}$$

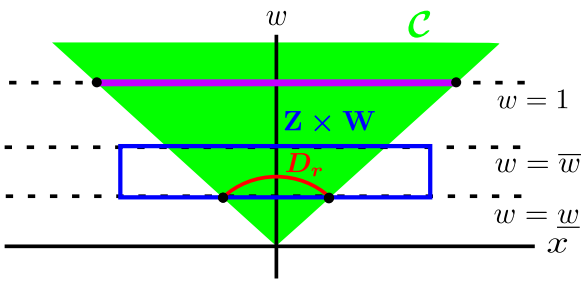

Figure 4.5: The sets Z × W (region contained in blue box), D_r (red spherical segment) and the cone $\mathscr{C}$ (green) from (4.18). The subset of the hyperplane $w = 1$ painted in purple represents the set B_1 from (4.20).

But, from (4.2), (3.9c) and Theorem (4.4.1) we get:

$$\begin{aligned}
&\bullet \sup\left\{\phi\left(\mathscr{X}_t^{\tilde{F}}(\lambda^{-1}(x,0,w))\right)\right\} = \lambda^{-\theta-1}\sup\left\{\phi\left(\mathscr{X}_{\lambda^{-\alpha}t}^{\tilde{F}}((x,0,w))\right)\right\}\\
&\bullet \mu\left(\lambda^{-1}(x,w),t\right) = \lambda^{-\theta-1}\mu\left((x,w),\lambda^{-\alpha}t\right)\\
&\bullet \tau\left(\lambda^{-1}(x,w)\right) = \lambda^{\alpha}\tau\left((x,w)\right)
\end{aligned} \tag{4.35}$$

Incorporating (4.35) into (4.34), we finally get:

$$\mu\left((x,w),t\right) \geq \sup\left\{\phi\left(\mathscr{X}_t^{\tilde{F}}((x,0,w))\right)\right\}, \forall (x,w) \in \mathscr{C} \text{ and } \forall t \in [0, \tau\left((x,w)\right)], \tag{4.36}$$

i.e. $\mu(\cdot)$ satisfies (3.9b) in $\mathscr{C}$.

Finally, let us prove that $\mu(\cdot)$ satisfies (3.9d). Observe that, since $\delta_0 \geq 0$, $\delta_1 > 0$ and (4.16b) holds, then $\mu\left((x,w),t\right)$ and $\dot{\mu}\left((x,w),t\right)$ are strictly increasing w.r.t. t (for a more detailed proof, see the proofs in Chapter 3). Thus, since $\mu\left((x,w),0\right) < 0$, then, for any $(x,w) \in \mathbb{R}^{n+1} \setminus \{0\}$, $\exists! \tau^{\downarrow}(x,w) > 0$ such that $\mu\left((x,w),\tau^{\downarrow}\left((x,w)\right)\right) = 0$. The proof is now complete. □

5

Abstracting the Sampling Behaviour of Nonlinear Event-Triggered Control Systems

In previous works [39]–[41], finite-state abstractions were created, capturing the sampling behaviour of LTI ETC systems with quadratic triggering functions. Offering an infinite-horizon look to ETC systems' sampling patterns, such abstractions have been used for versatile scheduling of ETC traffic. Here we significantly extend this framework, by abstracting perturbed uncertain nonlinear ETC systems with general triggering functions. To construct an ETC system's abstraction: a) the state space is partitioned into regions, b) for each region an interval is determined, containing all intersampling times of points in the region, and c) the abstraction's transitions are determined through reachability analysis. To determine intervals and transitions, we devise algorithms based on reachability analysis. For partitioning, we propose an approach based on isochronous manifolds, resulting into tighter intervals and providing control over them, thus containing the abstraction's non-determinism. Simulations showcase our developments.

This chapter has been published in [64]. Some changes have been made to streamline presentation. A preliminary version, focusing solely on homogeneous systems, and including the developments in Appendix 5.A, has been published in [65].

5.1. INTRODUCTION

According to abstraction-based approaches to ETC traffic scheduling [39]–[41], ETC systems are abstracted by finite-state *quotient systems* (abstractions), capturing the ETC systems' sampling behaviour. The abstraction's set of output sequences contains all possible sequences of intersampling times that the given ETC system may exhibit, thus providing an infinite-horizon look into its sampling patterns. Employing this property, [39]–[41] showed that such abstractions can be employed for scheduling of ETC traffic.

To construct the abstraction, the system's state-space is partitioned into finitely many regions $\tilde{\mathcal{R}}_{i,j}$ (the i,j-index becomes clear later), representing the abstraction's states. For each region $\tilde{\mathcal{R}}_{i,j}$, an interval $[\underline{\tau}_{\tilde{\mathcal{R}}_{i,j}}, \overline{\tau}_{\tilde{\mathcal{R}}_{i,j}}]$ is determined, containing all intersampling times corresponding to states in the region. These intervals serve as the abstraction's output. Finally, the abstraction's transitions, given a starting region, indicate where the system's trajectories end up after an elapsed intersampling time. The abstraction's non-determinism, encoding how coarsely it captures the actual system's behaviours, depends on the intervals' tightness and the transition set's size. Previous works [39]–[41] abstracted LTI systems with quadratic triggering functions.

5

Here, we significantly extend the above framework by abstracting the traffic of nonlinear ETC systems with bounded disturbances or uncertainties and general triggering functions[1]. To determine the timing intervals and the transitions, we propose algorithms based on *reachability analysis* (e.g., see [66], [67]). Regarding state-space partitioning, we propose an approach that is based on approximations of IMs, derived in the previous chapters. By partially inheriting the merits of partitioning with actual IMs, this approach aims at providing control over the timing intervals and improving their tightness, thus containing one source of the abstraction's non-determinism. Simulation comparisons between the proposed partition and a naive partition support our arguments, as the proposed partition achieves tighter intervals (for metrics capturing tightness refer to Section 5.6).

5.2. NOTATION AND PRELIMINARIES

5.2.1. NOTATION

Given two sets $X_a, X_b \subseteq X$, $d_H(X_a, X_b)$ denotes their Hausdorff distance. Given an equivalence relation $Q \subseteq X \times X$, the set of all equivalence classes is denoted by X/Q.

5.2.2. SYSTEMS AND SIMULATION RELATIONS

Here we recall notions of systems and simulation relations from [68], which are employed later.

Definition 5.2.1 (System [68, Definition 1.1])**.** *A system* S *is a tuple* $(X, X_0, \longrightarrow, Y, H)$*, where* X *is the set of states,* X_0 *the set of initial states,* $\longrightarrow \subseteq X \times X$ *a transition relation,* Y *the set of outputs and* $H : X \to Y$ *the output map.*

[1] Throughout the chapter, we mainly focus on systems without disturbances or uncertainties, for the sake of clarity. Nonetheless, Remarks 5.4.4 and 5.5.3 describe how our approach directly extends to perturbed uncertain systems. Moreover, applicability of our approach to perturbed systems is demonstrated by a numerical example in Section 5.6.1.

We have omitted the action set U in Definition 5.2.1, since we focus on autonomous systems. If X is a finite (or infinite) set, then S is called finite-state (respectively infinite-state). A system S is called a *metric system* if Y is equipped with a metric $d : Y \times Y \to \mathbb{R}_0^+ \cup \{+\infty\}$.

Definition 5.2.2 (ϵ-Approximate Simulation Relation [68, Definition 9.2])**.** *Consider two metric systems* S_a, S_b *with* $Y_a = Y_b$ *and a constant* $\epsilon \geq 0$*. A relation* $Q \subseteq X_a \times X_b$ *is an* ϵ*-approximate simulation relation from* S_a *to* S_b *if it satisfies:*

- $\forall x_{0_a} \in X_{0_a}: \quad \exists x_{0_b} \in X_{0_b}$ *such that* $(x_{0_a}, x_{0_b}) \in Q$,
- $\forall (x_a, x_b) \in Q: \quad d(H_a(x_a), H_b(x_b)) \leq \epsilon$,
- $\forall x_a, x_a' \in X_a$ *with* $(x_a, x_a') \in \underset{a}{\longrightarrow}$*: if* $(x_a, x_b) \in Q$ *then* $\exists (x_b, x_b') \in \underset{b}{\longrightarrow}$ *such that* $(x_a', x_b') \in Q$.

If there exists an ϵ-approximate simulation relation from S_a to S_b, we say that S_b ϵ-approximately simulates S_a and write $S_a \overset{\epsilon}{\preceq} S_b$. Moreover, let us introduce an alternative definition of *power quotient systems*. For the original definition, see [68].

Definition 5.2.3 (Power Quotient System [40, Definition 6])**.** *Consider a system* $S = (X, X_0, \longrightarrow, Y, H)$ *and an equivalence relation* $Q \subseteq X \times X$*. The power quotient system of* S *is the tuple* $S_{/Q} = (X_{/Q}, X_{0_{/Q}}, \underset{/Q}{\longrightarrow}, Y_{/Q}, H_{/Q})$*, where:*

- $X_{/Q} = X/Q$ *and* $X_{0_{/Q}} = \{x_{/Q} \in X_{/Q} : x_{/Q} \cap X_0 \neq \emptyset\}$,
- $(x_{/Q}, x'_{/Q}) \in \underset{/Q}{\longrightarrow}$ *if* $\exists (x, x') \in \longrightarrow$ *such that* $x \in x_{/Q}$ *and* $x' \in x'_{/Q}$,
- $Y_{/Q} \subseteq 2^Y$ *and* $H_{/Q}(x_{/Q}) = \bigcup_{x \in x_{/Q}} H(x)$.

Lemma 5.2.1 ([40, Lemma 1])**.** *Consider a metric system* S*, a relation* $Q \subseteq X \times X$ *and the power quotient system* $S_{/Q}$*. For any* ϵ *such that* $\epsilon \geq \sup_{x \in x_{/Q},\, x_{/Q} \in X/Q} d_H(H(x), H_{/Q}(x_{/Q}))$, $S_{/Q}$ ϵ*-approximately simulates* S*, i.e.* $S \overset{\epsilon}{\preceq} S_{/Q}$.

5.3. PROBLEM STATEMENT

In this chapter, we abstract the sampling behaviour of nonlinear ETC systems; we construct finite-state systems, whose set of output sequences contains all possible intersampling time sequences of the given ETC system. For clarity, we mainly consider the case without disturbances or uncertainties, but we also point out through remarks (Remarks 5.4.4 and 5.5.3) and a numerical example (Section 5.6.1) how the proposed approach directly applies to systems with bounded disturbances or uncertainties.

We adopt a problem formulation similar to [40]. Recall the ETC system (2.5)-(2.6):

$$\dot{\zeta}(t) = f\Big(\zeta(t), v(\zeta(t) + \varepsilon_\zeta(t))\Big), \quad t \in [t_i, t_{i+1})$$
$$t_{i+1} = t_i + \inf\{t > 0 : \phi(\zeta(t; x_i), \varepsilon_\zeta(t)) \geq 0\}$$

and its extended form (2.8):

$$\dot{\xi}(t) = \begin{bmatrix} f\Big(\zeta(t), v(\zeta(t)+\varepsilon_\zeta(t))\Big) \\ -f\Big(\zeta(t), v(\zeta(t)+\varepsilon_\zeta(t))\Big) \end{bmatrix} = f_e(\xi(t)),\ t \in [t_i, t_{i+1})$$
$$\xi(t_{i+1}^+) = \begin{bmatrix} \zeta(t_{i+1}^-) \\ 0 \end{bmatrix}$$

Let us introduce the system:

$$\mathrm{S} = (X, X_0, \longrightarrow, Y, H), \tag{5.1}$$

where $X = X_0 \subseteq \mathbb{R}^n$, $Y \subseteq \mathbb{R}_{>0}$, $H(x) = \tau(x)$ and the transition relation $\longrightarrow \subseteq X \times X$ is such that $(x, x') \in \longrightarrow \iff \zeta(\tau(x); x) = x'$. Observe that the set of output sequences of system (5.1) contains all possible intersampling time sequences of the ETC system (2.5)-(2.6), that correspond to trajectories confined in X. However, it is infinite-state and cannot serve as a computationally handleable abstraction.

We, also, introduce the following set of assumptions:

Assumption 5.3.1.

1. *The origin is the only equilibrium of* (2.3).
2. *The vector field $f_e(\cdot)$ from* (2.8) *is locally bounded.*
3. $\phi\Big((0,0)\Big) \leq 0$ *and* $\phi\Big((x,0)\Big) < 0$ *for all* $x \in \mathbb{R}^n \setminus \{0\}$. *Moreover, for any compact set* $K \subset \mathbb{R}^n$ *there exists* $\epsilon_K > 0$ *such that for all* $x_0 \in K \setminus \{0\}$, $\phi(\xi(t; x_0)) < 0$ *for all* $t \in [0, \epsilon_K)$.
4. *The set X is compact and connected.*
5. *A heartbeat (maximum allowed intersampling time, see Remark 2.3.1)* $\tau_{\max}$ *is imposed on the system.*

Item 1 serves for clarity of presentation. Item 3 imposes that $\phi\Big((\cdot,0)\Big)$ is negative-definite and that the given ETC system cannot exhibit infinitely fast sampling; this is satisfied by most functions in the ETC literature (e.g. Tabuada's [7], dynamic triggering [8], mixed triggering [18], Lebesgue sampling [6]). Item 4 suggests that we are interested in trajectories of the system that stay in the compact connected set X. Finally, item 5 guarantees that there can be no infinite intersampling time, which is essential for the algorithms developed in Section 5.4.1. Recall, from Remark 2.3.1, that this is a reasonable assumption.

Since (5.1) captures exactly the sampling behaviour of the ETC system (2.5)-(2.6), abstracting the ETC system is equivalent to abstracting (5.1). This gives rise to the following:

Problem Statement. *Consider the system* S (5.1). *Let Assumption 5.3.1 hold. Construct a power-quotient system* $\mathrm{S}_{/Q} = (X_{/Q}, X_{0_{/Q}}, \underset{/Q}{\longrightarrow}, Y_{/Q}, H_{/Q})$ *with:*

- $X_{/Q} = X/Q := \{\tilde{\mathscr{R}}_{1,1}, \ldots, \tilde{\mathscr{R}}_{i,j}, \ldots, \tilde{\mathscr{R}}_{q,m}\}$ *and* $X_{0_{/Q}} = X_{/Q}$, *where* $\tilde{\mathscr{R}}_{i,j} \subseteq X$ *and* $\bigcup \tilde{\mathscr{R}}_{i,j} = X$.

- $(x_{/Q}, x'_{/Q}) \in \xrightarrow[/Q]{}$ *if* $\exists x \in x_{/Q}$ *and* $\exists x' \in x'_{/Q}$ *such that* $\zeta(H(x); x) = x'$,

- $Y_{/Q} \subseteq 2^Y = 2^{\mathbb{R}_{>0}}$ *and* $H_{/Q}(\tilde{\mathcal{R}}_{i,j}) := [\underline{\tau}_{\tilde{\mathcal{R}}_{i,j}}, \overline{\tau}_{\tilde{\mathcal{R}}_{i,j}}]$, *with:*

$$\underline{\tau}_{\tilde{\mathcal{R}}_{i,j}} \leq \inf_{x \in \tilde{\mathcal{R}}_{i,j}} H(x), \quad \overline{\tau}_{\tilde{\mathcal{R}}_{i,j}} \geq \sup_{x \in \tilde{\mathcal{R}}_{i,j}} H(x). \tag{5.2}$$

The states $\tilde{\mathcal{R}}_{i,j}$ of the abstraction are regions in the ETC system's state-space, i.e. $\tilde{\mathcal{R}}_{i,j} \subseteq X \subset \mathbb{R}^n$ (the i,j-subscript becomes clear later). A transition from $\tilde{\mathcal{R}}_{i,j}$ to $\tilde{\mathcal{R}}_{k,l}$ is defined if there exists a trajectory starting from $x \in \tilde{\mathcal{R}}_{i,j}$, which ends up in $\tilde{\mathcal{R}}_{k,l}$ after an elapsed intersampling time $\tau(x)$. Hence, a transition is taken every time the triggering condition (2.6) is satisfied. Finally, (5.2) indicates that the abstraction's output of a state $\tilde{\mathcal{R}}_{i,j}$ is an interval containing all intersampling times corresponding to states $x \in \tilde{\mathcal{R}}_{i,j}$. Thus, given a run of the ETC system, there is a corresponding run of the abstraction, whose output sequence is a sequence of intervals each of which containing the intersampling time that the ETC system exhibited at that particular step of the run. In fact, by Lemma 5.2.1, we conclude that $S \overset{\epsilon}{\preceq} S_{/Q}$ for all $\epsilon \geq \max_i \{\overline{\tau}_{\tilde{\mathcal{R}}_{i,j}} - \underline{\tau}_{\tilde{\mathcal{R}}_{i,j}}\}$.

As discussed in [40], the abstraction $S_{/Q}$ is semantically equivalent to a *timed automaton*. The automaton's guards are determined by the intervals $[\underline{\tau}_{\tilde{\mathcal{R}}_{i,j}}, \overline{\tau}_{\tilde{\mathcal{R}}_{i,j}}]$, and its transitions are the ones of $S_{/Q}$. The tighter the intervals and the smaller the transition set, the less non-deterministic becomes the automaton; hence it simulates more accurately the original system, and the scheduling algorithms provide less conservative results.

To address the problem, we have to partition X into regions $\tilde{\mathcal{R}}_{i,j}$ (which automatically generates the relation Q), derive the intervals, and determine the transitions. In what follows, partitioning the state-space is decoupled from determining the intervals and transitions. Specifically, in Section 5.4, we propose reachability-analysis-based algorithms to determine the timing intervals and transitions, *given any partition*. Later, in Section 5.5, we propose a specific partition, providing better control over the intervals and their tightness, thus containing one source of the abstraction's non-determinism.

5.4. TIMING INTERVALS AND TRANSITIONS

In this section, we assume that the partition is given and show how reachability analysis can be employed to determine timing intervals and transitions.

5.4.1. REACHABILITY ANALYSIS FOR TIMING INTERVALS

The following proposition, employing reachable sets and flowpipes, provides conditions that determine lower and upper bounds on intersampling times of points in a given region $\tilde{\mathcal{R}}_{i,j}$:

Proposition 5.4.1. *Consider the ETC system* (2.5)-(2.6) *and its extended form* (2.8). *Let*

Assumption 5.3.1 hold. Let $\tilde{\mathscr{R}}_{i,j} \subseteq X$. Define the sets:

$$\mathscr{I}_{i,j} := \{(x,0) \in \mathbb{R}^{2n} : x \in \tilde{\mathscr{R}}_{i,j}\}$$
$$\mathscr{U}_{\geq 0} := \{(x,e) \in \mathbb{R}^{2n} : \phi\Big((x,e)\Big) \geq 0\}$$
$$\mathscr{U}_{\leq 0} := \{(x,e) \in \mathbb{R}^{2n} : \phi\Big((x,e)\Big) \leq 0\}$$

If:

$$\mathscr{X}^{fe}_{[0,\tau_{low}]}(\mathscr{I}_{i,j}) \cap \mathscr{U}_{\geq 0} = \emptyset, \tag{5.3}$$

then for all $x \in \tilde{\mathscr{R}}_{i,j}$: $\tau(x) \geq \tau_{low}$, where $\tau(\cdot)$ is as in (2.7). Similarly, if:

$$\mathscr{X}^{fe}_{\tau_{high}}(\mathscr{I}_{i,j}) \cap \mathscr{U}_{\leq 0} = \emptyset, \tag{5.4}$$

then for all $x \in \tilde{\mathscr{R}}_{i,j}$: $\tau(x) \leq \tau_{high}$.

Proof. Equation (5.3) implies that $\forall x \in \tilde{\mathscr{R}}_{i,j}$ we have that: $\phi(\xi(t;x)) < 0$, for all $t \in [0, \tau_{\text{low}}]$. Thus, $\tau(x) \geq \tau_{\text{low}}$, i.e. τ_{low} is a lower bound on intersampling times of region $\tilde{\mathscr{R}}_{i,j}$.

Similarly, if $\mathscr{X}^{fe}_{\tau_{\text{high}}}(\mathscr{I}_{i,j}) \cap \mathscr{U}_{\leq 0} = \emptyset$, then for all $x \in \tilde{\mathscr{R}}_{i,j}$ we have that $\phi(\xi(\tau_{\text{high}};x)) > 0$. Thus, $\tau(x) \leq \tau_{\text{high}}$. □

To obtain the timing intervals $[\underline{\tau}_{\tilde{\mathscr{R}}_{i,j}}, \overline{\tau}_{\tilde{\mathscr{R}}_{i,j}}]$ for regions $\tilde{\mathscr{R}}_{i,j}$, we employ one line search for each one of the variables τ_{low} and τ_{high} and iterate until we find that (5.3) or (5.4), respectively, are satisfied. To check (5.3) and (5.4), we employ reachability-analysis computational tools (e.g. [66], [67]). Such tools, given a system (2.1), a set of initial conditions $\mathscr{I} \subset \mathbb{R}^n$ and a set $\mathscr{U} \subseteq \mathbb{R}^n$, overapproximate the reachable flowpipes $\mathscr{X}^{f}_{[\tau_1,\tau_2]}(\mathscr{I})$ and the set $\mathscr{U}$ by overapproximations $\hat{\mathscr{X}}^{f}_{[\tau_1,\tau_2]}(\mathscr{I}) \supseteq \mathscr{X}^{f}_{[\tau_1,\tau_2]}(\mathscr{I})$ and $\hat{\mathscr{U}} \supseteq \mathscr{U}$, and check if $\hat{\mathscr{X}}^{f}_{[\tau_1,\tau_2]}(\mathscr{I}) \cap \hat{\mathscr{U}} = \emptyset$. Moreover, by the implication:

$$\hat{\mathscr{X}}^{f}_{[\tau_1,\tau_2]}(\mathscr{I}) \cap \hat{\mathscr{U}} = \emptyset \implies \mathscr{X}^{f}_{[\tau_1,\tau_2]}(\mathscr{I}) \cap \mathscr{U} = \emptyset, \tag{5.5}$$

they can determine if $\mathscr{X}^{f}_{[\tau_1,\tau_2]}(\mathscr{I}) \cap \mathscr{U} = \emptyset$. Hence, by employing line searches on τ_{low} and τ_{high}, via a reachability analysis tool we check iteratively if $\hat{\mathscr{X}}^{fe}_{[0,\tau_{\text{low}}]}(\mathscr{I}_{i,j}) \cap \hat{\mathscr{U}}_{\geq 0} = \emptyset$ or $\hat{\mathscr{X}}^{fe}_{\tau_{\text{high}}}(\mathscr{I}_{i,j}) \cap \hat{\mathscr{U}}_{\leq 0} = \emptyset$, respectively, until these conditions are satisfied. Satisfaction of these conditions implies (5.3) and (5.4) (due to (5.5)), which imply that $\tau(x) \geq \tau_{\text{low}} = \underline{\tau}_{\tilde{\mathscr{R}}_{i,j}}$ and $\tau(x) \leq \tau_{\text{high}} = \overline{\tau}_{\tilde{\mathscr{R}}_{i,j}}$ for all $x \in \tilde{\mathscr{R}}_{i,j}$, respectively, by Proposition 5.4.1. Finally, if no $\tau_{\text{high}} \leq \tau_{\max}$ is found via the line-search, which satisfies (5.4), then the region's timing upper bound is fixed equal to the heartbeat: $\overline{\tau}_{\tilde{\mathscr{R}}_{i,j}} = \tau_{\max}$.

Remark 5.4.1. *If a heartbeat $\tau_{\max}$ is not imposed, then certain regions (e.g. the ones containing equilibria) might not admit upper bounds on their intersampling times. For these regions, the proposed line-search algorithm would not terminate.*

5.4.2. REACHABILITY ANALYSIS FOR TRANSITIONS

Let us show how the abstraction's transitions can be derived via reachability analysis. Recall the transitions' definition, from the Problem Statement:

$$(\tilde{\mathcal{R}}_{i,j}, \tilde{\mathcal{R}}_{k,l}) \in \underset{/Q}{\longrightarrow}, \text{ if :}$$

$$\exists x \in \tilde{\mathcal{R}}_{i,j} \text{ and } \exists x' \in \tilde{\mathcal{R}}_{k,l} \text{ such that } \zeta(H(x); x) = x'.$$

This definition can be relaxed as follows:

$$(\tilde{\mathcal{R}}_{i,j}, \tilde{\mathcal{R}}_{k,l}) \in \underset{/Q}{\longrightarrow}, \text{ if : } \mathcal{X}^{f}_{[\underline{\tau}_{\tilde{\mathcal{R}}_{i,j}}, \overline{\tau}_{\tilde{\mathcal{R}}_{i,j}}]}(\tilde{\mathcal{R}}_{i,j}) \cap \tilde{\mathcal{R}}_{k,l} \neq \emptyset. \tag{5.6}$$

Thus, inspired by (5.5), via a reachability analysis tool we check if $\hat{\mathcal{X}}^{f}_{[\underline{\tau}_{\tilde{\mathcal{R}}_{i,j}}, \overline{\tau}_{\tilde{\mathcal{R}}_{i,j}}]}(\tilde{\mathcal{R}}_{i,j}) \cap \tilde{\mathcal{R}}_{k,l} \neq \emptyset$, which approximates condition (5.6), and if satisfied we define a transition $(\tilde{\mathcal{R}}_{i,j}, \tilde{\mathcal{R}}_{k,l}) \in \underset{/Q}{\longrightarrow}$.

In this way, the constructed abstraction contains all possible transitions $(\tilde{\mathcal{R}}_{i,j}, \tilde{\mathcal{R}}_{k,l})$ defined as in (5.6). Notice that, since (5.6) is a relaxation of the original transitions' definition, and $\hat{\mathcal{X}}^{f}_{[\underline{\tau}_{\tilde{\mathcal{R}}_{i,j}}, \overline{\tau}_{\tilde{\mathcal{R}}_{i,j}}]}(\tilde{\mathcal{R}}_{i,j}) \cap \tilde{\mathcal{R}}_{k,l} \neq \emptyset$ does not necessarily imply that $\mathcal{X}^{f}_{[\underline{\tau}_{\tilde{\mathcal{R}}_{i,j}}, \overline{\tau}_{\tilde{\mathcal{R}}_{i,j}}]}(\tilde{\mathcal{R}}_{i,j}) \cap \tilde{\mathcal{R}}_{k,l} \neq \emptyset$, the abstraction may contain additional transitions $(\tilde{\mathcal{R}}_{i,j}, \tilde{\mathcal{R}}_{k,l})$ for which $\nexists x \in \tilde{\mathcal{R}}_{i,j}$ and $\nexists x' \in \tilde{\mathcal{R}}_{k,l}$ such that $\zeta(H(x); x) = x'$. Nonetheless, the existence of spurious transitions does not affect the fact that $S_{/Q}$ ϵ-approximately simulates S.

Remark 5.4.2. *Since reachability analysis uses overapproximations, the computed intervals and transitions are not exact. Nonetheless, higher accuracy settings for reachability analysis imply more accurate intervals and transitions, establishing a trade-off between accuracy and offline computations.*

Remark 5.4.3. *Overapproximations $\hat{\mathcal{X}}^{f}_{[\underline{\tau}_{\tilde{\mathcal{R}}_{i,j}}, \overline{\tau}_{\tilde{\mathcal{R}}_{i,j}}]}(\tilde{\mathcal{R}}_{i,j})$ of the flowpipes of the ETC system (2.5) can be readily obtained by the -already computed from the previous step- flowpipes $\hat{\mathcal{X}}^{f_e}_{[\underline{\tau}_{\tilde{\mathcal{R}}_{i,j}}, \overline{\tau}_{\tilde{\mathcal{R}}_{i,j}}]}(\mathcal{I}_{i,j})$ of the extended system (2.8), by projecting to the ζ-variables: $\hat{\mathcal{X}}^{f}_{[\underline{\tau}_{\tilde{\mathcal{R}}_{i,j}}, \overline{\tau}_{\tilde{\mathcal{R}}_{i,j}}]}(\tilde{\mathcal{R}}_{i,j}) = \boldsymbol{\pi}_{\zeta} \hat{\mathcal{X}}^{f_e}_{[\underline{\tau}_{\tilde{\mathcal{R}}_{i,j}}, \overline{\tau}_{\tilde{\mathcal{R}}_{i,j}}]}(\mathcal{I}_{i,j})$. Thus, the only computation needed to determine transitions is calculating the intersections $\boldsymbol{\pi}_{\zeta} \hat{\mathcal{X}}^{f_e}_{[\underline{\tau}_{\tilde{\mathcal{R}}_{i,j}}, \overline{\tau}_{\tilde{\mathcal{R}}_{i,j}}]}(\mathcal{I}_{i,j}) \cap \tilde{\mathcal{R}}_{k,l}$. This is in contrast to [40], where computing timing intervals and determining transitions are two distinct computational steps.*

Remark 5.4.4. *The above method directly extends to systems with bounded disturbances and uncertainties, since many reachability analysis tools, such as Flow* [67], can handle bounded unknown signals.*

5.5. PARTITIONING THE STATE SPACE

Here, we propose a way of partitioning the state space into regions $\tilde{\mathcal{R}}_{i,j}$, based on approximations of IMs, derived in Chapters 3 and 4, providing control over the timing intervals

and improving their tightness, compared to naively partitioning X into polytopes. First, we present the ideal (albeit non-achievable) partitioning in these terms, which employs IMs. Afterwards, we show how to approximate it via inner approximations of IMs: we start with homogeneous ETC systems, and then we generalize employing a homogenization procedure. Finally, we provide a thorough discussion on the advantages of the proposed approach. For this section, we add the following mild assumptions:

Assumption 5.5.1. *The function $\phi(\cdot)$ is p-times continuously differentiable, the vector field $f_e(\cdot)$ of (2.8) is $p-1$-times continuously differentiable, and $p \geq 1$.*

Assumption 5.5.1 is necessary in order to be able to derive inner-approximations of IMs, as described in Chapters 3 and 4.

5.5.1. ISOCHRONOUS MANIFOLDS AND IDEAL PARTITIONING

Here, we demonstrate how IMs, if obtained exactly, enable a partition (hereby termed IM-partition) which is ideal w.r.t. the timing intervals: it a) provides complete control over the intervals, and b) is optimal in terms of correspondence between timing intervals and state-space regions. Let us, first, focus on homogeneous systems and triggering functions, for clarity.

From their very definition (Definition 3.4.1), it becomes clear how IMs constitute a notion relating regions in a system's state-space and intersampling times. In fact, due to Proposition 3.4.1, the sets R_i consisting of the points lying between two manifolds of times τ_i, τ_j with $\tau_i \leq \tau_j$ (see Fig. 5.1) satisfy:

$$R_i = \{x \in \mathbb{R}^n : \tau(x) \in [\tau_i, \tau_j]\}, \tag{5.7}$$

i.e. R_i is the set of all points with intersampling times in $[\tau_i, \tau_j]$. Thus, if IMs were obtained exactly, one could: choose a set of times $\{\tau_1, \tau_2, ..., \tau_q\}$, generate the IMs M_{τ_i}, and use the regions R_i between successive IMs to partition the state-space.

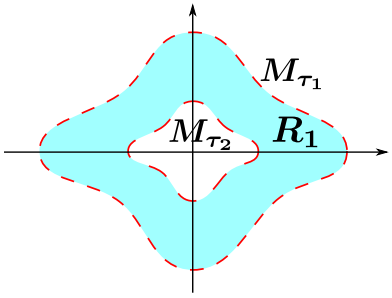

Figure 5.1: IMs (dashed lines) of a homogeneous ETC system for times $\tau_1 < \tau_2$. The region R_1 (filled region) satisfies (5.7).

The advantages of IM-partitioning are the following. First, complete control over the timing intervals is obtained, as the regions R_i are generated such that the corresponding timing intervals are equal to the chosen ones $[\tau_i, \tau_{i+1}]$ (due to (5.7)). Moreover, the IM-partition is optimal w.r.t. correspondence between regions and intervals: due to (5.7),

there is no set with bigger volume (Lebesgue measure) than R_i that corresponds to the same timing interval. This implies that IM-partitioning achieves the tightest intervals possible than any other partition, given a certain volume (or number) of regions.

The above advantages of IM-partitioning motivate us to employ the inner approximations of IMs derived earlier, in order to approximate this ideal way of partitioning.

5.5.2. STATE SPACE PARTITIONING FOR HOMOGENEOUS SYSTEMS VIA INNER APPROXIMATIONS OF IMS

For clarity, we first present how to partition with inner-approximations of IMs, in the context of homogeneous systems and triggering functions. To approximate IM-partitioning, one could divide the set X into regions $\mathscr{R}_i$ defined in (3.16), exactly as done in Chapter 3. However, the sets (3.16) are large for the reachability-analysis algorithms of Section 5.4 to be applied (e.g. see Fig. 5.1). Thus, we further partition them via cones $\mathscr{C}_j$ pointed at the origin and spanning $\mathbb{R}^n$. Hence, we obtain new sets $\mathscr{R}_{i,j}$ as intersections of approximations $\underline{M}_{\tau_i}$ and cones $\mathscr{C}_j$ (see Fig. 5.2):

$$\mathscr{R}_{i,j} = \mathscr{R}_i \cap \mathscr{C}_j \tag{5.8}$$

Finally, the regions $\tilde{\mathscr{R}}_{i,j}$ representing the states of the abstraction are obtained as intersections of sets $\mathscr{R}_{i,j}$ and the set of interest X (the compact state space):

$$\tilde{\mathscr{R}}_{i,j} = \mathscr{R}_{i,j} \cap X \tag{5.9}$$

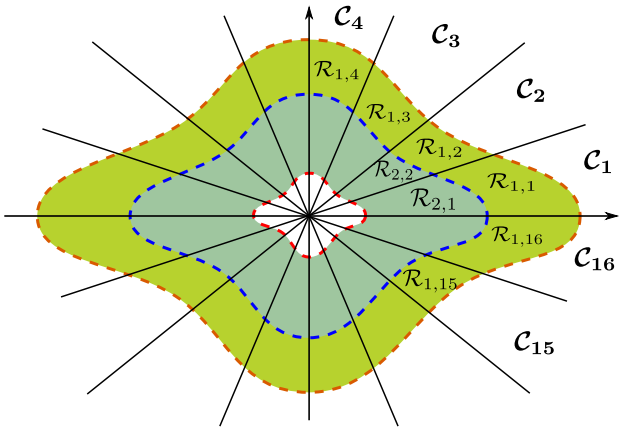

Figure 5.2: Regions $\mathscr{R}_{i,j}$ obtained as intersections of inner-approximations of IMs $\underline{M}_{\tau_i}$ (dashed lines) and cones $\mathscr{C}_j$.

To summarize the partitioning method:

1. Define a finite set of times $\{\tau_1, \ldots, \tau_q\}$ with $\tau_i < \tau_{i+1}$ and obtain the sets $\mathscr{R}_i$ according to (3.16).
2. Define a conic covering into cones $\mathscr{C}_j$ and obtain the sets $\mathscr{R}_{i,j}$ by (5.8).

3. Obtain the regions $\tilde{\mathcal{R}}_{i,j}$ by (5.9), which constitute the partition.

Note that some regions $\tilde{\mathcal{R}}_{i,j}$ might be empty sets, due to the intersection $\mathcal{R}_{i,j} \cap X$ being empty; such regions are discarded from the abstraction.

Remark 5.5.1. *Although the selected times τ_i provide a priori lower bounds on intersampling times for regions $\tilde{\mathcal{R}}_{i,j}$ (according to Corollary 3.4.1), simulations indicate that sometimes the algorithm of Section 5.4.1 provides less conservative bounds. Thus, the two ways of inferring timing lower bounds could be employed in a complementary way. Nonetheless, with the proposed partitioning method, reachability analysis for timing lower-bounds could be skipped, to reduce the offline computation time needed to compute the abstraction.*

5.5.3. STATE SPACE PARTITIONING FOR GENERAL NONLINEAR SYSTEMS

To extend the above partitioning method to general nonlinear systems and triggering functions, we employ the homogenization procedure (3.19). The state space of the ETC system is embedded in $\mathbb{R}^{n+1}$ and the sets $\mathcal{R}_{i,j}$ (5.8) are subsets of $\mathbb{R}^{n+1}$. Since X is now mapped to the set $\{(x,1) \in \mathbb{R}^{n+1} : x \in X\}$ (as commented in Section 3.7), which becomes our set of interest, the regions $\tilde{\mathcal{R}}_{i,j}$ are now obtained as:

$$\tilde{\mathcal{R}}_{i,j} = \mathcal{R}_{i,j} \cap \{(x,w) \in \mathbb{R}^{n+1} : x \in X, w = 1\},$$

Remark 5.5.2. *As discussed in Section 3.7.1, in cases where the origin is the equilibrium of the system and $\phi\Big((0,0)\Big) = 0$ (e.g. the ϕ from [7]), there is always a small region $\tilde{\mathcal{R}}_\star$ on the $(w=1)$-hyperplane containing $(0,0,\ldots,0,1)$ which is not covered by partitioning with approximations $\underline{M}_{\tau_i}$. This region can be defined as $\tilde{\mathcal{R}}_\star = \{(x,w) \in \mathbb{R}^{n+1} : x \in X, w = 1\} \setminus \bigcup_{i,j} \tilde{\mathcal{R}}_{i,j}$ and treated as an extra state of the abstraction.*

Remark 5.5.3. *The proposed partitioning method trivially extends to systems with bounded disturbances/uncertainties, by employing the approximations of IMs of perturbed uncertain systems derived in Chapter 4.*

5.5.4. DISCUSSION

Let us discuss the advantages of the proposed partition, compared to naively partitioning X into polytopes. The proposed method is certainly not ideal, as we only have inner approximations of IMs to work with. Nonetheless, our aim was to approximate the ideal IM-partition that was presented in Section 5.5.1, in order to partially gain some of the IM-partition's advantages.

First, the regions $\tilde{\mathcal{R}}_{i,j}$ generated by the proposed partition are expected to result into tighter intervals, compared to random polytopes of approximately the same volume. That is because they approximate the ideal shape of the regions R_i of Section 5.5.1, which are optimal in terms of correspondence between intersampling interval and volume. This claim is supported by simulation results in Section 5.6, which show that we can partition X with fewer regions (5.9) than polytopes and still obtain tighter intervals. Hence, with the proposed partition we contain one source of the abstraction's non-determinism.

In addition, due to Corollary 3.4.1, a region $\tilde{\mathscr{R}}_{i,j}$ is generated such that τ_i, which is chosen freely, is a lower bound on intersampling times. This provides some partial control over the intervals, in contrast to partitioning into random polytopes, where there is no obvious way of relating regions and timing bounds beforehand. Moreover, as a future direction, if outer approximations of IMs were obtained[2], they could be used to partition and gain control over the intervals' upper bounds as well (due to the scaling law 2.9). Finally, the proposed partitioning approach has the potential of approximating arbitrarily well IM-partitioning, by improving the method of approximating IMs.

5.6. NUMERICAL EXAMPLES

Here, we present simulation results supporting our theoretical developments. First, we apply the techniques of Section 5.4 combined with a naive partition, to abstract a perturbed nonlinear ETC system. Afterwards, we compare the partition proposed in Section 5.5 with naive partitioning, on an unperturbed system.

In the first example we use Flow*, whereas in the second we use dReach. Moreover, the sets $\mathscr{R}_{i,j}$ (5.8) are overapproximated by ball segments as described in Appendix 5.A, as they originally admit a transcendental representation which is currently not effectively handled by either Flow* or dReach. Ball segments can indeed be handled by dReach, but not by Flow*. On the other hand, dReach cannot handle disturbances, but Flow* can. That is why we employ naive partitioning in the perturbed system case. To abstract a perturbed system using the partition of Section 5.5, other options have to be explored, such as approximating the sets (5.8) by taylor models, which are handled by Flow*.

To measure the tightness of intervals of a given abstraction, we devise the two following metrics:

$$\text{AvgRatio} = \frac{\sum_{i,j} \frac{\overline{\tau}_{\tilde{\mathscr{R}}_{i,j}}}{\underline{\tau}_{\tilde{\mathscr{R}}_{i,j}}}}{\#\text{Regions}}, \quad \text{AvgDiff} = \frac{\sum_{i,j} \overline{\tau}_{\tilde{\mathscr{R}}_{i,j}} - \underline{\tau}_{\tilde{\mathscr{R}}_{i,j}}}{\#\text{Regions}} \tag{5.10}$$

The smaller these metrics the tighter the intervals. The difference between them is: in AvgDiff regions with larger intersampling times contribute more to the metric's value, while in AvgRatio all regions contribute the same, regardless of the time scales in which they operate. For our purposes, AvgRatio is more representative; we have also included AvgDiff, because it is closely connected to the definition of an abstraction's *precision* (the ϵ constant from Definition 5.2.2).

5.6.1. ABSTRACTING A PERTURBED NONLINEAR ETC SYSTEM

Consider the following nonlinear ETC system:

$$\dot{\zeta}_1 = -\zeta_1, \quad \dot{\zeta}_2 = \zeta_1^2\zeta_2 + \zeta_2^3 + u + d, \quad \dot{\varepsilon}_{\zeta_1} = -\dot{\zeta}_1, \quad \dot{\varepsilon}_{\zeta_2} = -\dot{\zeta}_2$$

with a Lebesgue-sampling triggering function $\phi\Big((\zeta(t),\varepsilon_\zeta(t))\Big) = \varepsilon_\zeta^2 - 0.01^2$, where $u = -(\zeta_2+\varepsilon_{\zeta_2}) - (\zeta_1+\varepsilon_{\zeta_1})^2(\zeta_2+\varepsilon_{\zeta_2}) - (\zeta_2+\varepsilon_{\zeta_2})^3$ is the control input, and $d \in [-0.1, 0.1]$ is a bounded unknown parameter (e.g. a disturbance or a model uncertainty).

[2] Deriving outer approximations of IMs is a difficult problem; e.g. there is no guarantee that a lower bound of the triggering function, derived as in Lemma 3.5.1, exhibits a zero-crossing w.r.t. time for any initial condition.

Let $X = [-2,2]^2$, and we partition it via 56 equal rectangles. The heartbeat is $\tau_{\max} = 0.022$. To compute the intervals $[\underline{\tau}_{\tilde{\mathcal{R}}_{i,j}}, \overline{\tau}_{\tilde{\mathcal{R}}_{i,j}}]$ and the transitions, we employ the algorithms of Section 5.4 and Flow*. Figure 5.3 depicts the computed timing lower and upper bounds for each region. The tightness metrics are AvgRatio ≈ 3.14 and AvgDiff ≈ 0.011. Figure 5.4 depicts the abstraction's transitions (418 in total).

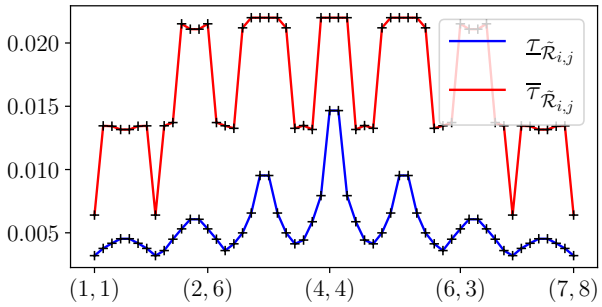

Figure 5.3: Perturbed ETC System: Timing lower and upper bounds for each region. The horizontal axis shows the regions' indices.

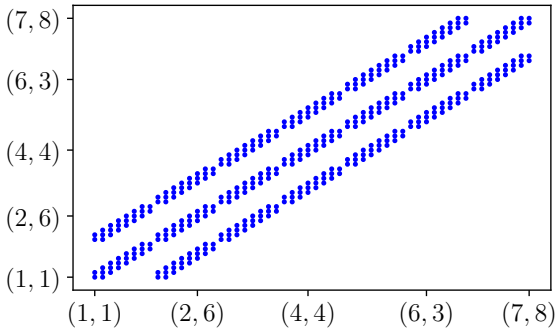

Figure 5.4: Perturbed ETC System: Transitions of the abstraction. Each dot $[(i,j),(k,l)]$ represents a transition $\tilde{\mathcal{R}}_{i,j} \to \tilde{\mathcal{R}}_{k,l}$.

Finally, we simulate a run of the ETC system to showcase our results' validity. Specifically, the system is initialized at $(1.3, 1.3)$, and the disturbance is $d(t) = 0.1\sin(10t)$. The duration is 2s. Figure 5.5 depicts the results. The red line is the evolution of the actual ETC intersampling times during the run, while the blue lines represent the intervals $[\underline{\tau}_{\tilde{\mathcal{R}}_{i,j}}, \overline{\tau}_{\tilde{\mathcal{R}}_{i,j}}]$ generated by the abstraction (by checking at which region $\tilde{\mathcal{R}}_{i,j}$ the state belonged at each time, and plotting its associated interval). As expected, the intersampling time is always confined in $[\underline{\tau}_{\tilde{\mathcal{R}}_{i,j}}, \overline{\tau}_{\tilde{\mathcal{R}}_{i,j}}]$. Moreover, it caps at $\tau_{\max} = 0.022$. The system's trajectory followed the spatial path: $\tilde{\mathcal{R}}_{6,7} \to \cdots \to \tilde{\mathcal{R}}_{6,6} \to \cdots \to \tilde{\mathcal{R}}_{5,6} \to \cdots \to \tilde{\mathcal{R}}_{5,5} \to \cdots \to \tilde{\mathcal{R}}_{4,5} \to \ldots$, where the dots indicate that the trajectory stayed in the previous region for multiple intersampling intervals. Note that all transitions taken during the run are contained in

the transition set of the abstraction (Fig. 5.4).

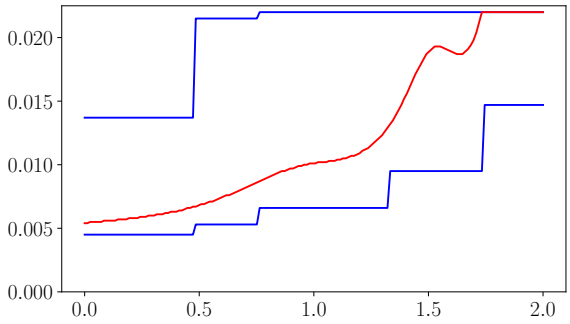

Figure 5.5: Time evolution of the ETC system's intersampling times (red line) and the intervals $[\underline{\tau}_{\tilde{\mathscr{R}}_{i,j}}, \overline{\tau}_{\tilde{\mathscr{R}}_{i,j}}]$ (blue lines) generated by the abstraction, during a run.

5.6.2. PERFORMANCE OF THE PARTITIONING APPROACH OF SECTION 5.5

To compare our proposed partition with naive partitioning, consider the unperturbed version of the ETC system presented in the previous numerical example, let $X = [-2,2]^2$ and $\tau_{\max} = 0.021$. For naive partitioning, we divide again X into 56 equal rectangles and calculate the intervals $[\underline{\tau}_{\tilde{\mathscr{R}}_{i,j}}, \overline{\tau}_{\tilde{\mathscr{R}}_{i,j}}]$. The results appear in Fig. 5.6. The tightness metrics are AvgRatio ≈ 1.74 and AvgDiff ≈ 0.0045. The total transitions of the abstraction are 367. We observe that the timing intervals are considerably tighter and the number of transitions is smaller, when the disturbance is absent. That is because unknown parameters in the dynamics give rise to infinite possible behaviours, implying larger non-determinism. Moreover, reachability-analysis tools behave more conservatively, when unknown parameters are present.

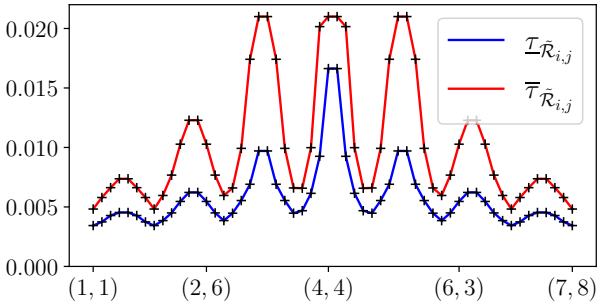

Figure 5.6: Naive Partition: Lower and upper bounds of intersampling times for each region.

For the partitioning approach of Section 5.5, after homogenizing the system and the triggering function as in (3.19) with $\alpha = 2$ and $\theta = 1$, we define the set of times $\{.002, .0028, .0038, .005, .0065, .0075\}$ and derive inner-approximations of the corresponding IMs and the sets $\mathscr{R}_i$, as per (3.16). To further divide $\mathscr{R}_i$ into $\mathscr{R}_{i,j}$, we use 9 polyhedral

cones $\mathscr{C}_j$ pointed at the origin of $\mathbb{R}^{n+1}$, that cover the set of interest $\{(x,w) \in \mathbb{R}^{n+1} : x \in X, w = 1\}$; i.e. $\bigcup_j (\mathscr{C}_j \cap \{(x,w) \in \mathbb{R}^{n+1} : w = 1\}) = \{(x,w) \in \mathbb{R}^{n+1} : x \in X, w = 1\}$[3]. Finally, after obtaining the regions $\tilde{\mathscr{R}}_{i,j}$ (5.9), the total number of abstraction states is 49 (recall that the number of regions $\tilde{\mathscr{R}}_{i,j}$ can be smaller than $|\{\mathscr{R}_i\}| \cdot |\{\mathscr{C}_j\}|$, where $|\cdot|$ denotes set cardinality, since empty intersections (5.9) are discarded). The computed intervals $[\underline{\tau}_{\tilde{\mathscr{R}}_{i,j}}, \overline{\tau}_{\tilde{\mathscr{R}}_{i,j}}]$ are depicted in Fig. 5.7. The tightness metrics are AvgRatio ≈ 1.54 and AvgDiff ≈ 0.0032. The total number of transitions is 471.

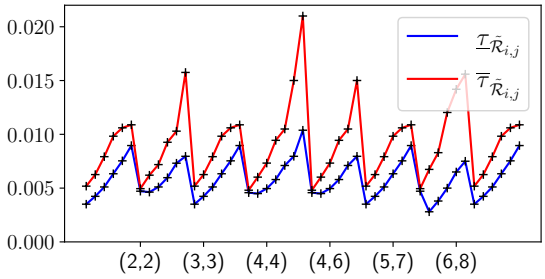

Figure 5.7: Proposed Partition: Lower and upper bounds of intersampling times for each region.

The partition of Section 5.5 achieves considerably tighter intervals even with a smaller amount of regions, compared to the naive one. This supports the claims of Section 5.5.4: it leads to tighter intervals, thus containing one of the sources of non-determinism. On the other hand, we observe that it has led to an abstraction with larger transition set. That may be because the sets (5.8) have been overapproximated by ball segments, which in some cases might be a crude approximation, while the naive partition's rectangles are fed directly to the reachability-analysis algorithm. In other words, while tighter intervals are an inherent characteristic of the partition of Section 5.5, the large number of transitions is probably due to coarse overapproximations.

5.7. CONCLUSION

We abstracted the sampling behaviour of perturbed uncertain nonlinear ETC systems with general triggering functions. Thus, we have significantly extended the applicability of abstraction-based scheduling of traffic in networks of ETC loops. To capture the sets of intersampling times that the given ETC system may generate, we formulated and solved reachability-analysis problems. In addition, we proposed a state-space partitioning method based on IMs, which provides partial control over the abstraction's accuracy and leads to tighter timing intervals, compared to naive partitioning. However, in the performed simulations it has led to larger transition sets, probably because of the crude overapproximations used to facilitate reachability analysis. This effect could be alleviated by employing more accurate approximations of the sets (5.8) (e.g. polynomial zonotopes or Taylor models), to reduce the size of the transition set, while keeping the timing

[3] A way to create this conic covering is to divide $\{(x,w) : x \in X, w = 1\}$ into 9 squares, and obtain $\mathscr{C}_j$ as the conic hull of the j-th square's vertices.

intervals tight, thus overall containing the abstraction's non-determinism. Finally, it has to be emphasized that the constructed abstractions suffer from the curse of dimensionality, like many abstraction-based approaches.

5.A. APPROXIMATING THE REGIONS $\mathscr{R}_{i,j}$ BY BALL SEGMENTS

To obtain the timing bounds $[\underline{\tau}_{\tilde{\mathscr{R}}_{i,j}}, \overline{\tau}_{\tilde{\mathscr{R}}_{i,j}}]$ and the state transitions, reachability analysis on the regions $\tilde{\mathscr{R}}_{i,j}$ is conducted. However, it is obvious from (3.15) and (3.16) that the sets $\mathscr{R}_{i,j}$ (which make up $\tilde{\mathscr{R}}_{i,j}$ through (5.9)) are transcendental, which renders their computational handling very difficult. To the authors' knowledge, there are no reachability analysis tools that can handle effectively such sets. Hence, we have provided an algorithm to overapproximate them.

In general, the overapproximation of transcendental sets is very challenging. However, leveraging special characteristics of the specific representation, we devised an algorithm that overapproximates the sets $\mathscr{R}_{i,j}$ by ball segments (Fig. 5.8):

$$\hat{\mathscr{R}}_{i,j} := \{x \in \mathscr{C}_j : \underline{r}_{i+1,j} \le |x| \le \overline{r}_{i,j}\}. \tag{5.11}$$

To obtain the ball segments (5.11), $\underline{r}_{i+1,j}$ and $\overline{r}_{i,j}$ must be determined; i.e. spherical

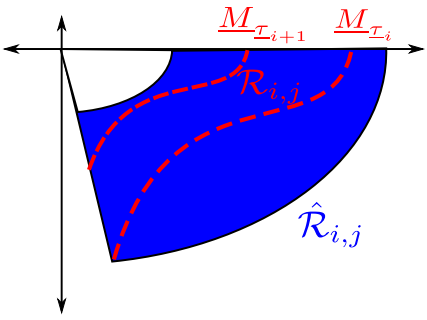

Figure 5.8: Ball segment $\hat{\mathscr{R}}_{i,j}$ (blue region) overapproximating $\mathscr{R}_{i,j}$ (region delimited by the red lines and the cone).

segments (intersections of spheres with cones) that inner- and outer- approximate the conic sections $\underline{M}_{\underline{\tau}_{i+1}} \cap \mathscr{C}_j$ and $\underline{M}_{\underline{\tau}_i} \cap \mathscr{C}_j$, respectively, have to be found (see Fig. 5.8), where $\underline{M}_{\underline{\tau}_i}$ represents the inner-approximation of IM $M_{\underline{\tau}_i}$ that has been used to define $\mathscr{R}_{i,j}$.

A whole sphere $S_r := \{x \in \mathbb{R}^n : |x| = r\}$ inner-approximates the whole $\underline{M}_{\underline{\tau}_\star}$ if it lies entirely in the region enclosed by $\underline{M}_{\underline{\tau}_\star}$, that is if $\mu(x, \underline{\tau}_\star) \le 0$ for all $x \in S_r$. Likewise, a spherical segment $S_{\underline{r}_{\star,j}} \cap \mathscr{C}_j$ inner-approximates $\underline{M}_{\underline{\tau}_\star} \cap \mathscr{C}_j$ if the following holds:

$$\forall x \in S_{\underline{r}_{\star,j}} \cap \mathscr{C}_j : \quad \mu(x, \underline{\tau}_\star) \le 0. \tag{5.12}$$

Formulas like (5.12) can be verified or disproved by SMT solvers, like dReal [53]. Thus, a line search on $\underline{r}_{\star,j}$ could be employed, by iteratively checking (5.12). In our case though, $\mu(x, \underline{\tau}_\star) \le 0$ implies the numerically non-robust symbolic computation of the

matrix exponential $e^{A(\frac{|x|}{\rho})^\alpha \underline{\tau}_\star}$ over the symbolic variable x. Luckily, since we want to verify $\mu(x, \underline{\tau}_\star) \leq 0$ on a spherical segment $S_{\underline{r}_{\star,j}} \cap \mathscr{C}_j$, we can fix $|x| \leftarrow \underline{r}_{\star,j}$, which renders the symbolic matrix exponential a regular numerical one and severely relaxes computations, i.e. $e^{A(\frac{|x|}{\rho})^\alpha \underline{\tau}_\star} = e^{A(\frac{\underline{r}_{\star,j}}{\rho})^\alpha \underline{\tau}_\star}$ for all $x \in S_{\underline{r}_{\star,j}} \cap \mathscr{C}_j$. This is done by fixing the first argument of $\mu(\cdot, \underline{\tau}_\star)$ as: $\mu(\frac{x}{|x|}\underline{r}_{\star,j}, \underline{\tau}_\star)$. Consequently, in order to find a spherical inner-approximation $S_{\underline{r}_{\star,j}} \cap \mathscr{C}_j$ of the conic section $\underline{M}_{\underline{\tau}_\star} \cap \mathscr{C}_j$, we employ a line search on the radius $\underline{r}_{\star,j}$ and check iteratively by an SMT solver the following condition:

$$\forall x \in S_{\underline{r}_{\star,j}} \cap \mathscr{C}_j : \quad \mu(\frac{x}{|x|}\underline{r}_{\star,j}, \underline{\tau}_\star) \leq 0. \tag{5.13}$$

By reversing inequality (5.13) we determine an outer-approximation $S_{\overline{r}_{\star,j}} \cap \mathscr{C}_j$ of $\underline{M}_{\underline{\tau}_\star} \cap \mathscr{C}_j$. Fig. 5.9 shows spherical inner/outer-approximations of $\underline{M}_{\underline{\tau}_\star}$ for each conic section.

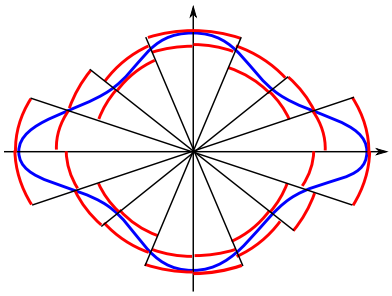

Figure 5.9: Spherical inner- and outer-approximations for each conic section of $\underline{M}_{\underline{\tau}_\star}$.

Finally, as soon as all radii $\underline{r}_{i,j}, \overline{r}_{i,j}$ are obtained, the regions $\mathscr{R}_{i,j}$ are overapproximated by ball segments $\hat{\mathscr{R}}_{i,j}$ (5.11). Then, reachability analysis can be conducted on the sets $\hat{\mathscr{R}}_{i,j} \cap X$, which are overapproximations of $\tilde{\mathscr{R}}_{i,j}$.

Remark 5.A.1. *The scaling property (3.9c) of μ, i.e. $\mu(\lambda x, t) = \lambda^{\theta+1}\mu(x, \lambda^\alpha t)$, can be employed to alleviate computations when computing the overapproximations. Specifically, as soon as the radii $\underline{r}_{\star,j}, \overline{r}_{\star,j}$ have been obtained for one approximation $\underline{M}_{\underline{\tau}_\star}$, we can use them and (3.9c) to derive all $\underline{r}_{i,j}, \overline{r}_{i,j}$. Observe that (3.9c) implies that $x \in \underline{M}_{\underline{\tau}_\star} \implies \lambda x \in \underline{M}_{\lambda^{-\alpha}\underline{\tau}_\star}$. Thus, if $S_{\underline{r}_{\star,j}} \cap \mathscr{C}_j$ is an inner-approximation of $\underline{M}_{\underline{\tau}_\star} \cap \mathscr{C}_j$, then $S_{\lambda\underline{r}_{\star,j}} \cap \mathscr{C}_j$ is an inner-approximation of $\underline{M}_{\lambda^{-\alpha}\underline{\tau}_\star} \cap \mathscr{C}_j$. Consequently, to obtain inner- and outer-approximations of all conic sections $\underline{M}_{\underline{\tau}_i} \cap \mathscr{C}_j$ $(i = 1, \ldots, q)$, we scale the obtained radii accordingly by corresponding factors $\lambda_i = \left(\frac{\underline{\tau}_\star}{\underline{\tau}_i}\right)^{\frac{1}{\alpha}}$, so that we get: $\underline{r}_{i,j} = \lambda_i \underline{r}_{\star,j}$ and $\overline{r}_{i,j} = \lambda_i \overline{r}_{\star,j}$.*

6

Formal Analysis of the Sampling Behaviour of Stochastic Event-Triggered Control

In this chapter, we formally analyze the sampling behaviour of stochastic linear periodic ETC (PETC) systems by computing bounds on associated metrics. Specifically, we consider functions over sequences of state measurements and intersampling times that can be expressed as average, multiplicative or cumulative rewards, and introduce their expectations as metrics on PETC's sampling behaviour. We compute bounds on these expectations, by constructing appropriate Interval Markov Chains equipped with suitable reward structures, that abstract stochastic PETC's sampling behaviour, and employing value iteration over these IMCs. Our results are illustrated on a numerical example, for which we compute bounds on the expected average intersampling time and on the probability of triggering with the maximum possible intersampling time in a finite horizon.

This chapter has been published in [69]. Some changes have been made to streamline presentation. A preliminary version has been published in [70]. The results of Appendix 6.C appear here for the first time.

6.1. INTRODUCTION

In this chapter, we formally analyze the sampling (vs. control) behaviour of stochastic ETC systems by computing bounds on associated metrics. In particular, we consider stochastic narrow-sense linear PETC systems with a Lebesgue-sampling triggering function. We define their sampling behaviour as the set Y of all possible sequences of state-measurements and intersampling times along with its associated probability measure. We introduce expectations of functions $g : \mathrm{Y} \to \mathbb{R}$ as metrics on ETC's sampling behaviour. Here, we focus on functions g described as cumulative, average or multiplicative rewards, i.e. $g_\star$ with $\star \in \{\mathrm{cum}, \mathrm{avg}, \mathrm{mul}\}$. This class of functions is rather standard in the context of quantitative analysis of stochastic systems, and it extends to including specifications of PCTL (Probabilistic Computation Tree Logic, see [71]). Besides, it is able to describe various metrics on ETC's sampling performance, as demonstrated through examples. The problem statement of this work is to obtain bounds on expectations of functions $g_\star$.

To address the problem, we construct IMCs (interval Markov chains; Markov chains with interval transition probabilities) that capture PETC's sampling behaviour. Then, we equip the IMCs with appropriate state-dependent rewards and prove that the {cum, avg, mul} reward over the paths of the IMC indeed bounds the expectation of $g_\star$ (Theorem 6.4.1). The IMC rewards can easily be computed via well-known value-iteration algorithms (see, e.g., [72]).

The main challenge in constructing the IMC is computing the IMC's probability intervals. For that, we study the joint probabilities of transitioning from one region of the state-space to another one with the intersampling time taking a specific value. Computation of these probabilities is more complicated than the traditional transition probabilities that appear in the literature of IMC-abstractions (e.g., [73]–[76]), due to the presence of intersampling time as an event. To cope with that, we employ a series of convex relaxations and the fact that the system's state is a Gaussian process. That way, we reformulate computing these probabilities as optimization problems of log-concave objective functions and hyperrectangle constraint sets, which are easy to solve. Our results are demonstrated through a numerical example, where we compute bounds on the expected average intersampling time and on the probability of triggering with the maximum possible intersampling time in a finite horizon.

Finally, it is worth noting that, as a side contribution, in Appendix 6.C, we provide a proof that Lebesgue sampling guarantees *practical mean-square stability* for linear stochastic PETC systems, under mild assumptions, as, to our knowledge, it is missing from the related literature [14]–[17].

6.2. NOTATION AND PRELIMINARIES

6.2.1. NOTATION

Given a set $X \subseteq \mathbb{R}$, $X_{[a,b]} = X \cap [a, b]$. Given a set S in some space X, we denote: its indicator function by $\mathbb{1}_S(\cdot)$, its Borel σ-algebra by $\mathscr{B}(S)$, its complement by $\overline{S} = X \setminus S$, and the k-times Cartesian product $S = S \times \cdots \times S$ by S^k. Given $x \in \mathbb{R}^n$, denote by $\{x\}^k$: both the k-times Cartesian product $\{x\} \times \cdots \times \{x\}$ and the kn-dimensional vector $\begin{bmatrix} x^\top & \dots & x^\top \end{bmatrix}^\top$. Given sets Q_1, Q_2 and $Q = Q_1 \times Q_2$, for any $q = (q_1, q_2) \in Q$ denote $\mathbf{proj}_{Q_1}(q) = q_1$ and $\mathbf{proj}_{Q_2}(q) = q_2$. Given two sets Q_1, Q_2 in some space, denote $Q_1 + Q_2 = \{q_1 + q_2 : q_1 \in Q_1, q_2 \in Q_2\}$

(Minkowski sum) and $Q_1 - Q_2 = \{q_1 - q_2 : q_1 \in Q_1, q_2 \in Q_2\}$ (Minkowski difference). Finally, consider a set $S(x) \subseteq \mathbb{R}^n$ that varies with a parameter $x \in \mathbb{R}^m$ (equivalent to a set-valued function $S : \mathbb{R}^m \to 2^{\mathbb{R}^n}$). We say that $S(x)$ is *linear on* x, if $S(x) = S' + \{Ax\}$, where $A \in \mathbb{R}^{n \times m}$ and $S' \subseteq \mathbb{R}^n$.

Given a random variable x and an associated probability measure $\mathbb{P}$, we denote its expectation w.r.t. $\mathbb{P}$ by $\mathrm{E}_{\mathbb{P}}[x]$ (when $\mathbb{P}$ is clear from the context, it might be omitted). We use the term 'path' or 'sequence' interchangeably. Given a finite path $\omega = q_0, q_1 \ldots, q_N$, denote $\omega(i) = q_i$ and $\omega(end) = \omega(N) = q_N$. Given a function $g(\omega)$ of paths ω, we denote $\mathrm{E}^{q_0}[g(\omega)] \equiv \mathrm{E}[g(\omega)|\omega(0) = q_0]$. Finally, $\mathcal{N}(\mu, \Sigma)$ denotes the Gaussian distribution with mean μ and covariance matrix Σ.

6.2.2. REWARDS OVER PATHS

Consider a set Q and a set Y of paths of length $N+1$, such that: $\omega(i) \in Q$, for all $\omega \in \mathrm{Y}$ and $0 \leq i \leq N$. Assume a probability measure $\mathbb{P}$ over $\mathscr{B}(\mathrm{Y})$ (for how to define $\mathscr{B}(\mathrm{Y})$ in our context, see Section 6.3.2). Define a *reward function* $R : Q \to [0, R_{\max}]$. We define the following expectations:

- *Cumulative (discounted) reward*: $\mathrm{E}_{\mathbb{P}}[g_{\mathrm{cum},N}(\omega)] \equiv \mathrm{E}_{\mathbb{P}}[\sum_{i=0}^{N} \gamma^i R(\omega(i))]$, where $\gamma \in [0,1]$.
- *Average reward*: $\mathrm{E}_{\mathbb{P}}[g_{\mathrm{avg},N}(\omega)] \equiv \mathrm{E}_{\mathbb{P}}[\frac{1}{N+1} \sum_{i=0}^{N} R(\omega(i))]$.
- *Multiplicative reward*: $\mathrm{E}_{\mathbb{P}}[g_{\mathrm{mul},N}(\omega)] \equiv \mathrm{E}_{\mathbb{P}}[\prod_{i=0}^{N} R(\omega(i))]$.

These expectations can describe a wide range of quantitative/qualitative properties of paths in Y, and they have been employed for verification in numerous settings, such as (interval) Markov chains (e.g. [73]–[76]), stochastic hybrid systems (e.g., [77]), etc. Later, we showcase their descriptive power within our framework (see Section 6.3.2).

6.2.3. INTERVAL MARKOV CHAINS (IMCS)

Interval Markov Chains are Markov models with interval transition probabilities, and they are defined as:

Definition 6.2.1 (Interval Markov Chain (IMC))**.** *An IMC is a tuple* $\mathrm{S}_{\mathrm{imc}} = \{Q, \check{P}, \hat{P}\}$, *where:* Q *is a finite set of states, and* $\check{P}, \hat{P} : Q \times Q \to [0,1]$ *are functions, with* $\check{P}(q,q')$ *and* $\hat{P}(q,q')$ *representing lower and upper bounds on the probability of transitioning from state* q *to* q', *respectively.*

For all $q \in Q$, we have that $\check{P}(q,q') \leq \hat{P}(q,q')$ and $\sum_{q' \in Q} \check{P}(q,q') \leq 1 \leq \sum_{q' \in Q} \hat{P}(q,q')$. A path of an IMC is a sequence of states $\omega = q_0, q_1, q_2, \ldots$, with $q_i \in Q$. Denote the set of the IMC's finite paths by $Paths(\mathrm{S}_{\mathrm{imc}})$. Given a state $q \in Q$, a transition probability distribution $p_q : Q \to [0,1]$ is called *feasible* if $\check{P}(q,q') \leq p_q(q') \leq \hat{P}(q,q')$ for all $q' \in Q$. Given $q \in Q$, its set of feasible distributions is denoted by Γ_q. We denote by $\Gamma_Q = \{p_q : p_q \in \Gamma_q, q \in Q\}$ the set of all feasible distributions for all states.

Definition 6.2.2 (Adversary)**.** *Given an IMC* $\mathrm{S}_{\mathrm{imc}}$, *an* adversary *is a function* $\boldsymbol{\pi} : Paths(\mathrm{S}_{\mathrm{imc}}) \to \Gamma_Q$, *such that* $\boldsymbol{\pi}(\omega) \in \Gamma_{\omega(end)}$, *i.e. given a finite path it returns a feasible distribution w.r.t. the path's last element.*

The set of all adversaries is denoted by Π. Given a $\boldsymbol{\pi} \in \Pi$ and $\omega(0) = q_0$, an IMC path evolves as follows: at any time-step $i > 0$, $\boldsymbol{\pi}$ chooses a distribution $p \in \Gamma_{\omega(i-1)}$ from which $\omega(i)$ is sampled.

IMCs may be equipped with a reward function $R : Q \to [0, R_{\max}]$. Given a $\boldsymbol{\pi} \in \Pi$ and an initial condition $q_0 \in Q$, all expectations listed in Section 6.2.2 are well-defined and single-valued: e.g., $\mathrm{E}^{q_0}_{\boldsymbol{\pi}}[g_{\mathrm{cum},N}(\omega)]$ (see [72]). However, due to the existence of infinite adversaries, the IMC produces whole ranges of such expectations. The bounds of these ranges, e.g. $(\sup_{\boldsymbol{\pi}\in\Pi}$ and) $\inf_{\boldsymbol{\pi}\in\Pi} \mathrm{E}^{q_0}_{\boldsymbol{\pi}}[g_{\mathrm{cum},N}(\omega)]$, can be computed via well-known *value iteration* algorithms (e.g., see [72], [78]).

6.3. THE SAMPLING BEHAVIOUR OF STOCHASTIC PETC: FRAMEWORK AND PROBLEM STATEMENT

6.3.1. LINEAR STOCHASTIC PETC SYSTEMS

Consider a state-feedback stochastic linear control system:

$$d\zeta(t) = A\zeta(t)dt + BK\zeta(t)dt + B_w dW(t),$$

where: A, B, K, B_w are matrices of appropriate dimensions, $\zeta(t) \in \mathbb{R}^n$ is the state, and $W(t)$ is an n_w-dimensional Wiener process on a complete probability space $(\Omega, \mathscr{F}, \{\mathscr{F}_t\}_{t\geq 0}, \mathbb{P})$. Ω denotes the sample space, $\mathscr{F}$ the σ-algebra generated by W, $\{\mathscr{F}_t\}_{t\geq 0}$ the natural filtration and $\mathbb{P}$ the probability measure. We denote the solution of the above stochastic differential equation with initial condition ζ_0 by $\zeta(t;\zeta_0)$.

In PETC, as in conventional ETC, the control input is held constant between consecutive sampling times t_i, t_{i+1} and is only updated on such times:

$$d\zeta(t) = A\zeta(t)dt + BK\zeta(t_i)dt + B_w dW(t), \quad t \in [t_i, t_{i+1}), \tag{6.1}$$

The sampling times are determined by the *triggering condition*:

$$t_{i+1} = t_i + \min\left\{k_{\max}h, \min\left\{kh : k \in \mathbb{N}, \phi\Big(\zeta(kh;\zeta(t_i)), \zeta(t_i)\Big) > 0\right\}\right\} \tag{6.2}$$

where $t_0 = 0$, $h > 0$ is a *checking period*, $k_{\max} \in \mathbb{N}_{>0}$, ϕ is the triggering function and $t_{i+1} - t_i$ is the intersampling time. Notice the presence of a maximum allowed intersampling time $k_{\max}h$. PETC works as follows during an intersampling interval $[t_i, t_{i+1})$: at time t_i the triggering function $\phi(\zeta(t_i), \zeta(t_i))$ is negative; the sensors check periodically, with period h, if the triggering function is positive; if it is found positive, or if $k_{\max}h$ time has elapsed since t_i, a new event t_{i+1} is triggered, the latest state-measurement is sent to the controller which updates the control action, and the whole process is repeated again. We call the combination (6.1)-(6.2) *(stochastic) PETC system.*

In stochastic PETC, intersampling time is a random variable that depends on the previously measured state and we denote it as follows:

$$\tau(x) = \min\left\{k_{\max}h, \min\left\{kh : k \in \mathbb{N}, \phi\Big(\zeta(kh;x), x\Big) > 0\right\}\right\}$$

where $x \in \mathbb{R}^n$ is the previously measured state. Note that, because the system is time-homogeneous, reasoning w.r.t. the interval $[t_i, t_{i+1})$ is equivalent to reasoning w.r.t. $[0, t_{i+1} - t_i)$.

Assumption 6.3.1. *We assume the following:*

1. *The matrix pair* (A, B_w) *is controllable.*
2. *The checking period* $h = 1$.
3. $\phi(\zeta(t;x), x) = |\zeta(t;x) - x|_\infty - \epsilon$, *where* $\epsilon > 0$ *is a predefined constant.*

Item 1 guarantees that $\zeta(t)$ is a non-degenerate Gaussian random variable (see [75]) and item 2 is for ease of presentation and without loss of generality. Regarding item 3, ϕ is the well-studied Lebesgue-sampling triggering function [6] with an ∞-norm instead of a 2-norm. In Appendix 6.C, we provide a proof that Lebesgue sampling guarantees *practical mean-square stability* for linear stochastic PETC systems, under mild assumptions, as, to our knowledge, it is missing from the related literature [14]–[17]. Finally, in Remark 6.5.2, we discuss briefly how our results can be extended to more general triggering functions.

6.3.2. SAMPLING BEHAVIOUR AND ASSOCIATED METRICS

A stochastic PETC system may exhibit different sequences of state-measurements and intersampling times $(\zeta_0, t_0), (\zeta(t_1), t_1 - t_0), (\zeta(t_2), t_2 - t_1), \ldots$, where t_i are sampling times. We call *sampling behaviour*, the set of all possible such sequences:

Definition 6.3.1 (Sampling Behaviour)**.** *We call* N-sampling behaviour *of stochastic PETC system* (6.1)-(6.2) *the set:*

$$\mathrm{Y}_N = \{(x_0, s_0), (x_1, s_1), (x_2, s_2), \ldots, (x_N, s_N) : \; x_i \in \mathbb{R}^n, s_i \in \mathbb{N}_{[0,k_{\max}]}\} \tag{6.3}$$

where $N \in \mathbb{N}$. *When* N *is clear from the context, it is omitted.*

We denote $Q := \mathbb{R}^n \times \mathbb{N}_{[0,k_{\max}]}$. Given an initial condition $y_0 = (x_0, s_0) \in Q$, the set Y_N is associated to a probability measure $\mathbb{P}^{y_0}_{\mathrm{Y}_N}$ (conditioned on y_0) which is inductively defined over $\mathscr{B}(\mathrm{Y}_N)$ as follows[1]:

$$\mathbb{P}^{y_0}_{\mathrm{Y}_N}(\omega(0) \in (X_0, s_0)) = \mathbb{1}_{(X_0,s_0)}(y_0) \tag{6.4}$$

$$\mathbb{P}^{y_0}_{\mathrm{Y}_N}(\omega(i+1) \in (X_{i+1}, s_{i+1}) \mid \omega(i) = (x_i, s_i)) = \mathbb{P}(\zeta(s_{i+1}; x_i) \in X_{i+1}, \tau(x_i) = s_{i+1}) \tag{6.5}$$

where $\omega \in \mathrm{Y}_N$, $s_0, s_i, s_{i+1} \in \mathbb{N}_{[0,k_{\max}]}$, $x_i \in \mathbb{R}^n$, $X_0, X_{i+1} \subseteq \mathbb{R}^n$ and we use (X, s) to denote the set $\{(x, s) : x \in X\}$. This measure is well-defined, even when the horizon $N = +\infty$, according to the Ionescu-Tulcea theorem [79].

Remark 6.3.1. *As noted in Section 6.3.1, typically it is assumed that the first sampling time* $t_0 = 0$, *which implies that the first intersampling time* $s_0 = t_0 - 0 = 0$ *and the initial condition is* $y_0 = (x_0, 0)$.

Remark 6.3.2. *Under item 3 of Assumption 6.3.1, and in every Zeno-free ETC scheme,* $\mathbb{P}(\tau(x) = 0) = 0$ *for any* $x \in \mathbb{R}^n$, *because the triggering function is strictly negative for* $k = 0$. *Thus, for any* $i \geq 1$ *and* $\omega \in \mathrm{Y}_N$: $\mathbb{P}_{\mathrm{Y}_N}(\boldsymbol{proj}_{\mathbb{N}_{[0,k_{\max}]}}(\omega(i)) = 0) = 0$. *Note that this is not in contrast with Remark 6.3.1 that only reasons about initial conditions* (x_0, s_0) *and not* (x_i, s_i) *with* $i \geq 1$.

[1] Consider Q^{N+1} endowed with its product topology. Then $\mathscr{B}(\mathrm{Y}_N)$ is the σ-algebra generated by cylinder sets of Q^{N+1}.

Studying PETC's sampling behaviour may be formalized by defining functions $g : \mathrm{Y}_N \to \mathbb{R}$ and computing their expectations $\mathrm{E}_{\mathbb{P}^{y_0}_{\mathrm{Y}_N}}[g(\omega)]$. Here, we focus on functions that can be described as cumulative $g_{\mathrm{cum},N}$, average $g_{\mathrm{avg},N}$ or multiplicative $g_{\mathrm{mul},N}$ rewards (see Section 6.2.2). By appropriately choosing the reward R, these classes of functions can describe many interesting properties of PETC's sampling behaviour:

- *Example 1:* Consider $R(x,s) = s$. Then $\mathrm{E}_{\mathbb{P}^{y_0}_{\mathrm{Y}_N}}[g_{\mathrm{avg},N}(\omega)]$ is the expected average intersampling time: the larger it is, the less frequently the system is expected to sample, saving more bandwidth and energy.

- *Example 2:* Consider $R(x,s) = \min(\alpha \frac{1}{|x|+\varepsilon} + \beta s, R_{\max})$, with $\alpha, \beta, \varepsilon > 0$, penalizing paths that overshoot far from the origin or exhibit a high sampling frequency. A bigger $\mathrm{E}_{\mathbb{P}^{y_0}_{\mathrm{Y}_N}}[g_{\mathrm{cum},N}(\omega)]$ implies better performance in terms of stabilization speed and sampling frequency. Observe how incorporating state-measurements x in our definition of sampling behaviour, allows to include control-performance related metrics, apart from sampling-performance metrics.

- *Example 3:* Consider the reward:

$$R(x,s) = \begin{cases} 0, & \text{if } s = k_{\max} \\ 1, & \text{otherwise} \end{cases}$$

Then, we have that:

$$\mathrm{E}_{\mathbb{P}^{y_0}_{\mathrm{Y}_N}}[g_{\mathrm{mul},N}(\omega)] = \mathbb{P}^{y_0}_{\mathrm{Y}_N}\left(\mathbf{proj}_{\mathbb{N}_{[0,k_{\max}]}}(\omega(i)) \neq k_{\max},\ \forall i\right)$$

$\mathrm{E}_{\mathbb{P}^{y_0}_{\mathrm{Y}_N}}[g_{\mathrm{mul},N}(\omega)]$ is the probability that there is no intersampling time $s = k_{\max}$ in the next N events. The smaller it is, the more probable it is that the system samples, at least once in the first N triggers, with intersampling time $s = k_{\max}$, implying that a bigger maximum intersampling time could be used, allowing the system to sample even less frequently and saving more bandwidth.

Observe that, if the initial condition (x_0, s_0) is only known to obey some distribution $p_0 : Q \to [0,1]$, the expected reward can be described as:

$$\mathrm{E}_{\mathbb{P}^{p_0}_{\mathrm{Y}_N}}[g_{\star,N}(\omega)] = \sum_{s_0 \in \mathbb{N}_{[0,k_{\max}]}} \int_{\mathbb{R}^n} \mathrm{E}_{\mathbb{P}^{(x_0,s_0)}_{\mathrm{Y}_N}}[g_{\star,N}(\omega)] p_0(x_0,s_0) dx_0$$

Thus, reasoning about individual initial conditions y_0 is sufficient and immediately extends to the general case of random initial conditions.

Overall, defining PETC's sampling behaviour Y_N, associating it to its induced probability measure $\mathbb{P}^{y_0}_{\mathrm{Y}_N}$ given in (6.4)-(6.5), and studying expectations $\mathrm{E}_{\mathbb{P}^{y_0}_{\mathrm{Y}_N}}[g(\omega)]$ constitutes a formal framework for the study of PETC's sampling behaviour.

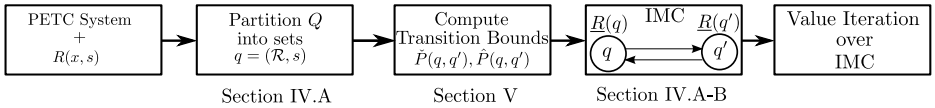

Figure 6.1: A flowchart showing the steps followed to compute bounds on the expected rewards $\mathrm{E}_{\mathbb{P}^{y_0}_{\mathrm{Y}_N}}[g_{\star,N}(\omega)]$.

6.3.3. PROBLEM STATEMENT

Unfortunately, exact computation of $\mathrm{E}_{\mathbb{P}^{y_0}_{\mathrm{Y}_N}}[g_{\star,N}(\omega)]$ is generally infeasible. Among others, how to obtain the measure $\mathbb{P}^{y_0}_{\mathrm{Y}_N}$ over the *uncountable* set of paths Y_N and then integrate over it? Hence, we aim at computing bounds over such expectations:

Problem Statement. *Consider the PETC system* (6.1)-(6.2) *and its sampling behaviour* Y_N*, for some* $N \in \mathbb{N}$*. Let Assumption* 6.3.1 *hold. Consider a reward function* $R : Q \to [0, R_{\max}]$*. For all initial conditions* $y_0 \in X \times \mathbb{N}_{[0,k_{\max}]}$*, where* $X \subset \mathbb{R}^n$ *is compact, compute (non-trivial) lower and upper bounds on* $\mathrm{E}_{\mathbb{P}^{y_0}_{\mathrm{Y}_N}}[g_{\star,N}(\omega)]$*, where* $\star \in \{\mathrm{cum}, \mathrm{avg}, \mathrm{mul}\}$.

In the rest of this article, we address the problem by constructing an IMC that *abstracts* the sampling behaviour Y_N along with $\mathbb{P}^{y_0}_{\mathrm{Y}_N}$, equipping it with suitable reward functions $\underline{R}, \overline{R}$, and computing (sup$_{\boldsymbol{\pi}\in\Pi}$ and) inf$_{\boldsymbol{\pi}\in\Pi} \mathrm{E}^{q_0}_{\boldsymbol{\pi}}[g_{\star,N}(\tilde{\omega})]$, with $\star \in \{\mathrm{cum}, \mathrm{avg}, \mathrm{mul}\}$, to obtain the bounds we are looking for. Specifically, in the next section we show how to construct such an IMC, by partitioning the state space and providing conditions (eq. (6.7)-(6.8)) that have to be satisfied by the IMC's transition probability intervals. We prove in Theorem 6.4.1 that this IMC equipped with suitable rewards gives rise to bounds on $\mathrm{E}_{\mathbb{P}^{y_0}_{\mathrm{Y}_N}}[g_{\star,N}(\omega)]$. Later, in Section 6.5, we show how to compute $\check{P}$ and $\hat{P}$ such that they satisfy (6.7)-(6.8), by solving optimization problems with log-concave objective functions. Finally, the desired bounds (sup$_{\boldsymbol{\pi}\in\Pi}$ and) inf$_{\boldsymbol{\pi}\in\Pi} \mathrm{E}^{q_0}_{\boldsymbol{\pi}}[g_{\star,N}(\tilde{\omega})]$ are obtained via well-known value iteration algorithms, as demonstrated through a numerical example in Section 6.6. A flowchart of the steps followed to compute the desired bounds is shown in Figure 6.1.

Remark 6.3.3. *By assuming that* $y_0 = (x_0, s_0) \in X \times \mathbb{N}_{[0,k_{\max}]}$*, we essentially assume that the initial state of the system* $x_0 \in X$*. Compactness of* X *is vital, to partition it into a finite number of subsets* $\mathcal{R}_i$ *and end up with a finite-state IMC. Nonetheless, this is not an unrealistic assumption, as in practice the initial conditions of the system are usually known to be bounded in some set. Furthermore,* $s_0 \in \mathbb{N}_{[0,k_{\max}]}$ *for generality, but, as mentioned in Remark* 6.3.1*, typically in ETC* $s_0 = 0$.

Remark 6.3.4. *We constrain ourselves to* {cum, avg, mul} *rewards for clarity, but our approach extends to a more general framework. As commented in Section* 6.4.2*, our IMCs can be employed for computing bounds on* bounded-until *probabilities:*

$$\mathbb{P}^{y_0}_{\mathrm{Y}_N}(\exists i \in \mathbb{N}_{[0,N]} \text{ s.t. } \omega(i) \in G \text{ and } \forall k \le i,\ \omega(k) \in S)$$

where $S, G \subseteq Q$*. Bounded-until constitutes the backbone of PCTL [73], as all PCTL formulas can be written with bounded-until operations. In short, our approach directly extends to PCTL. Moreover, by extending our proofs according to [74] and [76], we could incorporate probabilistic* $\omega-$*regular or LTL (Linear Temporal Logic) properties.*

6.4. IMCs ABSTRACTING PETC'S SAMPLING BEHAVIOUR

6.4.1. CONSTRUCTING THE IMC

Typically, to abstract a stochastic behaviour Y and its probability measure $\mathbb{P}_Y$ through an IMC: i) the state space is partitioned into a finite number of regions, each of which corresponds to an IMC-state, ii) if the state space is unbounded, then one of these regions is unbounded, and its IMC-state is made absorbing[2], and iii) the bounds on transition probabilities $\check{P}(q,q'), \hat{P}(q,q')$ are derived such that $\check{P}(q,q') \leq \mathbb{P}_Y(\omega(i+1) \in q' | \omega(i) = x) \leq \hat{P}(q,q')$ for all $x \in q$, where $\omega \in Y$.

In this work, we adopt the above methodology. Observe that the state space from which the sampling behaviour emerges is the set $Q = \mathbb{R}^n \times \mathbb{N}_{[0,k_{\max}]}$. Since $\mathbb{N}_{[0,k_{\max}]}$ is by-construction partitioned into the singletons $\{0\}, \{1\}, \ldots, \{k_{\max}\}$, it suffices to partition $\mathbb{R}^n$. Consider m non-overlapping compact regions $\mathscr{R}_i$ such that $\bigcup_{i \in \mathbb{N}_{[1,m]}} \mathscr{R}_i = X$. Then, $\mathbb{R}^n$ is partitioned into:

$$Q_{\mathscr{R}} \cup \{\overline{X}\}$$

where $Q_{\mathscr{R}} = \{\mathscr{R}_1, \ldots, \mathscr{R}_m\}$. According to the aforementioned methodology, the states of the IMC would be of the form $(q,s) \in \left(Q_{\mathscr{R}} \cup \{\overline{X}\}\right) \times \mathbb{N}_{[0,k_{\max}]}$. Nonetheless, for compactness of the IMC, we group all states $(\overline{X}, s)$ (for $s \in \mathbb{N}_{[0,k_{\max}]}$) that correspond to $\overline{X}$ into a single absorbing state q_{abs}:

$$q_{\text{abs}} = \overline{X} \times \mathbb{N}_{[0,k_{\max}]}$$

From now on, we abusively use $(\mathscr{R}_i, s)$ (resp. q_{abs}) to denote both the corresponding IMC-state and the set $\mathscr{R}_i \times \{s\}$ (resp. $\overline{X} \times \mathbb{N}_{[0,k_{\max}]}$). Finally, the set of the IMC-states is:

$$Q_{\text{imc}} = \left(Q_{\mathscr{R}} \times \mathbb{N}_{[0,k_{\max}]}\right) \cup \{q_{\text{abs}}\} \tag{6.6}$$

Regarding the transition probability bounds $\check{P}(q,q')$ and $\hat{P}(q,q')$, since we need to bound $\mathbb{P}(\omega(i+1) \in q' | \omega(i) = x)$ for all $x \in q$, by employing (6.5), we have that for all $(\mathscr{R}, k), (\mathscr{S}, s) \in Q_{\mathscr{R}} \times \mathbb{N}_{[0,k_{\max}]}$:

$$\begin{aligned}
\check{P}\Big((\mathscr{R},k),(\mathscr{S},s)\Big) &\leq \min_{x \in \mathscr{R}} \mathbb{P}(\zeta(s;x) \in \mathscr{S}, \tau(x) = s) \\
\hat{P}\Big((\mathscr{R},k),(\mathscr{S},s)\Big) &\geq \max_{x \in \mathscr{R}} \mathbb{P}(\zeta(s;x) \in \mathscr{S}, \tau(x) = s) \\
\check{P}\Big((\mathscr{R},k),q_{\text{abs}}\Big) &\leq \sum_{s \in \mathbb{N}_{[0,k_{\max}]}} \min_{x \in \mathscr{R}} \mathbb{P}(\zeta(s;x) \in \overline{X}, \tau(x) = s) \\
\hat{P}\Big((\mathscr{R},k),q_{\text{abs}}\Big) &\geq \sum_{s \in \mathbb{N}_{[0,k_{\max}]}} \max_{x \in \mathscr{R}} \mathbb{P}(\zeta(s;x) \in \overline{X}, \tau(x) = s)
\end{aligned} \tag{6.7}$$

and for all $q' \in Q_{\text{imc}}$:

$$\check{P}(q_{\text{abs}}, q') = \hat{P}(q_{\text{abs}}, q') = \begin{cases} 1, \text{ if } q' = q_{\text{abs}} \\ 0, \text{ otherwise} \end{cases} \tag{6.8}$$

[2] An IMC-state $q \in Q_{\text{imc}}$ is absorbing $\iff \check{P}(q,q) = 1$.

The computation of $\check{P}$ and $\hat{P}$ such that they satisfy (6.7)-(6.8) is addressed in Section 6.5 and it involves bounding the solutions to the optimization problems of (6.7). The summation in the last two inequalities of (6.7) results from the fact that q_{abs} is a grouping of all states $(\overline{X}, s)$ with $s \in \mathbb{N}_{[0,k_{\max}]}$, while (6.8) indicates that q_{abs} is indeed absorbing. In view of Remark 6.3.2, since we know that $\mathbb{P}(\tau(x) = 0) = 0$, then for any $q \in Q_{\text{imc}}$ and $\mathscr{S} \in Q_{\mathscr{R}}$, it suffices to write $\check{P}(q,(\mathscr{S},0)) = \hat{P}(q,(\mathscr{S},0)) = 0$; that is, states $(\mathscr{S},0)$ only have outgoing transitions and no incoming ones. Finally, we define the IMC that abstracts the sampling behaviour as follows:

$$\mathrm{S}_{\text{imc}} = (Q_{\text{imc}}, \check{P}, \hat{P}), \tag{6.9}$$

where Q_{imc} is given by (6.6) and $\check{P}, \hat{P}$ are given by (6.7)-(6.8).

To demonstrate how the constructed IMC abstracts the PETC system's sampling behaviour, let us relate paths $\omega \in \mathrm{Y}_N$ to paths $\tilde{\omega} \in Paths(\mathrm{S}_{\text{imc}})$. First, consider a path ω such that $\omega(i) \notin q_{\text{abs}}$ for all $i \leq N$. Then, this path is related to a path $\tilde{\omega} \in Paths(\mathrm{S}_{\text{imc}})$ of the same length, for which $\omega(i) \in \tilde{\omega}(i)$ for all $i \leq N$. Next, consider a path such that $\omega(i) \in q_{\text{abs}}$ for some $i \leq N$ and $\omega(j) \notin q_{\text{abs}}$ for all $j < i$. Then, ω is related to $\tilde{\omega} \in Paths(\mathrm{S}_{\text{imc}})$ of the same length, for which $\omega(j) \in \tilde{\omega}(j)$ for all $j \leq i$ and $\tilde{\omega}(k) = q_{\text{abs}}$ for all $k \geq i$. This latter relation indicates that all paths in Y_N that enter $\overline{X}$ (even those that eventually return to X) are mapped to IMC-paths that enter q_{abs} at the same time and stay there.

6.4.2. Bounds on Sampling-Behaviour Rewards via IMCs

The IMC described above, if equipped with suitable rewards $\underline{R}, \overline{R}$, can be employed for the computation of lower and upper bounds on $\mathrm{E}_{\mathbb{P}^{y_0}_{\mathrm{Y}_N}}[g_{\star,N}(\omega)]$:

Theorem 6.4.1. *Consider the IMC* S_{imc} *given by* (6.9). *Define reward functions* $\underline{R}, \overline{R} : Q_{\text{imc}} \to [0, R_{\max}]$ *such that:*

$$\underline{R}(q) = \begin{cases} \min\limits_{(x,s)\in q} R(x,s), & \text{if } q \neq q_{\text{abs}} \\ \min\limits_{(x,s)\in \mathbb{R}^n \times \mathbb{N}_{[1,k_{\max}]}} R(x,s), & \text{if } q = q_{\text{abs}} \end{cases}, \quad \overline{R}(q) = \begin{cases} \max\limits_{(x,s)\in q} R(x,s), & \text{if } q \neq q_{\text{abs}} \\ \max\limits_{(x,s)\in \mathbb{R}^n \times \mathbb{N}_{[1,k_{\max}]}} R(x,s), & \text{if } q = q_{\text{abs}} \end{cases} \tag{6.10}$$

and the associated rewards over paths $\tilde{\omega} \in Paths(\mathrm{S}_{\text{imc}})$ *denoted by* $\underline{g}_{\star,N}, \overline{g}_{\star,N}$, *where* $\star \in \{\text{cum}, \text{avg}, \text{mul}\}$. *Then, for any initial condition* $y_0 = (x_0, s_0) \in X \times \mathbb{N}_{[0,k_{\max}]}$ *and* $N \in \mathbb{N}$:

$$\inf_{\boldsymbol{\pi}\in\Pi} \mathrm{E}^{q_0}_{\boldsymbol{\pi}}[\underline{g}_{\star,N}(\tilde{\omega})] \leq \mathrm{E}_{\mathbb{P}^{y_0}_{\mathrm{Y}_N}}[g_{\star,N}(\omega)] \leq \sup_{\boldsymbol{\pi}\in\Pi} \mathrm{E}^{q_0}_{\boldsymbol{\pi}}[\overline{g}_{\star,N}(\tilde{\omega})]$$

where q_0 *is such that* $y_0 \in q_0$.

Proof Sketch. The above expectations are written as *value functions* defined via *value iteration* (see Lemma 6.A.1), and mathematical induction over the iteration is employed. For the full proof, see Appendix 6.A. □

Hence, to compute bounds on expectations $\mathrm{E}_{\mathbb{P}^{y_0}_{\mathrm{Y}_N}}[g_{\star,N}(\omega)]$, we equip the IMC (6.9) with the reward functions $\underline{R}, \overline{R}$ from (6.10) and compute the expectations $\inf_{\boldsymbol{\pi}\in\Pi} \mathrm{E}^{q_0}_{\boldsymbol{\pi}}[\underline{g}_{\star,N}(\tilde{\omega})]$

and $\sup_{\boldsymbol{\pi}\in\Pi}\mathrm{E}^{q_0}_{\boldsymbol{\pi}}[\overline{g}_{\star,N}(\tilde{\omega})]$. As mentioned in Section 6.2.3, these expectations can be computed via value-iteration algorithms (e.g. see [72]), with polynomial complexity in the number of IMC-states. In fact, the value iteration used for {cum, mul} rewards is given here by equations (6.26) and (6.37) respectively in Appendix 6.A (the avg reward is the same as cum with $\gamma = 1$, and in the last step we just divide by $N+1$). Moreover, since bounded-until probabilities on IMCs, and thus PCTL properties, may be computed through a similar value iteration [73], our proofs can be adapted to show that we can bound bounded-until probabilities defined over Y_N by using the constructed IMC.

Finally, Theorem 6.4.1 indicates that *the same IMC* can be used to derive bounds for any chosen {cum, avg, mul} reward, for any horizon N, and any initial condition $y_0 \in X \times \mathbb{N}_{[0,k_{\max}]}$. It is also worth noting that a proof like that of Theorem 6.4.1 was missing from the literature on IMC-abstractions [73]–[76], where it was (correctly) taken for granted that the quantitative metric (e.g., a reward) evaluated over the IMC bounds the metric evaluated over the original stochastic behaviour, due to the way that the transition probabilities are constructed.

Remark 6.4.1. *For any $q \in Q_{\mathrm{imc}}$, the rewards $\underline{R}$ and $\overline{R}$ serve as conservative estimates of the real reward obtained if the system operates in q. In fact, specifically for q_{abs}, $\underline{R}$ and $\overline{R}$ are* global *lower and upper bounds, respectively, on the actual reward $R(x,s)$ (except for the case $s = 0$, which happens with zero probability, except for initial conditions). Due to this, for states $(\mathscr{R}, s) \in Q_{\mathrm{imc}}$ with $\mathscr{R}$ being "near" $\overline{X}$ (i.e., near the boundary of X), which tend to obtain larger transition probabilities to q_{abs}, the lower and upper bounds $\inf_{\boldsymbol{\pi}\in\Pi}\mathrm{E}^{q_0}_{\boldsymbol{\pi}}[\underline{g}_{\star,N}(\tilde{\omega})]$ and $\sup_{\boldsymbol{\pi}\in\Pi}\mathrm{E}^{q_0}_{\boldsymbol{\pi}}[\overline{g}_{\star,N}(\tilde{\omega})]$ are more conservative, compared to when $\mathscr{R}$ is further inside X. This is showcased by Figure 6.4. For that reason, in practice, to construct the IMC, it is better to partition a superset $Y \supseteq X$ into regions $\mathscr{R}_i$, so that the regions that comprise X are further inside Y, and the corresponding bounds are not that conservative.*

Remark 6.4.2. *Our results extend to infinite horizons (i.e. $N = +\infty$), when the rewards are well-defined, as it has already been proven in [70, Theorem IV.1]; in fact, the proof for $N = +\infty$ is simpler, as it suffices to consider time-invariant adversaries.*

The only thing that remains is to describe how to compute the transition probability bounds given by (6.7). This is carried out in the coming section.

6.5. COMPUTING THE TRANSITION PROBABILITY BOUNDS

Here, we compute lower bounds on the minima and upper bounds on the maxima in (6.7), thus completing the IMC's construction. Through a series of convex relaxations, and employing Proposition 6.5.1 and Lemma 6.5.1, the min/max expressions in (6.7) are formulated as optimization problems of log-concave functions (in fact, Gaussian integrals) over hyperrectangles, which are straightforward to solve. To facilitate this analysis, we introduce the following assumption:

Assumption 6.5.1. *The set X and all sets $\mathscr{R}_i \in Q_{\mathscr{R}}$ are hyperrectangles.*

This assumption is without loss of generality, as in the case where X is not a hyperrectangle, our approach could be applied by under/overapproximating X by a hyperrectangle Y and partitioning Y into a finite set of hyperrectangles $\mathscr{R}_i$.

For the rest of the document, for any $s \in \mathbb{N}_{[1,N]}$, we denote $\zeta_{s,x} = \zeta(s;x)$ and $\tilde{\zeta}_{s,x} = [\zeta_{1,x}^\top \quad \zeta_{2,x}^\top \quad \dots \quad \zeta_{s,x}^\top]^\top$. The following statements are instrumental in our derivations:

Proposition 6.5.1. *For any $s \in \mathbb{N}_{[1,N]}$, we have that $\tilde{\zeta}_{s,x} \sim \mathcal{N}(\mu_{\tilde{\zeta}_{s,x}}, \Sigma_{\tilde{\zeta}_{s,x}})$ with:*

$$\mu_{\tilde{\zeta}_{s,x}} = \begin{bmatrix} \mathrm{E}(\zeta_{1,x}^\top) & \mathrm{E}(\zeta_{2,x}^\top) & \dots & \mathrm{E}(\zeta_{s,x}^\top) \end{bmatrix}^\top$$

$$\Sigma_{\tilde{\zeta}_{s,x}} = \begin{bmatrix} \mathrm{Cov}(1,1) & \mathrm{Cov}(1,2) & \dots & \mathrm{Cov}(1,s) \\ \vdots & \vdots & \dots & \vdots \\ \mathrm{Cov}(s,1) & \mathrm{Cov}(s,2) & \dots & \mathrm{Cov}(s,s) \end{bmatrix}$$

where $\mathrm{E}(\zeta(t;x)) = [e^{At}(I + A^{-1}BK) - A^{-1}BK]x$ *and:*

$$\mathrm{Cov}(t_1,t_2) = \int_0^{\min(t_1,t_2)} e^{A(t_1-s)} B_w B_w^\top e^{A^\top (t_2-s)} \, ds$$

Thus, given some set $S \subseteq \mathbb{R}^{sn}$, the following holds:

$$\mathbb{P}(\tilde{\zeta}(s;x) \in S) = \int_S \mathcal{N}(dz | \mu_{\tilde{\zeta}_{s,x}}, \Sigma_{\tilde{\zeta}_{s,x}}) \tag{6.11}$$

Proof. Application of the expectation and covariance operators to the solution of linear SDE (6.1) (see [80, pp. 96]). □

Lemma 6.5.1. *Consider a function $h : \mathbb{R}^n \to [0,1]$ with $n \in \mathbb{N}_{>0}$ defined by:*

$$h(x) = \int_{S(x)} \mathcal{N}(dz | f(x), \Sigma)$$

where Σ is a covariance matrix, $S(x) \subseteq \mathbb{R}^m$ with $m \in \mathbb{N}_{>0}$ is linear on x and convex for all $x \in \mathbb{R}^n$, and $f : \mathbb{R}^n \to \mathbb{R}^m$ is an affine function. The function $h(x)$ is log-concave on x.

Proof. See Appendix 6.B. □

In what follows we transform the probabilities involved in (6.7) to set-membership ones $\mathbb{P}(\tilde{\zeta}_{s,x} \in S(x))$, where $S(x)$ is a polytope, but neither necessarily convex nor linear on x. Afterwards, we break them down to simpler ones and employ some convex relaxations, such that the set of integration of the resulting Gaussian integrals is convex and linear on x and Lemma 6.5.1 is enabled. Finally, we end up with optimization problems of log-concave functions over the hyperrectangle $\mathscr{R}$, and solve them to obtain lower and upper bounds on the expressions in (6.7).

6.5.1. TRANSITION PROBABILITIES AS SET-MEMBERSHIP PROBABILITIES

For now, let us focus on transitions from any state $(\mathscr{R}, k) \in Q_{\mathrm{imc}} \setminus q_{\mathrm{abs}}$ to any state $(\mathscr{S}, s) \in Q_{\mathscr{R}} \times \mathbb{N}_{[1,k_{\max}]}$:

$$(\max_{x \in \mathscr{R}} \text{ or }) \quad \min_{x \in \mathscr{R}} \mathbb{P}(\zeta(s;x) \in \mathscr{S}, \tau(x) = s)$$

Later, in Section 6.5.4, we show how transitions to q_{abs} can be treated similarly to the case above. Moreover, remember that for $s = 0$ the above probability is trivially 0 (see Remark 6.3.2).

Define the following hyperrectangle:

$$\Phi(x) := \{y \in \mathbb{R}^n : \phi(y,x) \le 0\} = \{y \in \mathbb{R}^n : |y-x|_\infty \le \epsilon\},$$

Note that $\Phi(x)$ is convex and linear on x: $\Phi(x) = \Phi(0) + \{x\}$. Moreover, it is such that $\zeta(t;x) \in \Phi(x) \iff \phi(\zeta(t;x),x) \le 0$. Thus, the following equivalences hold:

$$\begin{aligned} &\text{if } s \in \mathbb{N}_{[1,k_{\max}-1]}: && \tau(x) = s \iff \tilde{\zeta}_{s,x} \in \Phi^{s-1}(x) \times \overline{\Phi}(x) \\ &\text{if } s = k_{\max}: && \tau(x) = s = k_{\max} \iff \tilde{\zeta}_{k_{\max}-1,x} \in \Phi^{k_{\max}-1}(x) \end{aligned}$$

where, for brevity, in the case where $s = 1$ we have abusively denoted $\Phi^0(x) \times \overline{\Phi}(x) = \overline{\Phi}(x)$. In words, when $s \neq k_{\max}$, the intersampling time is s if and only if the state belongs to $\Phi(x)$ at all checking times $1, 2, \dots, s-1$ and at time s it lies outside $\Phi(x)$. When $s = k_{\max}$, it suffices that the state belongs to $\Phi(x)$ at all checking times $1, 2, \dots, k_{\max}-1$. Thus, for $s \in \mathbb{N}_{[1,k_{\max}-1]}$:

$$\begin{aligned} \mathbb{P}(\zeta(s;x) \in \mathscr{S}, \tau(x) = s) &= \mathbb{P}\left(\tilde{\zeta}_{s,x} \in \Phi^{s-1}(x) \times (\overline{\Phi}(x) \cap \mathscr{S})\right) \\ &= \int_{\Phi^{s-1}(x) \times (\overline{\Phi}(x) \cap \mathscr{S})} \mathcal{N}(dz | \mu_{\tilde{\zeta}_{s,x}}, \Sigma_{\tilde{\zeta}_{s,x}}) \end{aligned} \tag{6.12}$$

and for $s = k_{\max}$:

$$\begin{aligned} \mathbb{P}(\zeta(k_{\max};x) \in \mathscr{S}, \tau(x) = k_{\max}) &= \mathbb{P}\left(\tilde{\zeta}_{k_{\max},x} \in \Phi^{k_{\max}-1}(x) \times \mathscr{S}\right) \\ &= \int_{\Phi^{k_{\max}-1}(x) \times \mathscr{S}} \mathcal{N}(dz | \mu_{\tilde{\zeta}_{k_{\max},x}}, \Sigma_{\tilde{\zeta}_{k_{\max},x}}) \end{aligned} \tag{6.13}$$

In the following we combine (6.12) and (6.13) with some convex relaxations, to enable Lemma 6.5.1 and obtain bounds on ($\max_{x \in \mathscr{R}}$ and) $\min_{x \in \mathscr{R}} \mathbb{P}(\zeta(s;x) \in \mathscr{S}, \tau(x) = s)$ through solving optimization problems with log-concave functions. In particular, observe that $\mu_{\tilde{\zeta}_{s,x}}$ is already an affine function of x (see Proposition 6.5.1), thus satisfying one of the two conditions of Lemma 6.5.1. Hence, our efforts focus on transforming the integration sets in (6.12)-(6.13) such that they become linear on x and convex.

6.5.2. LOWER BOUNDS ON TRANSITION PROBABILITIES

Let us start by determining lower bounds on:

$$\min_{x \in \mathscr{R}} \mathbb{P}(\zeta(s;x) \in \mathscr{S}, \tau(x) = s) \tag{6.14}$$

The special case when $s = k_{\max}$, which is given by (6.13), is simple. Observe that the set $\Phi^{k_{\max}-1}(x) \times \mathscr{S}$ is convex (since $\Phi(x)$ and $\mathscr{S} \in Q_{\mathscr{R}}$ are hyperrectangles) and linear on x, as it can be written as:

$$\Phi^{k_{\max}-1}(x) \times \mathscr{S} = \Phi^{k_{\max}-1}(0) \times \mathscr{S} + \begin{bmatrix} I_n & I_n & \dots & I_n & 0_n \end{bmatrix}^\top \{x\}$$

Thus, when $s = k_{\max}$, the objective function $\mathbb{P}(\zeta(s;x) \in \mathscr{S}, \tau(x) = s)$ of minimization problem (6.14) is log-concave (due to (6.13) and Lemma 6.5.1). The constraint set $\mathscr{R}$ is a

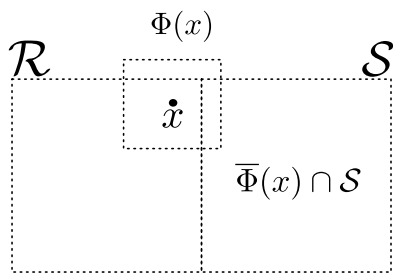

(a) The set $\mathscr{R}$ is the dashed square on the left, $\mathscr{S}$ is the one on the right, and $\Phi(x)$ is the one centered at x. For the given x on the figure, $\overline{\Phi}(x) \cap \mathscr{S}$ is non-convex. For different $x \in \mathscr{R}$ the set $\overline{\Phi}(x) \cap \mathscr{S}$ has a different shape; thus, $\overline{\Phi}(x) \cap \mathscr{S}$ is not linear on x.

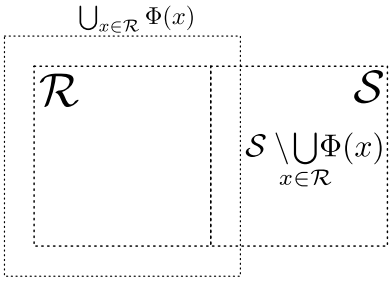

(b) The set $\bigcup_{x\in\mathscr{R}} \Phi(x)$, and consequently $\mathscr{S} \setminus \bigcup_{x\in\mathscr{R}} \Phi(x)$, does not depend on x. The set $\mathscr{S} \setminus \bigcup_{x\in\mathscr{R}} \Phi(x)$ can be partitioned into a finite number (minimum one, here) of hyperrectangles.

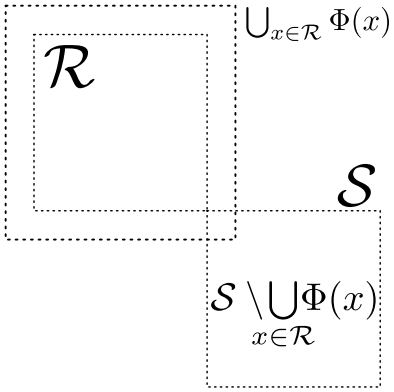

(c) The set $\mathscr{S} \setminus \bigcup_{x\in\mathscr{R}} \Phi(x)$ can be partitioned into a finite number (minimum two, here) of hyperrectangles.

Figure 6.2: The interplay between sets $\mathscr{R}$, $\mathscr{S}$, $\overline{\Phi}(x) \cap \mathscr{S}$ and $\mathscr{S} \setminus \bigcup_{x\in\mathscr{R}} \Phi(x)$.

hyperrectangle. Thus, the minimization problem attains its solution at one of the vertices of $\mathscr{R}$ [81, pp. 343, Theorem 32.2]; we simply have to evaluate the objective function for each of the vertices, to find the minimum.

When $s \neq k_{\max}$, the set of integration in (6.12) is neither convex nor linear on x due to $\overline{\Phi}(x) \cap \mathscr{S}$ (see Figure 6.2a); thus, we cannot invoke Lemma 6.5.1 and there is no indication that it is straightforward to compute (6.14). In this case, we resort to convex relaxations, each of which yield a lower bound on (6.14) that can be computed easily. These are the following:

Relaxation 1: Notice that $\overline{\Phi}(x) \cap \mathscr{S} = \mathscr{S} \setminus \Phi(x)$, for any $x \in \mathscr{R}$. Since $\Phi(x) \subseteq \bigcup_{x\in\mathscr{R}} \Phi(x)$ for all x, it follows that:

$$\overline{\Phi}(x) \cap \mathscr{S} = \mathscr{S} \setminus \Phi(x) \supseteq \mathscr{S} \setminus \bigcup_{x\in\mathscr{R}} \Phi(x)$$

For examples of $\mathscr{S} \setminus \bigcup_{x\in\mathscr{R}} \Phi(x)$ see Figures 6.2b and 6.2c. Observe that, since $\bigcup_{x\in\mathscr{R}} \Phi(x)$ does not depend on x, the set $\mathscr{S} \setminus \bigcup_{x\in\mathscr{R}} \Phi(x)$ does not depend on x; it is a fixed set,

in contrast to $\overline{\Phi}(x) \cap \mathscr{S}$. Moreover, since both $\mathscr{S}$ and $\bigcup_{x\in\mathscr{R}} \Phi(x)$ are hyperrectangles, then $\mathscr{S} \setminus \bigcup_{x\in\mathscr{R}} \Phi(x)$ can always be partitioned into a finite number of hyperrectangles $\mathscr{S}_1, \ldots, \mathscr{S}_r$, where $r \leq n$ and $r = 0$ in the case where $\mathscr{S} \setminus \bigcup_{x\in\mathscr{R}} \Phi(x)$ is empty. Thus:

$$\begin{aligned} &\min_{x\in\mathscr{R}} \int_{\Phi^{s-1}(x)\times(\overline{\Phi}(x)\cap\mathscr{S})} \mathscr{N}(dz|\mu_{\tilde{\zeta}_{s,x}}, \Sigma_{\tilde{\zeta}_{s,x}}) \geq \\ &\min_{x\in\mathscr{R}} \int_{\Phi^{s-1}(x)\times(\mathscr{S}\setminus\bigcup_{x\in\mathscr{R}}\Phi(x))} \mathscr{N}(dz|\mu_{\tilde{\zeta}_{s,x}}, \Sigma_{\tilde{\zeta}_{s,x}}) \geq \\ &\sum_{i=1}^{r} \min_{x\in\mathscr{R}} \int_{\Phi^{s-1}(x)\times\mathscr{S}_i} \mathscr{N}(dz|\mu_{\tilde{\zeta}_{s,x}}, \Sigma_{\tilde{\zeta}_{s,x}}) \end{aligned} \tag{6.15}$$

The integration sets $\Phi^{s-1}(x) \times \mathscr{S}_i$ are convex and linear on x. Thus, in the last expression of (6.15) we are dealing with log-concave objective functions, and the r minimization problems attain their minimum at vertices of $\mathscr{R}$. Hence, we easily solve the r minimization problems to obtain a lower bound on (6.14).

Relaxation 2: Here, we employ the law of total probability to write:

$$\mathbb{P}\left(\tilde{\zeta}_{s,x} \in \Phi^{s-1}(x) \times (\overline{\Phi}(x) \cap \mathscr{S})\right) = \mathbb{P}\left(\tilde{\zeta}_{s,x} \in \Phi^{s-1}(x) \times \mathscr{S}\right) - \mathbb{P}\left(\tilde{\zeta}_{s,x} \in \Phi^{s-1}(x) \times (\Phi(x) \cap \mathscr{S})\right)$$

which gives the following relationship:

$$\begin{aligned} &\min_{x\in\mathscr{R}} \mathbb{P}\left(\tilde{\zeta}_{s,x} \in \Phi^{s-1}(x) \times (\overline{\Phi}(x) \cap \mathscr{S})\right) \geq \\ &\min_{x\in\mathscr{R}} \mathbb{P}\left(\tilde{\zeta}_{s,x} \in \Phi^{s-1}(x) \times \mathscr{S}\right) - \max_{x\in\mathscr{R}} \mathbb{P}\left(\tilde{\zeta}_{s,x} \in \Phi^{s-1}(x) \times (\Phi(x) \cap \mathscr{S})\right) \end{aligned} \tag{6.16}$$

The minimization problem in the right-hand side of (6.16) is similar to the ones discussed before (log-concave objective function and hyperrectangle constraint set), and the minimum can be computed easily. However, the set $\Phi(x) \cap \mathscr{S}$ not being linear on x makes the maximization problem hard to solve. By employing that $\Phi(x) \cap \mathscr{S} \subseteq \mathscr{S} \cap \bigcup_{x\in\mathscr{R}} \Phi(x)$, we relax it by writing:

$$\max_{x\in\mathscr{R}} \mathbb{P}\left(\tilde{\zeta}_{s,x} \in \Phi^{s-1}(x) \times (\Phi(x) \cap \mathscr{S})\right) \leq \max_{x\in\mathscr{R}} \mathbb{P}\left(\tilde{\zeta}_{s,x} \in \Phi^{s-1}(x) \times \left(\mathscr{S} \cap \bigcup_{x\in\mathscr{R}} \Phi(x)\right)\right)$$

The set $\mathscr{S} \cap \bigcup_{x\in\mathscr{R}} \Phi(x)$ is a (possibly empty) hyperrectangle and does not depend on x; thus, $\Phi^{s-1}(x) \times \left(\mathscr{S} \cap \bigcup_{x\in\mathscr{R}} \Phi(x)\right)$ is convex and linear on x. Hence, the maximization problem in the right-hand side of the above equation is a convex program (log-concave objective function over the convex constraint set $\mathscr{R}$), and can be easily solved via regular convex optimization techniques. By computing the exact minimum in the right-hand side of (6.16) and an upper bound on the maximum-term as discussed here, we obtain a lower bound on (6.14).

Relaxation 3: Continuing from (6.16), we propose a different relaxation for the maximization problem in the right-hand side of (6.16). Specifically, by employing Bayes's

rule:

$$\max_{x\in\mathscr{R}}\mathbb{P}\Big(\tilde{\zeta}_{s,x}\in\Phi^{s-1}(x)\times(\Phi(x)\cap\mathscr{S})\Big)\leq\max_{x\in\mathscr{R}}\mathbb{P}\Big(\tilde{\zeta}_{s,x}\in\Phi^{s}(x)|\zeta_{s,x}\in\mathscr{S}\Big)\cdot\max_{x\in\mathscr{R}}\mathbb{P}(\zeta_{s,x}\in\mathscr{S}) \tag{6.17}$$

The term $\max_{x\in\mathscr{R}}\mathbb{P}(\zeta_{s,x}\in\mathscr{S})$ can be computed exactly easily, as $\mathbb{P}(\zeta_{s,x}\in\mathscr{S})$ is log-concave on x. For the term $\max_{x\in\mathscr{R}}\mathbb{P}\Big(\tilde{\zeta}_{s,x}\in\Phi^{s}(x)|\zeta_{s,x}\in\mathscr{S}\Big)$, we make use of the following bound:

Proposition 6.5.2. *The following holds:*

$$\max_{x\in\mathscr{R}}\mathbb{P}\Big(\tilde{\zeta}_{s,x}\in\Phi^{s}(x)|\zeta_{s,x}\in\mathscr{S}\Big)\leq\max_{(x,v)\in\mathscr{R}\times\mathscr{S}}\mathbb{P}\Big(\tilde{\zeta}_{s,x}\in\Phi^{s}(x)|\zeta_{s,x}=v\Big) \tag{6.18}$$

Proof. The proof is the same as in [82, Lemma 2]. □

To compute the right-hand side of (6.18), we use the fact that the random variable $\xi=(\tilde{\zeta}_{s,x}|\zeta_{l,x}=v)$ is normally distributed:

Corollary 6.5.1 (to Proposition 6.5.1)**.** *Consider the random variable $\xi=(\tilde{\zeta}_{s,x}|\zeta_{l,x}=v)$, where $l\in\mathbb{N}_{[0,s]}$, and $v\in\mathbb{R}^n$. Then $\xi\sim\mathscr{N}(\mu_\xi(x,v),\Sigma_\xi)$, where:*

$$\begin{aligned}\mu_\xi(x,v)&=\mathrm{E}(\tilde{\zeta}_{s,x})-\Sigma_{\tilde{\zeta}_{s,x},\zeta_{l,x}}\Sigma^{-1}_{\zeta_{l,x}}(v-\mathrm{E}(\zeta_{l,x}))\\ \Sigma_\xi&=\Sigma_{\tilde{\zeta}_{s,x}}-\Sigma_{\tilde{\zeta}_{s,x},\zeta_{l,x}}\Sigma^{-1}_{\zeta_{l,x}}\Sigma_{\zeta_{l,x},\tilde{\zeta}_{s,x}},\end{aligned}$$

where $\Sigma_{\zeta_{l,x}}=\mathrm{Cov}(l,l)$, $\Sigma_{\tilde{\zeta}_{s,x}}$, $\mathrm{E}(\tilde{\zeta}_{s,x})$ and $\mathrm{E}(\zeta_{l,x})$ are obtained from Proposition 6.5.1, and $\Sigma_{\zeta_{l,x},\tilde{\zeta}_{s,x}}=\Sigma^\top_{\tilde{\zeta}_{s,x},\zeta_{l,x}}=\begin{bmatrix}\mathrm{Cov}(l,1) & \mathrm{Cov}(l,2) & \dots & \mathrm{Cov}(l,s)\end{bmatrix}$.

Proof. Straightforward application of the well-known formula for conditional normal distributions [83]. □

Thus, we have that:

$$\max_{(x,v)\in\mathscr{R}\times\mathscr{S}}\mathbb{P}\Big(\tilde{\zeta}_{s,x}\in\Phi^{s}(x)|\zeta_{s,x}=v\Big)=\max_{(x,v)\in\mathscr{R}\times\mathscr{S}}\int_{\Phi^s(x)}\mathscr{N}(dz|\mu_\xi(x,v),\Sigma_\xi)$$

Observe that $\mu_\xi(x,v)$ is affine on the optimization variables (x,v), and $\Phi^s(x)$ is obviously convex and linear on x. Thus, the objective function of the above maximization problem is log-concave. Finally, since the set of constraints $\mathscr{R}\times\mathscr{S}$ is convex, we deduce that computing the right-hand side of (6.18) is a convex program. Combining (6.18) with (6.17) and (6.16) yields an easily computable bound on (6.14).

Remark 6.5.1. *Gaussian integrals over hyperrectangles are often encountered in fields such as statistics and learning, and many algorithms exist for their numerical computation (e.g., Genz's algorithm [84] or python's* scipy.stats.multivariate_normal *[85]).*

6.5.3. UPPER BOUNDS ON TRANSITION PROBABILITIES

We proceed to computing upper bounds on:

$$\max_{x\in\mathscr{R}} \mathbb{P}(\zeta(s;x)\in\mathscr{S}, \tau(x)=s) \tag{6.19}$$

Again, the case where $s=k_{\max}$ is easy: it corresponds to a convex program, and (6.19) is computed exactly. For the case where $s\neq k_{\max}$, we employ a relaxation similar to Relaxation 3 described in the previous. In particular, as in (6.16), we write:

$$\begin{aligned}\max_{x\in\mathscr{R}} \mathbb{P}\left(\tilde{\zeta}_{s,x}\in\Phi^{s-1}(x)\times(\overline{\Phi}(x)\cap\mathscr{S})\right)\leq\\ \max_{x\in\mathscr{R}} \mathbb{P}\left(\tilde{\zeta}_{s,x}\in\Phi^{s-1}(x)\times\mathscr{S}\right)-\min_{x\in\mathscr{R}} \mathbb{P}\left(\tilde{\zeta}_{s,x}\in\Phi^{s-1}(x)\times(\Phi(x)\cap\mathscr{S})\right)\end{aligned} \tag{6.20}$$

The term $\max_{x\in\mathscr{R}} \mathbb{P}\left(\tilde{\zeta}_{s,x}\in\Phi^{s-1}(x)\times\mathscr{S}\right)$ is computed easily, through convex optimization. For the other term in the right-hand side of (6.20), we write as in (6.17):

$$\min_{x\in\mathscr{R}} \mathbb{P}\left(\tilde{\zeta}_{s,x}\in\Phi^{s-1}(x)\times(\Phi(x)\cap\mathscr{S})\right)\geq\min_{x\in\mathscr{R}} \mathbb{P}\left(\tilde{\zeta}_{s,x}\in\Phi^{s}(x)|\zeta_{s,x}\in\mathscr{S}\right)\cdot\min_{x\in\mathscr{R}} \mathbb{P}(\zeta_{s,x}\in\mathscr{S}) \tag{6.21}$$

Given the discussion of the previous section, it is clear that: a) $\min_{x\in\mathscr{R}} \mathbb{P}(\zeta_{s,x}\in\mathscr{S})$ is computed exactly (by traversing the vertices of $\mathscr{R}$), and b) a lower bound on $\min_{x\in\mathscr{R}} \mathbb{P}\left(\tilde{\zeta}_{s,x}\in\Phi^{s}(x)|\zeta_{s,x}\in\mathscr{S}\right)$ is computed by employing Proposition 6.5.2 and Corollary 6.5.1, which yield log-concave minimization over the polytope $\mathscr{R}\times\mathscr{S}$.

6.5.4. TRANSITIONS TO q_{abs}

According to the last two inequalities in (6.7), for transitions to q_{abs} we are interested in:

$$(\min_{x\in\mathscr{R}} \text{ or }) \quad \max_{x\in\mathscr{R}} \mathbb{P}(\zeta(s;x)\in\overline{X}, \tau(x)=s)$$

We focus on the maximization, as minimization follows identical steps. By the law of total probability, we have:

$$\max_{x\in\mathscr{R}} \mathbb{P}(\zeta(s;x)\in\overline{X}, \tau(x)=s)\leq\max_{x\in\mathscr{R}} \mathbb{P}(\tau(x)=s)-\min_{x\in\mathscr{R}} \mathbb{P}(\zeta(s;x)\in X, \tau(x)=s) \tag{6.22}$$

Note that, since X is a hyperrectangle, the term $\min_{x\in\mathscr{R}} \mathbb{P}(\zeta(s;x)\in X, \tau(x)=s)$ can be treated exactly as discussed in the previous sections (where X takes the place of $\mathscr{S}$). Regarding $\mathbb{P}(\tau(x)=s)$, we have the following two cases:

- $s=k_{\max}$. In this case:
$$\mathbb{P}(\tau(x)=s)=\mathbb{P}(\tilde{\zeta}_{s,x}\in\Phi^{s-1}(x))$$
Thus, $\max_{x\in\mathscr{R}} \mathbb{P}(\tau(x)=s)=\max_{x\in\mathscr{R}} \mathbb{P}(\tilde{\zeta}_{s-1,x}\in\Phi^{s-1}(x))$, which can be computed easily (log-concave objective function and hyperrectangular constraint set).
- $s\neq k_{\max}$. In this case, by the law of total probability:
$$\mathbb{P}(\tau(x)=s)=\mathbb{P}(\tilde{\zeta}_{s,x}\in\Phi^{s-1}(x)\times\overline{\Phi}(x))=\mathbb{P}(\tilde{\zeta}_{s-1,x}\in\Phi^{s-1}(x))-\mathbb{P}(\tilde{\zeta}_{s,x}\in\Phi^{s}(x))$$

where when $s = 1$ we have abusively denoted $\tilde{\zeta}_{0,x} = x$ and $\Phi^0(x) = x$. Thus, we have:

$$\max_{x\in\mathscr{R}} \mathbb{P}(\tau(x) = s) \leq \max_{x\in\mathscr{R}} \mathbb{P}(\tilde{\zeta}_{s-1,x} \in \Phi^{s-1}(x)) - \min_{x\in\mathscr{R}} \mathbb{P}(\tilde{\zeta}_{s,x} \in \Phi^{s}(x))$$

and both terms in the right-hand side can be computed easily as discussed in the previous sections (log-concave objective functions and hyperrectangular constraint sets).

Remark 6.5.2. *To compute the transition probabilities, in several parts of the derivations, we have exploited the fact that $\Phi(x) := \{y \in \mathbb{R}^n : \phi(y,x) \leq 0\}$ is convex and linear on x, as well as that it is a hyperrectangle, which are consequences of the particular form of the triggering function $\phi(\zeta(t;x),x) = |\zeta(t;x) - x|_\infty - \epsilon$. To address more general triggering functions, where $\Phi(x)$ is neither convex nor linear on x, one could derive hyperrectangular approximations $\check{\Phi}(x)$ and $\hat{\Phi}(x)$ of the set $\Phi(x)$, such that both of them are convex and linear on x and $\check{\Phi}(x) \subseteq \Phi(x) \subseteq \hat{\Phi}(x)$ for all $x \in \mathscr{R}$. Nonetheless, this would introduce additional conservativeness.*

6.6. NUMERICAL EXAMPLES

We, now, demonstrate our theoretical results with a numerical example. Consider a stochastic PETC system (6.1)-(6.2) with:

$$A = \begin{bmatrix} -4 & 3 \\ -2 & 1 \end{bmatrix}, B = \begin{bmatrix} 1 \\ 0 \end{bmatrix}, K = \begin{bmatrix} -2 & 3 \end{bmatrix}, B_w = \begin{bmatrix} 2.5 & 0 \\ 0 & 2.5 \end{bmatrix}$$

and $\epsilon = 0.25$, $h = 0.006$, $k_{\max} = 3$. We are interested in analyzing the sampling behaviour of the system for initial conditions in $X = [-1.2, 1.2]^2$. Following Remark 6.4.1, we partition $Y = [-2,2]^2$ into 2500 equal rectangles, and construct the IMC as described in the previous.

First, consider the multiplicative reward from Example 3 in Section 6.3.2 and a horizon $N = 5$. Recall that, in this case, the expected reward expresses the probability that there is no intersampling time $s = k_{\max}$ in the first 5 triggers. As dictated by Theorem 6.4.1, we equip the IMC with rewards $\underline{R}, \overline{R}$, which are as follows for any $q \in Q_{\text{imc}}$:

$$\underline{R}(q) = \begin{cases} 0, & \text{if } q = q_{\text{abs}} \text{ or } \mathbf{proj}_{\mathbb{N}}(q) = k_{\max} \\ 1, & \text{otherwise} \end{cases}, \quad \overline{R}(q) = \begin{cases} 0, & \text{if } \mathbf{proj}_{\mathbb{N}}(q) = k_{\max} \\ 1, & \text{otherwise} \end{cases}$$

For all $q_0 \in Q_{\text{imc}} \setminus q_{\text{abs}}$, we calculate $\inf_{\boldsymbol{\pi}\in\Pi} \mathrm{E}^{q_0}_{\boldsymbol{\pi}}[\underline{g}_{\text{mul},N}(\tilde{\omega})]$ and $\sup_{\boldsymbol{\pi}\in\Pi} \mathrm{E}^{q_0}_{\boldsymbol{\pi}}[\overline{g}_{\text{mul},N}(\tilde{\omega})]$, by employing the value iteration introduced in (6.37). The adversary that gives rise to each bound is the so-called *o-maximizing MDP* and can be found easily (see [72] and [73]).

The obtained bounds for all $q_0 = (\mathscr{R}, 0) \in Q_{\mathscr{R}} \times \{0\}$, with $\mathscr{R} \subset [-1.2, 1.2]^2$, are shown in Figure 6.3. We only consider the case where the initial intersampling time $s_0 = 0$, as commented in Remark 6.3.1[3]. From the obtained bounds, one can expect from the system a high probability of sampling with intersampling time $k_{\max}$. Thus, based on that observation, an engineer who is to implement the PETC system, could decide to further increase the maximum allowed intersampling time, in order to allow the system to sample even less frequently.

[3] This is with no loss to generality, as s_0 does not affect the evolution of the system: for different s_0 and the same realization of the Wiener process, the sample path evolves exactly the same.

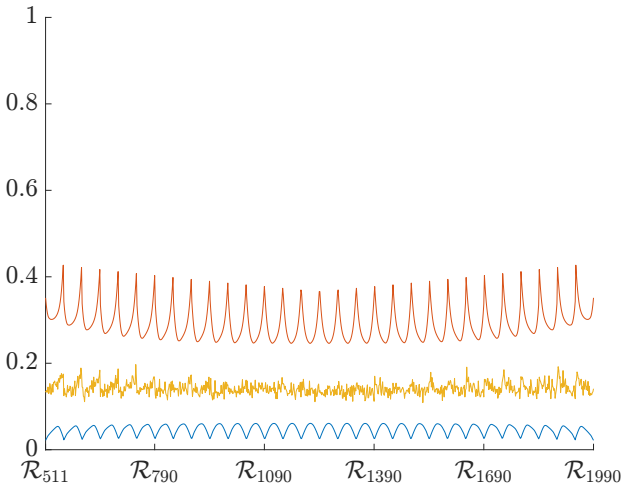

Figure 6.3: The blue and red lines are the computed lower and upper bounds, respectively, on the expected multiplicative reward from Example 3 in Section 6.3.2 starting from any initial condition $x_0 \in \mathscr{R}_i$ (initial intersampling time is assumed $s_0 = 0$), for all regions $\mathscr{R}_i \subset [-1.2, 1.2]^2$ in the partition. The yellow (middle) line is the statistical estimate of the expected reward for a random initial condition from each region.

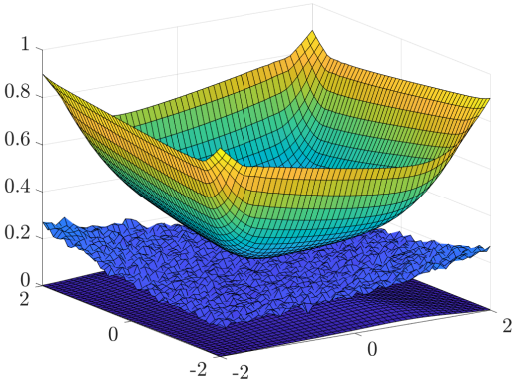

Figure 6.4: Surface plot of the obtained lower and upper bounds on the expected multiplicative reward from Example 3 in Section 6.3.2 for all regions $\mathscr{R}_i \subset [-2, 2]^2$ in the partition (x-axis). The surface on the bottom is the lower bound, the surface at the top is the upper bound, and the one in the middle is the statistical estimate of the expected reward for a random initial condition from each region, as obtained from simulations.

Figure 6.3, also, shows the statistical estimate of the expected reward, as derived by simulations. Specifically, for all $q_0 \in Q_{\mathscr{R}} \times \{0\}$ with $\mathscr{R} \subset [-1.2, 1.2]^2$, we pick a random initial condition $y_0 \in q_0$ and simulate 1000 sample paths, with a horizon of 5 triggers (the simulation stops after the 5th trigger). Each sample path that does not generate any intersampling time $s = k_{\max}$ is counted, and the total count is divided by 1000 to obtain a statistical estimate of the true probability. Figure 6.3 shows that, as expected by Theorem

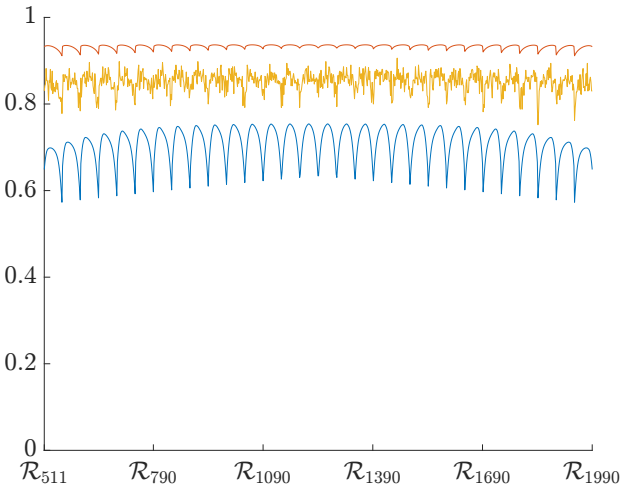

Figure 6.5: The blue and red lines are lower and upper bounds, respectively, on the bounded-until probability (6.23) starting from any initial condition $x_0 \in \mathscr{R}_i$ (initial intersampling time is assumed $s_0 = 0$), for all regions $\mathscr{R}_i \subset [-1.2, 1.2]^2$. The yellow line (the one in the middle) is the statistical estimate of the probability for a random initial condition from each region.

6.4.1, the statistical estimate is confined within the computed bounds. Finally, Figure 6.4 is a surface plot illustrating the obtained bounds and the statistical estimate for all regions $\mathscr{R}_i \in [-2, 2]^2$, supporting what is discussed in Remark 6.4.1: regions closer to the boundary of the partition correspond to more conservative bounds.

Next, to demonstrate our results' extension to PCTL, we derive bounds on the following bounded-until probability:

$$\mathbb{P}^{y_0}_{Y_N}\Big(\exists i \in \mathbb{N}_{[0,5]} \text{ s.t. } \mathbf{proj}_{\mathbb{N}}(\omega(i)) = k_{\max} \text{ and } \forall k \leq i,\ \omega(k) \notin q_{\text{abs}}\Big) \tag{6.23}$$

This is the probability that the state stays in Y *until* there is a trigger $s = k_{\max}$, in a horizon $N = 5$. Figure 6.5 shows the results.

Finally, for completeness, we calculate bounds on the expected average intersampling time for $N = 5$, as introduced in Example 1, Section 6.3.2. Since we assume $s_0 = 0$, which implies that we are only interested in the average of the 5 subsequent triggers, we use N in the denominator, instead of $N + 1$. The results are illustrated in Figure 6.6. The obtained bounds could be used to compare the average sampling performance of this particular PETC design with some other implementation; e.g. it is evident that, on average, it samples considerably more efficiently than a periodic implementation with period h. Alternatively, they could be used to forecast the expected average occupation of the communication channel.

6.7. CONCLUSION

In this chapter, we have computed bounds on metrics associated to the sampling behaviour of linear stochastic PETC systems, by constructing IMCs abstracting the sampling behaviour and equipping them with suitable rewards. The metrics are expectations of

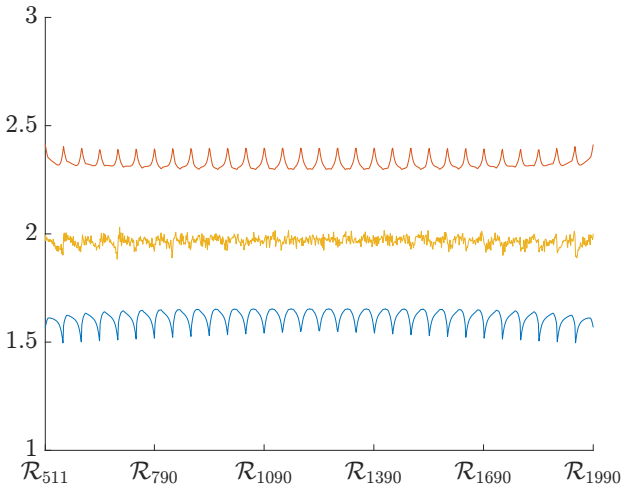

Figure 6.6: The blue and red lines are lower and upper bounds on the expected average intersampling time starting from any initial condition $x_0 \in \mathscr{R}_i$ (initial intersampling time is assumed $s_0 = 0$), for regions $\mathscr{R}_i \subset [-1.2, 1.2]^2$. The yellow line (the one in the middle) is the statistical estimate of the expected average for a random initial condition from each region.

functions of sequences of intersampling times and state measurements, that take the form of cumulative, average or multiplicative rewards. Numerical examples have been provided to demonstrate the effectiveness of the proposed framework in practice. Specifically, for a given system, we have computed the expected average intersampling time and the probability of triggering with the maximum allowed intersampling time, in a finite horizon. Moreover, we have computed bounds on a bounded-until probability, demonstrating extensibility of our approach to PCTL properties. Overall, the framework presented here, enables the formal study of PETC's sampling behaviour and the assessment of its sampling (vs. control) performance.

6.A. TECHNICAL LEMMATA AND PROOF OF THEOREM 6.4.1

In this subsection, we first provide some technical lemmata, and then prove Theorem 6.4.1. Let us introduce some notation and terminology. We constrain ourselves to Markovian adversaries. The value of such adversaries depends only on the time-step i and the given state $q \in Q_{\text{imc}}$, i.e. $\boldsymbol{\pi}(i,q) = p_{i,q} \in \Gamma_q$. From now on, we abusively write $\boldsymbol{\pi}(i,q,q') = p_{i,q}(q')$, for any $q' \in Q_{\text{imc}}$, to denote the transition probability from q to q' at time i, under adversary $\boldsymbol{\pi}$. Moreover, for $s_i, s_{i+1} \in \mathbb{N}_{[0,k_{\max}]}$, $x_i \in \mathbb{R}^n$, $X_{i+1} \subseteq \mathbb{R}^n$, denote:

$$T((X_{i+1}, s_{i+1})|(x_i, s_i)) := \mathbb{P}^{y_0}_{Y_N}(\omega(i+1) \in (X_{i+1}, s_{i+1})|\omega(i) = (x_i, s_i)) \tag{6.24}$$

This notation is common in the literature of stochastic systems and T is often called *transition kernel*. Let us abuse notation and write $\int_Q T(dy'|y)$, for some $y \in Q$, to denote $\sum_{s' \in \mathbb{N}_{[0,k_{\max}]}} \int_{\mathbb{R}^n} T((dx', s')|y)$.

We proceed to stating the technical lemmata. The first one provides a relationship indicating that the expected cumulative reward can be written as a *value function* defined

via *value iteration*, which is a trivial extension of the value iteration in [72] to finite horizons and time-varying adversaries. The second and third lemmata provide some useful bounds, which are employed in the proof of Theorem 6.4.1.

Lemma 6.A.1. *Given IMC* $\mathrm{S}_{\mathrm{imc}}$ *from* (6.9)*, equipped with a reward function* $\underline{R} : Q_{\mathrm{imc}} \to \underline{R}_{\max}$*, any Markovian adversary* $\boldsymbol{\pi} \in \Pi$ *and any* $q_0 \in Q_{\mathrm{imc}}$*, we have that:*

$$\mathrm{E}_{\boldsymbol{\pi}}[\sum_{j=i}^{N} \gamma^{j-i} \underline{R}(\tilde{\omega}(j)) | \tilde{\omega}(i) = q_0] = \underline{V}_{\boldsymbol{\pi},i}(q_0) \tag{6.25}$$

where for all $q \in Q_{\mathrm{imc}}$ *and* $i \in \mathbb{N}_{[0,N-1]}$*:*

$$\underline{V}_{\boldsymbol{\pi},N}(q) = \underline{R}(q) \tag{6.26a}$$

$$\underline{V}_{\boldsymbol{\pi},i}(q) = \underline{R}(q) + \gamma \sum_{q' \in Q_{\mathrm{imc}}} \underline{V}_{\boldsymbol{\pi},i+1}(q') \boldsymbol{\pi}(i,q,q') \tag{6.26b}$$

Similarly, for all $y_0 \in Q$*:*

$$\mathrm{E}_{\mathbb{P}_{\mathrm{Y}}^{y_0}}[\sum_{j=i}^{N} \gamma^{j-i} R(\omega(j)) | \omega(i) = y_0] = V_i(y_0) \tag{6.27}$$

where for all $y \in Q$ *and* $i \in \mathbb{N}_{[0,N-1]}$*:*

$$V_N(y) = R(y) \tag{6.28a}$$

$$V_i(y) = R(y) + \gamma \int_Q V_{i+1}(y') T(dy'|y) \tag{6.28b}$$

Consequently, we have:

$$\begin{aligned} \mathrm{E}_{\boldsymbol{\pi}}^{q_0}[\underline{g}_{\mathrm{cum},N}(\tilde{\omega})] &= \mathrm{E}_{\boldsymbol{\pi}}[\sum_{j=0}^{N} \gamma^{j} \underline{R}(\tilde{\omega}(j)) | \tilde{\omega}(0) = q_0] \\ &= \underline{V}_{\boldsymbol{\pi},0}(q_0) \\ \mathrm{E}_{\mathbb{P}_{\mathrm{Y}}^{y_0}}[g_{\mathrm{cum},N}(\omega)] &= \mathrm{E}_{\mathbb{P}_{\mathrm{Y}}^{y_0}}[\sum_{j=0}^{N} \gamma^{j} R(\omega(j)) | \omega(0) = y_0] \\ &= V_0(y_0) \end{aligned} \tag{6.29}$$

Proof. We prove (6.25) by induction. The proof of (6.27) is identical, and then (6.29) follows immediately. It obviously holds that $\underline{V}_{\boldsymbol{\pi},N}(q_0) = R(q_0) = \mathrm{E}_{\boldsymbol{\pi}}[\sum_{j=N}^{N} \gamma^{j-N} \underline{R}(\tilde{\omega}(j)) | \tilde{\omega}(N) =$

$q_0]$ for all $q_0 \in Q_{\text{imc}}$. Now, assume that (6.25) holds for some $i \in \mathbb{N}_{[1,N]}$. Then:

$$\begin{aligned}
&\underline{V}_{\boldsymbol{\pi},i-1}(q_0) = \\
&\underline{R}(q_0) + \gamma \sum_{q' \in Q_{\text{imc}}} \underline{V}_{\boldsymbol{\pi},i}(q')\boldsymbol{\pi}(i-1,q_0,q') = \\
&\underline{R}(q_0) + \gamma \sum_{q' \in Q_{\text{imc}}} \mathrm{E}_{\boldsymbol{\pi}}\Big[\sum_{j=i}^{N} \gamma^{j-i}\underline{R}(\tilde{\omega}(j))|\tilde{\omega}(i) = q'\Big]\boldsymbol{\pi}(i-1,q_0,q') = \\
&\underline{R}(q_0) + \mathrm{E}_{\boldsymbol{\pi}}\Big[\sum_{j=i}^{N} \gamma^{j-i+1}\underline{R}(\tilde{\omega}(j))|\tilde{\omega}(i-1) = q_0\Big] = \\
&\mathrm{E}_{\boldsymbol{\pi}}\Big[\underline{R}(q_0) + \sum_{j=i}^{N} \gamma^{j-i+1}\underline{R}(\tilde{\omega}(j))|\tilde{\omega}(i-1) = q_0\Big] = \\
&\mathrm{E}_{\boldsymbol{\pi}}\Big[\underline{R}(q_0) + \gamma\underline{R}(\tilde{\omega}(i)) + \gamma^2\underline{R}(\tilde{\omega}(i+1)) + \ldots|\tilde{\omega}(i-1) = q_0\Big] = \\
&\mathrm{E}_{\boldsymbol{\pi}}[\sum_{j=i-1}^{N} \gamma^{j-i+1}\underline{R}(\tilde{\omega}(j))|\tilde{\omega}(i-1) = q_0]
\end{aligned}$$

where:

- in the second equality we used the induction assumption that we made;
- in the third equality we put γ inside the expectation, and we used the law of total expectation;
- and in the fourth equality we put $\underline{R}(q_0)$ inside the expectation.

Thus (6.25) is proven by induction, and the proof is completed. □

Lemma 6.A.2. *Given any adversary $\boldsymbol{\pi} \in \Pi$, for all $y \in \mathbb{R}^n \times \mathbb{N}_{[1,k_{\max}]}$ and for all $i \in \mathbb{N}_{[1,N]}$:*

$$\underline{V}_{\boldsymbol{\pi},i}(q_{\text{abs}}) \leq V_i(y) \tag{6.30}$$

Proof. From Lemma 6.A.1, we know that:

$$\begin{aligned}
&V_i(y) = \mathrm{E}_{\mathbb{P}_{\mathrm{Y}}^{y}}[\sum_{j=i}^{N} \gamma^{j-i}R(\omega(j))|\omega(i) = y] \\
&\underline{V}_{\boldsymbol{\pi},i}(q_{\text{abs}}) = \mathrm{E}_{\boldsymbol{\pi}}[\sum_{j=i}^{N} \gamma^{j-i}\underline{R}(\tilde{\omega}(j))|\tilde{\omega}(i) = q_{\text{abs}}] = \sum_{j=i}^{N} \gamma^{j-i}\underline{R}(q_{\text{abs}}) = \sum_{j=i}^{N} \gamma^{j-i} \min_{(x,s)\in\mathbb{R}^n\times\mathbb{N}_{[1,k_{\max}]}} R(x,s)
\end{aligned} \tag{6.31}$$

where in the second equation, the second equality comes from the fact that q_{abs} is absorbing for any $\boldsymbol{\pi} \in \Pi$ and the third equality comes from (6.10).

From Remark 6.3.2, since $y \in \mathbb{R}^n \times \mathbb{N}_{[1,k_{\max}]}$ we can deduce that for all $j \in \mathbb{N}_{[i,N]}$ we have:

$$\mathbb{P}_{\mathrm{Y}_N}(\omega(j) \in \mathbb{R}^n \times \mathbb{N}_{[1,k_{\max}]}|\omega(i) = y) = 1$$

Thus, we have:

$$\min_{(x,s)\in\mathbb{R}^n\times\mathbb{N}_{[1,k_{\max}]}} R(x,s) \leq R(\omega(j)), \text{ for all } j \in \mathbb{N}_{[i,N]} \text{ a.s.} \tag{6.32}$$

where a.s. means “almost surely". By combining the above equation with (6.31), equation (6.30) follows. □

Lemma 6.A.3. *Given any adversary $\boldsymbol{\pi} \in \Pi$ and any $y \in Q$:*

$$\underline{V}_{\boldsymbol{\pi},i}(q_{\text{abs}}) \int_{q_{\text{abs}}} T(dy'|y) \leq \int_{q_{\text{abs}}} V_i(y')\, T(dy'|y) \tag{6.33}$$

Proof. We have that:

$$\begin{aligned}
&\int_{q_{\text{abs}}} V_i(y')\, T(dy'|y) = \\
&\int_{\overline{X}\times\mathbb{N}_{[1,k_{\max}]}} V_i(y')\, T(dy'|y) + \cancelto{0}{\int_{\overline{X}\times\{0\}} V_i(y')\, T(dy'|y)} \geq \\
&\underline{V}_{\boldsymbol{\pi},i}(q_{\text{abs}}) \int_{\overline{X}\times\mathbb{N}_{[1,k_{\max}]}} T(dy'|y) = \\
&\underline{V}_{\boldsymbol{\pi},i}(q_{\text{abs}}) \int_{\overline{X}\times\mathbb{N}_{[1,k_{\max}]}} T(dy'|y) + \underline{V}_{\boldsymbol{\pi},i}(q_{\text{abs}}) \underbrace{\int_{\overline{X}\times\{0\}} T(dy'|y)}_{0} = \\
&\underline{V}_{\boldsymbol{\pi},i}(q_{\text{abs}}) \int_{q_{\text{abs}}} T(dy'|y)
\end{aligned}$$

where for crossing out the term $\int_{\overline{X}\times\{0\}} V_i(y')\, T(dy'|y)$ we used the fact that $\int_{\overline{X}\times\{0\}} T(dy'|y) = 0$ (due to what is discussed in Remark 6.3.2), and for the inequality we used Lemma 6.A.2. □

Now, we are ready to prove Theorem 6.4.1:

Proof of Theorem 6.4.1. First, we prove the statement for cumulative rewards, and then we show how the proof is adapted for average and multiplicative rewards. We focus on the lower bound as the proof for the upper bound is similar. It suffices to show that there exists an adversary $\boldsymbol{\pi}^* \in \Pi$ such that:

$$\mathrm{E}^{q_0}_{\boldsymbol{\pi}^*}[\underline{g}_{\text{cum},N}(\tilde{\omega})] \leq \mathrm{E}_{\mathbb{P}^{y_0}_{\mathrm{Y}}}[g_{\text{cum},N}(\omega)] \tag{6.34}$$

By employing Lemma 6.A.1, specifically equation (6.29), to prove (6.34) it suffices to prove that there exists a $\boldsymbol{\pi}^* \in \Pi$ such that for any $q_0 \in Q_{\text{imc}} \setminus \{q_{\text{abs}}\}$ and any $y_0 \in q_0$:

$$\underline{V}_{\boldsymbol{\pi}^*,0}(q_0) \leq V_0(y_0) \tag{6.35}$$

Consider the following adversary for all $q \in Q_{\text{imc}}$, $i \in \mathbb{N}_{[0,N-1]}$:

$$\boldsymbol{\pi}^*(i,q,q') = \begin{cases} \displaystyle\int_{q'} T(dy'|y_i^*(q)), \text{ if } q \neq q_{\text{abs}} \\ 1, \text{ if } q = q' = q_{\text{abs}}, \\ 0, \text{ otherwise} \end{cases} \tag{6.36}$$

where $y_i^*(q) = \arg\min_{y \in q} V_i(y)$. Indeed $\boldsymbol{\pi}^* \in \Pi$, since $\sum_{q' \in Q_{\text{imc}}} \boldsymbol{\pi}^*(i,q,q') = 1$ for all $q \in Q_{\text{imc}}$, and from (6.7) and (6.24) it easily follows that $\check{P}(q,q') \leq \boldsymbol{\pi}^*(i,q,q') \leq \hat{P}(q,q')$[4].

Now, we are ready to prove (6.35), by induction. First, from (6.10) it is obvious that $\underline{V}_{\boldsymbol{\pi},N}(q_0) \leq V_N(y_0)$ for any $q_0 \in Q_{\text{imc}} \setminus \{q_{\text{abs}}\}$ and any $y_0 \in q_0$, since:

$$\underline{V}_{\boldsymbol{\pi},N}(q_0) = \underline{R}(q_0) \leq R(y_0) = V_N(y_0)$$

Assume that $\underline{V}_{\boldsymbol{\pi},i}(q_0) \leq V_i(y_0)$ for any $q_0 \in Q_{\text{imc}} \setminus \{q_{\text{abs}}\}$ and any $y_0 \in q_0$, for some $i \in \mathbb{N}_{[1,N]}$. Then:

$$\begin{aligned}
&\underline{V}_{\boldsymbol{\pi},i-1}(q_0) = \\
&\underline{R}(q_0) + \gamma \sum_{q' \in Q_{\text{imc}}} \underline{V}_{\boldsymbol{\pi},i}(q') \boldsymbol{\pi}(i-1,q_0,q') = \\
&\underline{R}(q_0) + \gamma \sum_{q' \in Q_{\text{imc}} \setminus \{q_{\text{abs}}\}} \underline{V}_{\boldsymbol{\pi},i}(q') \int_{q'} T(dy' | y_{i-1}^*(q_0)) + \gamma \underline{V}_{\boldsymbol{\pi},i}(q_{\text{abs}}) \int_{q_{\text{abs}}} T(dy' | y_{i-1}^*(q_0)) \leq \\
&\min_{y \in q_0} R(y) + \gamma \sum_{q' \in Q_{\text{imc}} \setminus \{q_{\text{abs}}\}} \min_{y \in q'}(V_i(y)) \int_{q'} T(dy' | y_{i-1}^*(q_0)) + \gamma \underline{V}_{\boldsymbol{\pi},i}(q_{\text{abs}}) \int_{q_{\text{abs}}} T(dy' | y_{i-1}^*(q_0)) \leq \\
&\min_{y \in q_0} R(y) + \gamma \sum_{q' \in Q_{\text{imc}} \setminus \{q_{\text{abs}}\}} \int_{q'} V_i(y') T(dy' | y_{i-1}^*(q_0)) + \gamma \int_{q_{\text{abs}}} V_i(y') T(dy' | y_{i-1}^*(q_0)) \leq \\
&R(y_{i-1}^*(q_0)) + \gamma \sum_{q' \in Q_{\text{imc}}} \int_{q'} V_i(y') T(dy' | y_{i-1}^*(q_0)) = \\
&R(y_{i-1}^*(q_0)) + \gamma \int_{Q} V_i(y') T(dy' | y_{i-1}^*(q_0)) = \\
&V_{i-1}(y_{i-1}^*(q_0)) = \min_{y \in q_0} V_{i-1}(y)
\end{aligned}$$

where:

- in the first step we used (6.26); in the second step we used the definition (6.36) of $\boldsymbol{\pi}^*$;
- in the third step we used that $\underline{R}(q_0) = \min_{y \in q_0} R(y)$ (from (6.10)) and that $\underline{V}_{\boldsymbol{\pi},i}(q_0) \leq V_i(y_0)$ for any $q_0 \in Q_{\text{imc}} \setminus \{q_{\text{abs}}\}$ and any $y_0 \in q_0$ (from the induction assumption);
- in the fourth step we used that $\min_{y \in q'}(V_i(y)) \leq V(y')$ for all $y' \in q'$, and the inequality given by Lemma 6.A.3;
- in the sixth step we used that $\bigcup_{q' \in q_{\text{imc}}} q' = Q$, in the seventh step we used (6.28), and in the last step we used that $y_{i-1}^*(q_0) = \arg\min_{y \in q_0} V_{i-1}(y)$.

Hence, since $\underline{V}_{\boldsymbol{\pi},i-1}(q_0) \leq \min_{y \in_0} V_{i-1}(y)$, we have that (6.35) is proven by induction, thus proving (6.34).

Only thing remaining is to explain how this proof generalizes to average and multiplicative rewards. The average reward is very simple, as it is just the time-average of a

[4] Adopting the transition-kernel notation, it can be written that for $q \in Q_{\text{imc}} \setminus \{q_{\text{abs}}\}$, $\check{P}(q,q') \leq \min_{y \in q} \int_{q'} T(dy'|y)$, for any $q' \in Q_{\text{imc}}$. Similarly for $\hat{P}$. Indeed it follows that $\check{P}(q,q') \leq \boldsymbol{\pi}^*(i,q,q') \leq \hat{P}(q,q')$

cumulative reward with $\gamma = 1$: $\mathrm{E}[g_{\mathrm{avg},N}(\omega)] = \frac{1}{N+1}\mathrm{E}[\sum_0^N R(\omega(i))]$. Finally, for multiplicative rewards, only thing that changes w.r.t. cumulative rewards is the value iteration, which becomes:

$$\begin{aligned} \underline{V}_{\boldsymbol{\pi},N}(q) &= \underline{R}(q) \\ \underline{V}_{\boldsymbol{\pi},i}(q) &= \underline{R}(q) \cdot \sum_{q' \in Q_{\mathrm{imc}}} \underline{V}_{\boldsymbol{\pi},i+1}(q')\boldsymbol{\pi}(i,q,q') \end{aligned} \tag{6.37}$$

□

6.B. PROOF OF LEMMA 6.5.1

Proof of Lemma 6.5.1. This proof draws inspiration from the proof of [86, Proposition 2]. Let us first prove log-concavity of the following simpler case:

$$g(x) = \int_S \mathcal{N}(dz|x,\Sigma)$$

with $S \subseteq \mathbb{R}^n$ not dependent on x. Observe that:

$$g(x) = \int_{S-\{x\}} \mathcal{N}(dz|0,\Sigma),$$

where $S - \{x\}$ is still a convex set as a mere translation of S. Then, $g(x)$ can be written as:

$$g(x) = P(S - \{x\}),$$

where $P(\cdot)$ is a probability measure over $\mathscr{B}(\mathbb{R}^n)$ induced by the distribution $\mathcal{N}(0,\Sigma)$. Since $\mathcal{N}(z|0,\Sigma)$ is log-concave, from [87, Theorem 2] we know that P is a log-concave measure, meaning that for every pair of convex sets $S_1, S_2 \subseteq \mathbb{R}^n$ and any $\lambda \in (0,1)$:

$$P(\lambda S_1 + (1-\lambda)S_2) \geq (P(S_1))^{\lambda}(P(S_2))^{1-\lambda} \tag{6.38}$$

Moreover, for any $x_1, x_2 \in \mathbb{R}^n$ and any $\lambda \in (0,1)$ we have:

$$\begin{aligned} \lambda(S - \{x_1\}) + (1-\lambda)(S - \{x_2\}) = \\ \{\lambda(y - x_1) : y \in S\} + \{(1-\lambda)(w - x_1) : w \in S\} = \\ \{\lambda(y - x_1) + (1-\lambda)(w - x_1) : y, w \in S\} = \\ \{\lambda y + (1-\lambda)w - \lambda x_1 - (1-\lambda)x_2 : y, w \in S\} = \\ \{\lambda y + (1-\lambda)w : y, w \in S\} - \lambda\{x_1\} - (1-\lambda)\{x_2\} = \\ S - \lambda\{x_1\} - (1-\lambda)\{x_2\} \end{aligned} \tag{6.39}$$

where the last equality is because $v = \lambda y + (1-\lambda)w$ is a convex combination of any two points $y, w \in S$ and S is convex[5].

[5] Since S is convex, then for any two $y, w \in S$ and any $\lambda \in (0,1)$ we have that $v = \lambda y + (1-\lambda)w \in S$. Thus, for a given λ, $\{\lambda y + (1-\lambda)w : y, w \in S\} \subseteq S$. But, also, $S = \{\lambda y + (1-\lambda)y \in S : y \in S\} \subseteq \{\lambda y + (1-\lambda)w : y, w \in S\}$. Thus, it has to be $S = \{\lambda y + (1-\lambda)w : y, w \in S\}$.

Finally, for any $x_1, x_2 \in \mathbb{R}^n$ and any $\lambda \in (0,1)$ we have:

$$\begin{aligned} g(\lambda x_1 + (1-\lambda)x_2) = \\ P\Big(S - \lambda\{x_1\} + (1-\lambda)\{x_2\}\Big) = \\ P\Big(\lambda(S-\{x_1\}) + (1-\lambda)(S-\{x_2\})\Big) \geq \\ \Big(P(S-\{x_1\})\Big)^{\lambda}\Big(P(S-\{x_2\})\Big)^{(1-\lambda)} = \\ (g(x_1))^{\lambda}(g(x_2))^{1-\lambda} \end{aligned}$$

where in the second equality we used (6.39) and for the inequality we used (6.38). Thus, it follows that $g(x)$ is log-concave.

For the general case, since $S(x) \subseteq \mathbb{R}^m$ is linear on x and convex, then it can be written as $S(x) = S' + \{Gx\}$, where $S' \subseteq \mathbb{R}^m$ is convex and $G \in \mathbb{R}^{m\times n}$. Thus we have:

$$\begin{aligned} h(x) = \int_{S(x)} \mathcal{N}(dz|f(x),\Sigma) = \int_{S'+\{Gx\}} \mathcal{N}(dz|f(x),\Sigma) = \int_{S'} \mathcal{N}(dz|f(x)-Gx,\Sigma) \\ = g(f(x)-Gx) \end{aligned}$$

where $g(x) = \int_{S'} \mathcal{N}(dz|x,\Sigma)$. The function $h(x) = g(f(x)-Gx)$ is log-concave as the composition of the log-concave function $g(x)$ with the affine function $f(x)-Gx$. □

6

6.C. LEBESGUE SAMPLING AND PRACTICAL MEAN-SQUARE STABILITY

In this section, we show that under mild assumptions, with the right choice of the checking period h, stochastic PETC system (6.1)-(6.2) can be rendered *practically mean-square stable*. To the author's knowledge, the proof that Lebesgue sampling can guarantee practical mean-square stability for linear stochastic systems with non-vanishing noise is missing from the related literature [14]–[17]. Apart from anything else, all these works assume dynamics with vanishing noise. Nonetheless, the proof is inspired by the techniques introduced in [17, Theorem 1], although there are significant modifications.

6.C.1. PRELIMINARY NOTIONS

First, let us introduce some auxiliary mathematical definitions and results. In the following, given a square matrix A, $\mathrm{tr}(A)$ denotes its trace.

Definition 6.C.1 (Class-$\mathcal{K}$, Class-$\mathcal{K}_\infty$ [63, Definition 4.2]). *A continuous function $\alpha : [0,a) \to [0,+\infty)$ is said to belong to class-$\mathcal{K}$ if it is strictly increasing and $\alpha(0) = 0$. It is said to belong to class-$\mathcal{K}_\infty$ if $a = +\infty$ and $\lim_{r\to+\infty} \alpha(r) = +\infty$.*

Definition 6.C.2 (Class-$\mathcal{KL}$, [63, Definition 4.3]). *A continuous function $\beta : [0,a) \times [0,+\infty) \to [0,+\infty)$ is said to belong to class-$\mathcal{KL}$ if, for each fixed s, the mapping $\beta(r,s)$ belongs to class-$\mathcal{K}$ w.r.t. r, and, for each fixed r, the mapping $\beta(r,s)$ is decreasing w.r.t. s and $\lim_{s\to+\infty} \beta(r,s) = 0$.*

Definition 6.C.3 (Mean-Square Practical Stability [88, Definition 2.1])**.** *Consider a stochastic system:*

$$d\zeta(t) = f(\zeta(t),t)dt + g(\zeta(t),t)dW(t) \tag{6.40}$$

where W is an n_w-dimensional Wiener process on an associated complete filtered probability space $(\Omega,\mathscr{F},\{\mathscr{F}_t\}_{t\geq 0},\mathbb{P})$, $f:\mathbb{R}^n\times\mathbb{R}_{\geq 0}\to\mathbb{R}^n$ and $g:\mathbb{R}^n\times\mathbb{R}_{\geq 0}\to\mathbb{R}^{n\times n_w}$. The system is called practically mean-square stable *if there exist a class-$\mathcal{KL}$ function β and a constant $d>0$, such that:*

$$\mathrm{E}[|\zeta(t)|^2] \leq \beta\Big(\mathrm{E}[|\zeta(0)|^2], t\Big) + d$$

Definition 6.C.4 (Infinitesimal Generator $\mathscr{L}$, [89] and [90, Definition 7.3.1 and Theorem 7.3.3])**.** *Consider the Itô diffusion (6.40). Given any function $V:\mathbb{R}^n\times\mathbb{R}_{\geq 0}\to\mathbb{R}$, which is twice differentiable on the first argument and differentiable on the second argument, the infinitesimal generator $\mathscr{L}$ is defined by:*

$$\mathscr{L}V(x,t) = \frac{\partial V(x,t)}{\partial t} + \frac{\partial V^\top(x,t)}{\partial x} f(x,t) + \frac{1}{2}\mathrm{tr}\Big(g^\top(x,t)\frac{\partial^2 V(x,t)}{\partial x^2} g(x,t)\Big)$$

Theorem 6.C.1 ([88, Theorem 1, modified])**.** *Consider the Itô diffusion (6.40). Suppose that there exist a convex class-$\mathcal{K}_\infty$ function $\underline{\alpha}:\mathbb{R}\to\mathbb{R}$, a class-$\mathcal{K}_\infty$ function $\overline{\alpha}:\mathbb{R}\to\mathbb{R}$, a non-negative function $\alpha:\mathbb{R}\to\mathbb{R}$, a constant $c\geq 0$, and a non-negative function $V:\mathbb{R}^n\times\mathbb{R}_{\geq 0}\to\mathbb{R}$, which is twice differentiable on the first argument and differentiable on the second argument, such that:*

$$\underline{\alpha}(|x|^2) \leq V(x,t) \leq \overline{\alpha}(|x|^2), \quad \forall x\in\mathbb{R}^n \tag{6.41}$$

$$\mathrm{E}[\mathscr{L}V(\zeta(t),t)] \leq -\mathrm{E}[\alpha(|\zeta(t)|)] + c, \quad \forall t\geq 0 \tag{6.42}$$

where $\lim\limits_{|x|\to\infty}\frac{\alpha(|x|)}{\overline{\alpha}(|x|^2)} > 0$. Then, the system (6.40) is practically mean-square stable.

6.C.2. PRACTICAL MEAN-SQUARE STABILITY OF STOCHASTIC PETC WITH LEBESGUE SAMPLING

Let us write the linear stochastic PETC system (6.1)-(6.2) in an alternative form, by incorporating the measurement error $\varepsilon(t)$ as an exogenous time-varying input:

$$\begin{aligned} d\zeta(t) &= (A-BK)\zeta(t)dt + BK\varepsilon(t)dt + B_w dW(t)\\ \varepsilon(t) &= \zeta(t_i)-\zeta(t), \quad t\in[t_i,t_{i+1})\\ t_{i+1} &= t_i + \min\Big\{k_{\max}h, \min\Big\{kh : k\in\mathbb{N}, \phi\Big(\zeta(kh;\zeta(t_i)),\varepsilon(t)\Big)>0\Big\}\Big\} \end{aligned} \tag{6.43}$$

For the remaining, let us denote by $s_k^i := t_i + kh$, i.e. s_k^i is the k-th checking time after sampling instant t_i, where $k\in\mathbb{N}$. Whenever we use the notation s_k^i, it is always suggested that $t_i\leq s_k^i\leq t_{i+1}$. That is, s_k^i is a time instant in the intersampling interval $[t_i,t_{i+1}]$. Moreover, we introduce the following assumptions:

Assumption 6.C.1. *We assume the following:*

- *Lebesgue sampling: $\phi(\zeta(t;x),\varepsilon(t)) = |\varepsilon(t)|-\epsilon$, where $\epsilon>0$ is a predefined constant.*

- *The gain K is selected such that there exists a symmetric positive-definite matrix $P \in \mathbb{R}^{n\times n}$ for which:*

$$P(A-BK)+(A-BK)^\top P + PBKK^\top B^\top P \preceq -I_n, \tag{6.44}$$

Such a pair of (K,P) always exists, if we assume that (A,B) is stabilizable (a reasonable and mild assumption), because this would amount to solving an LQR problem with $Q=I$ and $R^{-1}=KK^\top$.

Before stating and proving the main result of this section, we prove a technical lemma:

Lemma 6.C.1. *Consider the stochastic PETC system (6.43) and let Assumption 6.C.1 hold. For any given $i,k\in\mathbb{N}$, the following hold for all $t\in[s_k^i, s_{k+1}^i)$:*

$$\mathrm{E}[-|\zeta(t)|^2|\mathscr{F}_{t_i}] \leq \begin{cases} 0, & \text{if: } |\zeta(t_i)|<2\epsilon \\ -\frac{1}{4}|\zeta(t_i)|^2 e^{-\lambda_1 h} + \frac{|\zeta(t_i)|^2}{\lambda_1}(1-e^{-\lambda_1 h}), & \text{if: } |\zeta(t_i)|\geq 2\epsilon \end{cases} \tag{6.45}$$

$$\mathrm{E}[|\varepsilon(t)|^2|\mathscr{F}_{t_i}] \leq \epsilon^2 e^{(1+\lambda_2)h} + \frac{|\zeta(t_i)|^2+\mathrm{tr}(B_w^\top B_w)}{1+\lambda_2}(e^{(1+\lambda_2)h}-1) \tag{6.46}$$

where:

$$\lambda_1 = \max\left\{|\lambda_{\min}(-A^\top - A + BKK^\top B^\top)|, |\lambda_{\max}(-A^\top - A + BKK^\top B^\top)|\right\}$$
$$\lambda_2 = \max\left\{|\lambda_{\min}(\frac{1}{2}G^\top G - BK - K^\top B^\top)|, |\lambda_{\max}(\frac{1}{2}G^\top G - BK - K^\top B^\top)|\right\}$$

and $\lambda_{\min}(\cdot), \lambda_{\max}(\cdot)$ denote minimum and maximum eigenvalues, respectively, and $G = (A-BK)+(A-BK)^\top$.

Proof. First of all, since $s_k^i, s_{k+1}^i \in [t_i, t_{i+1}]$ and $s_k^i < s_{k+1}^i$, we know that the triggering condition has not been violated at s_k^i and thus $|\varepsilon(s_k^i)|\leq\epsilon$. Let us start with proving (6.46). We have that for all $t\in[s_k^i, s_{k+1}^i)$:

$$\begin{aligned}\mathscr{L}|\varepsilon(t)|^2 &= -\varepsilon^\top(t)\underbrace{[(A-BK)+(A-BK)^\top]}_{G}\zeta(t) - \varepsilon^\top(t)(BK+K^\top B^\top)\varepsilon(t) + \mathrm{tr}(B_w^\top B_w) \\ &\leq \frac{1}{2}|\zeta(t)|^2 + \varepsilon^\top(t)(\frac{1}{2}G^\top G - BK - K^\top B^\top)\varepsilon(t) + \mathrm{tr}(B_w^\top B_w) \\ &\leq |\zeta(t_i)|^2 + (1+\lambda_2)|\varepsilon(t)|^2 + \mathrm{tr}(B_w^\top B_w),\end{aligned}$$

where for the equality we used that $d\varepsilon(t) = -d\zeta(t)$, for the first inequality we used that $-\varepsilon^\top(t)G\zeta(t) \leq \frac{1}{2}|\zeta(t)|^2 + \frac{1}{2}\varepsilon^\top(t)G^\top G\varepsilon(t)$, and for the third inequality we used that $|\zeta(t)| - |\zeta(t_i)| \leq |\varepsilon(t)| \implies |\zeta(t)|^2 \leq 2|\zeta(t_i)|^2 + 2|\varepsilon(t)|^2$.

By Dynkin's formula [90, Theorem 7.4.1], we have:

$$\frac{d}{dt}\mathrm{E}[|\varepsilon(t)|^2|\mathscr{F}_{s_k^i}] = \mathrm{E}[\mathscr{L}|\varepsilon(t)|^2|\mathscr{F}_{s_k^i}] \leq |\zeta(t_i)|^2 + (1+\lambda_2)\mathrm{E}[|\varepsilon(t)|^2|\mathscr{F}_{s_k^i}] + \mathrm{tr}(B_w^\top B_w),$$

where $\zeta(t_i)$ is known since we are working in the time interval $t \in [s_k^i, s_{k+1}^i) \subseteq [t_i, t_{i+1})$ (i.e. $\zeta(t_i)$ is not a random variable). By applying the comparison lemma [63, pp. 102-103] to the inequality above, we obtain:

$$\mathrm{E}[|\varepsilon(t)|^2|\mathscr{F}_{s_k^i}] \leq |\varepsilon(s_k^i)|^2 e^{(1+\lambda_2)(t-s_k^i)} + \frac{|\zeta(t_i)|^2 + \mathrm{tr}(B_w^\top B_w)}{1+\lambda_2}(e^{(1+\lambda_2)(t-s_k^i)} - 1), \quad \forall\, t \in [s_k^i, s_{k+1}^i)$$

Since the function on the right-hand side is increasing w.r.t t, we can further extend this inequality by substituting $(t - s_k^i) \leftarrow h$. Finally, by using that $|\varepsilon(s_k^i)| \leq \epsilon$ and applying the expectation operator $\mathrm{E}[\cdot|\mathscr{F}_{t_i}]$, we get (6.46).

Let us proceed to proving (6.45). The first inequality of (6.45) (i.e., the one when $|\zeta(t_i)| < 2\epsilon$) is trivial, since $\mathrm{E}[-|\zeta(t)|^2|\mathscr{F}_{t_i}]$ is by definition non-positive. Let us focus on the second inequality of (6.45), i.e., on the case where $|\zeta(t_i)| \geq 2\epsilon$. Similarly to $\varepsilon(t)$, we obtain:

$$\begin{aligned}
\mathscr{L}(-|\zeta(t)|^2) &= -\zeta^\top(t)(A^\top + A)\zeta(t) - 2\zeta^\top(t)BK\zeta(t_i) - \mathrm{tr}(B_w^\top B_w) \\
&\leq \zeta^\top(t)(-A^\top - A + BKK^\top B^\top)\zeta(t) + |\zeta(t_i)|^2 - \mathrm{tr}(B_w^\top B_w) \\
&\leq \lambda_1|\zeta(t)|^2 + |\zeta(t_i)|^2,
\end{aligned}$$

where for the first inequality we used the fact that $-2\zeta^\top(t)BK\zeta(t_i) = 2(-\zeta^\top(t)BK)\zeta(t_i) \leq \zeta^\top(t)BKK^\top B^\top\zeta(t) + |\zeta(t_i)|^2$, and we also used that $-\mathrm{tr}(B_w^\top B_w)$ is always negative. Again, by Dynkin's formula, we obtain:

$$\frac{d}{dt}\mathrm{E}[-|\zeta(t)|^2|\mathscr{F}_{s_k^i}] = \mathrm{E}[\mathscr{L} - |\zeta(t)|^2|\mathscr{F}_{s_k^i}] \leq -\lambda_1\mathrm{E}[-|\zeta(t)|^2|\mathscr{F}_{s_k^i}] + |\zeta(t_i)|^2$$

By the comparison lemma (and the same argument regarding substituting $(t - s_k^i) \leftarrow h$), we get:

$$\mathrm{E}[-|\zeta(t)|^2|\mathscr{F}_{s_k^i}] \leq -|\zeta(s_k^i)|^2 e^{-\lambda_1 h} + \frac{|\zeta(t_i)|^2}{\lambda_1}(1 - e^{-\lambda_1 h})$$

Since $|\zeta(t_i)| \geq 2\epsilon$, we obtain: $|\varepsilon(s_k^i)| \leq \epsilon \implies -|\zeta(s_k^i)| + |\zeta(t_i)| \leq \epsilon \leq \frac{1}{2}\|\zeta(t_i)| \implies -|\zeta(s_k^i)|^2 \leq -\frac{1}{4}|\zeta(t_i)|^2$. By incorporating this to the above inequality, we get the second inequality of (6.45). □

We are ready to state and prove this section's main result, i.e. that with the right choice of h the stochastic PETC system can be rendered practically mean-square stable under Lebesgue sampling:

Theorem 6.C.2. *Consider the stochastic PETC system* (6.43) *and let Assumption* 6.C.1 *hold. Let* $\gamma \in (0,1)$ *and choose* $h > 0$ *such that:*[6]

$$\gamma\Big(-\frac{1}{4}e^{-\lambda_1 h} + \frac{1}{\lambda_1}(1 - e^{-\lambda_1 h})\Big) + \frac{1}{1+\lambda_2}(e^{(1+\lambda_2)h} - 1) \leq 0$$

The stochastic PETC system (6.43) *is practically mean-square stable.*

[6] We can always find such an h, since $\gamma\Big(-\frac{1}{4}e^{-\lambda_1 h} + \frac{1}{\lambda_1}(1 - e^{-\lambda_1 h})\Big) + \frac{1}{1+\lambda_2}(e^{(1+\lambda_2)h} - 1)$ is negative for $h = 0$ and it is strictly increasing.

Proof. We make use of Theorem 6.C.1. Consider the non-negative function $V : \mathbb{R}^n \times \mathbb{R}_{\geq 0} \to \mathbb{R}$, such that $V(x,t) = x^\top P x$, which is indeed twice-differentiable on its first argument and differentiable on its second.

First, it is obvious that (6.41) holds with $\underline{\alpha}(|x|) = \lambda_{\min}(P)|x|^2$ and $\overline{\alpha}(|x|) = \lambda_{\max}(P)|x|^2$. Moreover, for $\mathscr{L}V(\zeta(t),t)$ we have:

$$\begin{aligned}\mathscr{L}V(\zeta(t),t) &= \zeta^\top(t)(P(A-BK)+(A-BK)^\top P)\zeta(t) + 2\zeta^\top(t)PBK\varepsilon(t) + \operatorname{tr}(B_w^\top P B_w)\\ &\leq \zeta^\top(t)(P(A-BK)+(A-BK)^\top P + PBKK^\top B^\top P)\zeta(t) + |\varepsilon(t)|^2 + \operatorname{tr}(B_w^\top P B_w)\\ &\leq -|\zeta(t)|^2 + |\varepsilon(t)|^2 + \operatorname{tr}(B_w^\top P B_w), \quad \forall\, t \geq 0\end{aligned} \tag{6.47}$$

where the first inequality comes from the fact that $2\zeta^\top(t)PBK\varepsilon(t) \leq \zeta^\top(t)PBKK^\top B^\top P\zeta(t) + |\varepsilon(t)|^2$ and the second inequality comes from Assumption 6.C.1. We want to prove that, for a properly designed period $h = s_{k+1}^i - s_k^i$, (6.42) holds for all $t \in [s_k^i, s_{k+1}^i)$ and any $i,k \in \mathbb{N}$. For any $t \in [s_k^i, s_{k+1}^i)$ and any $i,k \in \mathbb{N}$, from (6.47) we obtain:

$$\mathrm{E}[\mathscr{L}V(\zeta(t),t)|\mathscr{F}_{t_i}] \leq -\mathrm{E}[|\zeta(t)|^2|\mathscr{F}_{t_i}] + \mathrm{E}[|\varepsilon(t)|^2|\mathscr{F}_{t_i}] + \operatorname{tr}(B_w^\top P B_w)$$

Case 1, $|\zeta(t_i)| \geq 2\epsilon$**:** Consider any $\gamma \in (0,1)$. In this case, from (6.45) and (6.46) we have:

$$\begin{aligned}\mathrm{E}[\mathscr{L}V(\zeta(t),t)|\mathscr{F}_{t_i}] &\leq (-1+\gamma)\mathrm{E}(|\zeta(t)|^2|\mathscr{F}_{t_i}) + \gamma\mathrm{E}[-|\zeta(t)|^2|\mathscr{F}_{t_i}] + \mathrm{E}[|\varepsilon(t)|^2|\mathscr{F}_{t_i}] + \operatorname{tr}(B_w^\top P B_w)\\ &\leq (-1+\gamma)\mathrm{E}[|\zeta(t)|^2|\mathscr{F}_{t_i}] +\\ &\quad + |\zeta(t_i)|^2 \underbrace{\left[\gamma\left(-\frac{1}{4}e^{-\lambda_1 h} + \frac{1}{\lambda_1}(1-e^{-\lambda_1 h})\right) + \frac{1}{1+\lambda_2}(e^{(1+\lambda_2)h}-1)\right]}_{\leq 0} +\\ &\quad + \underbrace{\epsilon^2 e^{(1+\lambda_2)h} + \frac{\operatorname{tr}(B_w^\top B_w)}{1+\lambda_2}(e^{(1+\lambda_2)h}-1) + \operatorname{tr}(B_w^\top P B_w)}_{c_1}\\ &\leq (-1+\gamma)\mathrm{E}[|\zeta(t)|^2|\mathscr{F}_{t_i}] + c_1\end{aligned}$$

Case 2, $|\zeta(t_i)| < 2\epsilon$**:** Consider any $\gamma \in (0,1)$. In this case, from (6.46) we have:

$$\begin{aligned}\mathrm{E}[\mathscr{L}V(\zeta(t),t)|\mathscr{F}_{t_i}] &\leq (-1+\gamma)\mathrm{E}[|\zeta(t)|^2|\mathscr{F}_{t_i}] + \gamma\mathrm{E}[-|\zeta(t)|^2|\mathscr{F}_{t_i}] + \mathrm{E}[|\varepsilon(t)|^2|\mathscr{F}_{t_i}] + \operatorname{tr}(B_w^\top P B_w)\\ &\leq (-1+\gamma)\mathrm{E}[|\zeta(t)|^2|\mathscr{F}_{t_i}] +\\ &\quad + \underbrace{\epsilon^2 e^{(1+\lambda_2)h} + \frac{4\epsilon^2 + \operatorname{tr}(B_w^\top B_w)}{1+\lambda_2}(e^{(1+\lambda_2)h}-1) + \operatorname{tr}(B_w^\top P B_w)}_{c_2}\\ &\leq (-1+\gamma)\mathrm{E}[|\zeta(t)|^2|\mathscr{F}_{t_i}] + c_2\end{aligned}$$

where we used that: a) $\gamma\mathrm{E}[-|\zeta(t)|^2|\mathscr{F}_{t_i}]$ is always negative and neglected it from the right-hand side, and b) that $|\zeta(t_i)| < 2\epsilon$.

Observe that $c_2 = c_1 + \frac{4\epsilon^2}{1+\lambda_2}(e^{(1+\lambda_2)h}-1) \geq c_1$. Thus, from both cases 1 and 2, we obtain that for all $t \in [s_k^i, s_{k+1}^i)$:

$$\mathrm{E}[\mathscr{L}V(\zeta(t),t)|\mathscr{F}_{t_i}] \leq (-1+\gamma)\mathrm{E}[|\zeta(t)|^2|\mathscr{F}_{t_i}] + c_2$$

Finally, by noticing that the above inequality holds for any interval $[s_k^i, s_{k+1}^i)$, and by applying the expectation operator $\mathrm{E}[\cdot]$, we obtain:

$$\mathrm{E}[\mathscr{L}V(\zeta(t),t)] \leq (-1+\gamma)\mathrm{E}[|\zeta(t)|^2] + c_2, \quad \forall\, t \geq 0$$

Thus, (6.42) is satisfied with $\alpha(|\zeta(t)|) = (1-\gamma)|\zeta(t)|^2$, which is class-$\mathscr{K}_\infty$. Finally, it is obvious that $\lim_{|x|\to\infty} \frac{\alpha(|x|)}{\overline{\alpha}(|x|^2)} = \frac{1-\gamma}{\lambda_{\max}(P)} > 0$. The proof is complete. □

7

Conclusions and Recommendations for Future Research

This chapter concludes the dissertation, summarizes the main contributions along with their practical implications, discusses limitations and suggests directions for future research.

7.1. GENERAL CONCLUSION

This dissertation started with a quote: *"An ounce of action is worth a ton of theory"*. This quote can be interpreted in two ways, which are certainly intertwined. The first and obvious way is that a tiny bit of action might be more valuable than a big amount of theory; this often proves true in sciences, as, sometimes, it takes only an observation or an experiment to start a whole theory. Arguably, this is how the whole field of ETC started, with the experimental study in [5]. The second way, in the author's opinion, suggests that it often takes a lot of theoretical work to arrive to (even a bit of) action. This is definitely the case for the field of control in general, but also for the field of ETC, in particular. More than two decades of predominantly theoretical research, and, still, ETC has not been adopted widely in practice.

In the introduction, we discussed how there is still critical knowledge missing, specifically, regarding ETC's sampling behaviour and predictions thereof. We argued about the (practical) implications that unravelling ETC's sampling behaviour can have, by bringing forth three different contexts: self-triggered control, traffic scheduling, and formal assessment of the sampling behaviour. This dissertation has studied the sampling behaviour of ETC in all three aforementioned contexts, aiming to contribute some missing pieces in that theoretical gap, such that widespread adoption of ETC in practice comes (a bit) closer.

7.2. CONTRIBUTIONS, LIMITATIONS AND FURTHER RESEARCH

In what follows, we discuss practical implications of this work's contributions, we point out its limitations and suggest future research directions.

CHAPTERS 3 AND 4: REGION-BASED SELF-TRIGGERED CONTROL

The region-based STC scheme that has been developed in Chapters 3 and 4, by providing a generic framework to incorporate different performance specifications (by emulating different triggering conditions) and a way to trade off sampling performance and online computational load, arguably constitutes a generally practical proposal for implementation of STC in practice. The engineer, to implement STC, mainly has to decide on the desired specification and specify a corresponding triggering function (which can be done by going through the literature of ETC). Moreover, computational load and sampling performance are tuned easily and intuitively, by simply tuning the number of regions.

Nevertheless, there are certain limitations and a lot of room for further research:

- In both Chapters 3 and 4 only static state-feedback has been studied. Extensions to dynamic output-feedback have to be made, in order to facilitate practical implementations of region-based STC. One possible way to do this is to incorporate the controller's and observer's dynamics into the system description (2.8).

- There are even more general types of triggering conditions that have to be addressed:

  – First, dynamic triggering conditions, originally introduced in [8], have been established as a very efficient proposal for stabilization purposes. In fact, a

very recent work [91] demonstrated that dynamic STC has the potential of significantly reducing the sampling frequency of STC. Thus, the extension of region-based STC to dynamic triggering conditions has to be studied. Let us recall the dynamic triggering condition proposed in [8]:

$$t_{i+1} = t_i + \inf\Big\{t > 0 : \ -\eta(t) - \sigma_2 \cdot \Big(\sigma_1 \beta_1(\zeta(t)) - \beta_2(\varepsilon(t))\Big) \geq 0\Big\},$$

where $\sigma_i \in (0,1)$ and $\beta_i \in \mathcal{K}_\infty$. Thus, the triggering function to be considered is:

$$\phi(\zeta(t), \varepsilon(t), \eta(t)) = -\eta(t) - \sigma_2 \cdot \Big(\sigma_1 \beta_1(\zeta(t)) - \beta_2(\varepsilon(t))\Big). \tag{7.1}$$

To emulate such a triggering function, with the proposed scheme, the dynamic variable η can be included as a part of the state of the system, and the extended state-vector reads as $\xi = \begin{pmatrix} \zeta^\top & \eta^\top & \varepsilon_\zeta^\top & \varepsilon_\eta^\top \end{pmatrix}^\top$, where ε_η is the dummy measurement error corresponding to η, with dynamics $\dot{\varepsilon}_\eta = 0$.

– Triggering conditions that address complex specifications, such as signal temporal logic tasks [92], should also be studied.

- The cases where (approximations of) IMs exhibit singularities have to be thoroughly studied, to gain further insight on their shapes and properties. Moreover, we have assumed the origin to be the only equilibrium in Chapters 3 and 4, because this is typical in many ETC studies. However, we have not (directly) invoked this assumption in any of our proofs, so it might not be needed. This needs a more careful study.

- As mentioned in Chapter 3, isochronous manifolds are inherent in any system with an output. Applications of approximations of isochronous manifolds outside the context of ETC and STC could, then, be explored.

CHAPTER 5: ABSTRACTIONS OF NONLINEAR ETC SYSTEMS FOR TRAFFIC SCHEDULING

Having constructed traffic abstractions of general nonlinear ETC systems with disturbances or uncertainties, we extended the applicability of versatile abstraction-based scheduling of ETC traffic to a considerably wider class of systems. However, there are a few things that have to be addressed:

- The constructed abstractions suffer from the curse of dimensionality: the size of the abstraction's state set scales exponentially with the system's dimensions. A potential way to introduce scalability is to use IM-based partitioning, without partitioning via cones, as in Chapters 3 and 4 (and similar to [41] for linear systems). However, as already argued in Chapter 5, the resulting regions would be too large for reachability-analysis purposes. Thus, this direction is not straightforward.

- Towards gaining complete control over the abstraction's timing intervals, by gaining control over the regions' timing upper bounds as well, outer approximations of isochronous manifolds could be explored, as commented in a footnote in Chapter 5.

However, deriving outer approximations of IMs is not as simple as merely altering the direction of inequality (3.10). For example, there is no straightforward way to enforce that the obtained lower bound of the triggering function exhibits a zero-crossing w.r.t. time (e.g., by enforcing monotonicity like what was done with the lower bound).

- Experimental results showcasing abstraction-based scheduling in networks of nonlinear ETC systems are the natural next step to the work presented in Chapter 5. These results are expected to demonstrate how conservative (or not) the constructed abstractions are for scheduling purposes and if there is a need for further improvement.

- The constructed abstractions could be employed for assessing the sampling performance of nonlinear ETC systems, similar to what has been done in [43]. Note, however, that extending certain results from [43], which studies linear PETC systems, to nonlinear systems is not straightforward.

CHAPTER 6: FORMAL ANALYSIS OF THE SAMPLING BEHAVIOUR OF STOCHASTIC PETC

The developments of Chapter 6 enable the formal assessment of the sampling (vs. control) performance and behaviour of stochastic PETC systems, through the computation of bounds on associated metrics. Employing these results, an engineer, who has to implement an ETC system, obtains knowledge on how frequently the system is expected to communicate, what sampling time patterns are the most probable to arise, what is the achieved trade off between sampling frequency and some control performance metric, etc. Nonetheless, there is still plenty of room for further research:

- Like the abstractions created in Chapter 5, the IMCs constructed in Chapter 6 suffer from the curse of dimensionality. Thus, more scalable solutions have to be explored.

- Extending the developed method to more general classes of systems, both in terms of nominal system dynamics and in terms of the way noise affects them, is a natural next step. For that, comparison theorems such as [93] could be used, to bound a nonlinear SDE with linear ones (similar to what we did in Chapters 3 and 4, to bound the evolution of the triggering function), and then apply the methodology developed in Chapter 6. An alternative way to approach the problem is by approximating the nonlinear SDE with Gaussian processes [94].

- The constructed IMCs can be endowed with controllable actions (in the spirit of what is done for non-stochastic ETC systems in [39] or [41]), becoming interval Markov decision processes, such that they are employed for traffic scheduling with probabilistic guarantees (e.g., minimizing the probability of packet collisions).

Finally, it is worth noting that incorporating the developments of Chapter 6 to the Python toolbox ETCetera [47] has not been finalized yet. The code that automates the developments of Chapter 6 and reproduces its results will be made publicly available through the release of the next version of ETCetera.

BIBLIOGRAPHY

[1] I. S. Lanka, "Event-triggered control for automotive systems: Theoretical analysis and experimental research", 2021.

[2] R. S. Raji, "Smart networks for control", *IEEE spectrum*, vol. 31, no. 6, pp. 49–55, 1994.

[3] W. P. M. H. Heemels, K. H. Johansson, and P. Tabuada, "An introduction to event-triggered and self-triggered control", in *Proceedings of the IEEE Conference on Decision and Control*, 2012, pp. 3270–3285.

[4] C. Peng and F. Li, "A survey on recent advances in event-triggered communication and control", *Information Sciences*, vol. 457, pp. 113–125, 2018.

[5] K.-E. Åarzén, "A simple event-based pid controller", *IFAC Proceedings Volumes*, vol. 32, no. 2, pp. 8687–8692, 1999.

[6] K. J. Astrom and B. M. Bernhardsson, "Comparison of riemann and lebesgue sampling for first order stochastic systems", in *Proceedings of the 41st IEEE Conference on Decision and Control, 2002.*, IEEE, vol. 2, 2002, pp. 2011–2016.

[7] P. Tabuada, "Event-triggered real-time scheduling of stabilizing control tasks", *IEEE Transactions on Automatic Control*, vol. 52, no. 9, pp. 1680–1685, 2007.

[8] A. Girard, "Dynamic triggering mechanisms for event-triggered control", *IEEE Transactions on Automatic Control*, vol. 60, no. 7, pp. 1992–1997, 2015.

[9] J. Lunze and D. Lehmann, "A state-feedback approach to event-based control", *Automatica*, vol. 46, no. 1, pp. 211–215, 2010.

[10] W. H. Heemels, M. Donkers, and A. R. Teel, "Periodic event-triggered control for linear systems", *IEEE Transactions on Automatic Control*, vol. 58, no. 4, pp. 847–861, 2012.

[11] M. Mazo Jr. and P. Tabuada, "Decentralized event-triggered control over wireless sensor/actuator networks", *IEEE Transactions on Automatic Control*, vol. 56, no. 10, pp. 2456–2461, 2011.

[12] R. Postoyan, P. Tabuada, D. Nesic, and A. A. Martinez, "A framework for the event-triggered stabilization of nonlinear systems.", *IEEE Transactions on Automatic Control*, vol. 60, no. 4, pp. 982–996, 2015.

[13] D. Antunes and W. Heemels, "Rollout event-triggered control: Beyond periodic control performance", *IEEE Transactions on Automatic Control*, vol. 59, no. 12, pp. 3296–3311, 2014.

[14] Y. Wang, W. X. Zheng, and H. Zhang, "Dynamic event-based control of nonlinear stochastic systems", *IEEE Transactions on Automatic Control*, vol. 62, no. 12, pp. 6544–6551, 2017.

[15] F. Li and Y. Liu, "Periodic event-triggered output-feedback stabilization for stochastic systems", *IEEE Transactions on Cybernetics*, 2019.

[16] Q. Zhu, "Stabilization of stochastic nonlinear delay systems with exogenous disturbances and the event-triggered feedback control", *IEEE Transactions on Automatic Control*, vol. 64, no. 9, pp. 3764–3771, 2018.

[17] S. Luo and F. Deng, "On event-triggered control of nonlinear stochastic systems", *IEEE Transactions on Automatic Control*, vol. 65, no. 1, pp. 369–375, 2019.

[18] T. Liu and Z.-P. Jiang, "A small-gain approach to robust event-triggered control of nonlinear systems", *IEEE Transactions on Automatic Control*, vol. 60, no. 8, pp. 2072–2085, 2015.

[19] U. Tiberi and K. H. Johansson, "A simple self-triggered sampler for perturbed nonlinear systems", *Nonlinear Analysis: Hybrid Systems*, vol. 10, no. 1, pp. 126–140, 2013.

[20] M. D. Di Benedetto, S. Di Gennaro, and A. D'innocenzo, "Digital self-triggered robust control of nonlinear systems", *International Journal of Control*, vol. 86, no. 9, pp. 1664–1672, 2013.

[21] D. Tolic, R. G. Sanfelice, and R. Fierro, "Self-triggering in nonlinear systems: A small gain theorem approach", in *Mediterranean Conference on Control and Automation*, 2012, pp. 941–947.

[22] D. Theodosis and D. V. Dimarogonas, "Self-triggered control under actuator delays", in *2018 IEEE Conference on Decision and Control*, IEEE, 2018, pp. 1524–1529.

[23] A. Anta and P. Tabuada, "To sample or not to sample: Self-triggered control for nonlinear systems", *IEEE Transactions on Automatic Control*, vol. 55, no. 9, pp. 2030–2042, 2010.

[24] A. Anta and P. Tabuada, "Exploiting isochrony in self-triggered control", *IEEE Transactions on Automatic Control*, vol. 57, no. 4, pp. 950–962, 2012.

[25] M. Velasco, J. Fuertes, and P. Marti, "The self triggered task model for real-time control systems", in *Work-in-Progress Session of the 24th IEEE Real-Time Systems Symposium*, vol. 384, 2003.

[26] M. Mazo Jr., A. Anta, and P. Tabuada, "An iss self-triggered implementation of linear controllers", *Automatica*, vol. 46, no. 8, pp. 1310–1314, 2010.

[27] ——, "On self-triggered control for linear systems: Guarantees and complexity", in *European Control Conference*, 2009, pp. 3767–3772.

[28] T. Gommans, D. Antunes, T. Donkers, P. Tabuada, and M. Heemels, "Self-triggered linear quadratic control", *Automatica*, vol. 50, no. 4, pp. 1279–1287, 2014.

[29] C. Fiter, L. Hetel, W. Perruquetti, and J.-P. Richard, "A state dependent sampling for linear state feedback", *Automatica*, vol. 48, no. 8, pp. 1860–1867, 2012.

[30] X. Wang and M. D. Lemmon, "Self-triggered feedback control systems with finite-gain l2stability", *IEEE Transactions on Automatic Control*, vol. 54, no. 3, pp. 452–467, 2009.

[31] ——, "Self-triggering under state-independent disturbances", *IEEE Transactions on Automatic Control*, vol. 55, no. 6, pp. 1494–1500, 2010.

[32] G. C. Buttazzo, G. Lipari, and L. Abeni, "Elastic task model for adaptive rate control", in *Proceedings 19th IEEE Real-Time Systems Symposium (Cat. No. 98CB36279)*, IEEE, 1998, pp. 286–295.

[33] M. Caccamo, G. Buttazzo, and L. Sha, "Elastic feedback control", in *Proceedings 12th Euromicro Conference on Real-Time Systems. Euromicro RTS 2000*, IEEE, 2000, pp. 121–128.

[34] R. Bhattacharya and G. J. Balas, "Anytime control algorithm: Model reduction approach", *Journal of Guidance, Control, and Dynamics*, vol. 27, no. 5, pp. 767–776, 2004.

[35] D. Fontanelli, L. Greco, and A. Bicchi, "Anytime control algorithms for embedded real-time systems", *Lecture Notes in Computer Science (including subseries Lecture Notes in Artificial Intelligence and Lecture Notes in Bioinformatics)*, vol. 4981 LNCS, pp. 158–171, 2008.

[36] S. Al-Areqi, D. Görges, and S. Liu, "Event-based networked control and scheduling codesign with guaranteed performance", *Automatica*, vol. 57, pp. 128–134, 2015.

[37] C. Lu, J. A. Stankovic, S. H. Son, and G. Tao, "Feedback control real-time scheduling: Framework, modeling, and algorithms", *Real-Time Systems*, vol. 23, no. 1-2, pp. 85–126, 2002.

[38] A. Cervin and J. Eker, "Control-scheduling codesign of real-time systems: The control server approach", *Journal of Embedded Computing*, vol. 1, no. 2, pp. 209–224, 2005.

[39] A. S. Kolarijani, D. Adzkiya, and M. Mazo Jr., "Symbolic abstractions for the scheduling of event-triggered control systems", in *2015 54th IEEE Conference on Decision and Control (CDC)*, IEEE, 2015, pp. 6153–6158.

[40] A. Kolarijani and M. Mazo Jr., "A formal traffic characterization of lti event-triggered control systems", *IEEE Transactions on Control of Network Systems*, 2016.

[41] G. de A. Gleizer and M. Mazo Jr., "Scalable traffic models for scheduling of linear periodic event-triggered controllers", *IFAC-PapersOnLine*, vol. 53, no. 2, pp. 2726–2732, 2020, 21st IFAC World Congress, ISSN: 2405-8963.

[42] P. Bouyer, F. Cassez, E. Fleury, and K. G. Larsen, "Optimal strategies in priced timed game automata", in *International Conference on Foundations of Software Technology and Theoretical Computer Science*, Springer, 2004, pp. 148–160.

[43] G. de A. Gleizer and M. Mazo Jr., "Computing the sampling performance of event-triggered control", in *Proceedings of the 24th International Conference on Hybrid Systems: Computation and Control*, 2021, pp. 1–7.

[44] B. Demirel, V. Gupta, D. E. Quevedo, and M. Johansson, "On the trade-off between communication and control cost in event-triggered dead-beat control", *IEEE Transactions on Automatic Control*, vol. 62, no. 6, pp. 2973–2980, 2016.

[45] R. Postoyan, R. G. Sanfelice, and W. P. M. H. Heemels, "Inter-event times analysis for planar linear event-triggered controlled systems", in *2019 IEEE 58th Conference on Decision and Control (CDC)*, 2019, pp. 1662–1667. DOI: 10.1109/CDC40024.2019.9028888.

[46] A. Rajan and P. Tallapragada, "Analysis of inter-event times for planar linear systems under a general class of event triggering rules", in *2020 59th IEEE Conference on Decision and Control (CDC)*, 2020, pp. 5206–5211. DOI: 10.1109/CDC42340.2020.9304406.

[47] G. Delimpaltadakis, G. de A. Gleizer, I. van Straalen, and M. Mazo Jr., "Etcetera: Beyond event-triggered control", in *Proceedings of the 25th International Conference on Hybrid Systems: Computation and Control*, 2022.

[48] M. Kawski, "Geometric homogeneity and stabilization", in *Nonlinear Control Systems Design 1995*, Elsevier, 1995, pp. 147–152.

[49] G. Delimpaltadakis and M. Mazo Jr., "Isochronous partitions for region-based self-triggered control", *IEEE Transactions on Automatic Control*, vol. 66, no. 3, pp. 1160–1173, 2020. DOI: 10.1109/TAC.2020.2994020.

[50] S. Prajna, A. Papachristodoulou, and P. A. Parrilo, "Introducing sostools: A general purpose sum of squares programming solver", in *Proceedings of the 41st IEEE Conference on Decision and Control*, IEEE, vol. 1, 2002, pp. 741–746.

[51] R. Gunderson, "A comparison lemma for higher order trajectory derivatives", *Proceedings of the American Mathematical Society*, pp. 543–548, 1971.

[52] J. Kapinski, S. Sankaranarayanan, J. V. Deshmukh, and N. Aréchiga, "Simulation-guided lyapunov analysis for hybrid dynamical systems", in *Proceedings of the 17th International Conference on Hybrid Systems: Computation and Control*, 2014, pp. 133–142.

[53] S. Gao, S. Kong, and E. M. Clarke, "Dreal: An smt solver for nonlinear theories over the reals", in *International Conference on Automated Deduction*, Springer, 2013, pp. 208–214.

[54] M. Krstic and P. V. Kokotovic, "Lean backstepping design for a jet engine compressor model", in *Proceedings of the 4th IEEE Conference on Control Applications*, IEEE, 1995, pp. 1047–1052.

[55] V. Meigoli and S. K. Y. Nikravesh, "A new theorem on higher order derivatives of lyapunov functions", *ISA transactions*, vol. 48, no. 2, pp. 173–179, 2009.

[56] D. Carnevale, A. R. Teel, and D. Nesic, "A lyapunov proof of an improved maximum allowable transfer interval for networked control systems", *IEEE Transactions on Automatic Control*, vol. 52, no. 5, pp. 892–897, 2007.

[57] H. L. Smith, *Monotone dynamical systems: an introduction to the theory of competitive and cooperative systems*, 41. American Mathematical Soc., 2008.

[58] Y. P. (https://math.stackexchange.com/users/360408/yuval-peres), *Existence (and uniqueness) of root of function with positive and strictly increasing derivative*, Mathematics Stack Exchange, URL:https://math.stackexchange.com/q/4459874 (version: 2022-05-27). eprint: https://math.stackexchange.com/q/4459874. [Online]. Available: https://math.stackexchange.com/q/4459874.

[59] G. Delimpaltadakis and M. Mazo Jr., "Region-based self-triggered control for perturbed and uncertain nonlinear systems", *IEEE Transactions on Control of Network Systems*, vol. 8, no. 2, pp. 757–768, 2021. DOI: 10.1109/TCNS.2021.3050121.

[60] E. Bernuau, D. Efimov, W. Perruquetti, and A. Polyakov, "On an extension of homogeneity notion for differential inclusions", in *2013 European Control Conference (ECC)*, IEEE, 2013, pp. 2204–2209.

[61] A. F. Filippov, *Differential Equations with Discontinuous Righthand Sides*. Kluwer Academic Publishers, Dordrecht, 1988.

[62] U. Tiberi and K. H. Johansson, "A simple self-triggered sampler for perturbed nonlinear systems", *Nonlinear Analysis: Hybrid Systems*, vol. 10, no. 1, pp. 126–140, 2013.

[63] H. K. Khalil, "Noninear systems", *Prentice-Hall, New Jersey*, vol. 2, no. 5, pp. 5–1, 1996.

[64] G. Delimpaltadakis and M. Mazo Jr., "Abstracting the traffic of nonlinear event-triggered control systems", *arXiv preprint arXiv:2010.12341, under review*, 2020.

[65] ——, "Traffic abstractions of nonlinear homogeneous event-triggered control systems", in *2020 IEEE 59th Conference on Decision and Control (CDC)*, 2020, pp. 4991–4998.

[66] S. Kong, S. Gao, W. Chen, and E. Clarke, "Dreach: Delta-reachability analysis for hybrid systems", in *International Conference on TOOLS and Algorithms for the Construction and Analysis of Systems*, Springer, 2015, pp. 200–205.

[67] X. Chen, E. Ábrahám, and S. Sankaranarayanan, "Flow*: An analyzer for nonlinear hybrid systems", in *International Conference on Computer Aided Verification*, Springer, 2013, pp. 258–263.

[68] P. Tabuada, *Verification and control of hybrid systems: a symbolic approach*. Springer Science & Business Media, 2009.

[69] G. Delimpaltadakis, L. Laurenti, and M. Mazo Jr., "Formal analysis of the sampling behaviour of stochastic event-triggered control", *arXiv preprint arXiv:2202.10178, under review*, 2022.

[70] ——, "Abstracting the sampling behaviour of stochastic linear periodic event-triggered control systems", in *2021 60th IEEE Conference on Decision and Control (CDC)*, 2021, pp. 1287–1294. DOI: 10.1109/CDC45484.2021.9683751.

[71] E. M. Hahn, V. Hashemi, H. Hermanns, M. Lahijanian, and A. Turrini, "Interval markov decision processes with multiple objectives: From robust strategies to pareto curves", *ACM Transactions on Modeling and Computer Simulation (TOMACS)*, vol. 29, no. 4, pp. 1–31, 2019.

[72] R. Givan, S. Leach, and T. Dean, "Bounded-parameter markov decision processes", *Artificial Intelligence*, vol. 122, no. 1-2, pp. 71–109, 2000.

[73] M. Lahijanian, S. B. Andersson, and C. Belta, "Formal verification and synthesis for discrete-time stochastic systems", *IEEE Transactions on Automatic Control*, vol. 60, no. 8, pp. 2031–2045, 2015.

[74] M. Dutreix and S. Coogan, "Specification-guided verification and abstraction refinement of mixed monotone stochastic systems", *IEEE Transactions on Automatic Control*, vol. 66, no. 7, pp. 2975–2990, 2021.

[75] L. Laurenti, M. Lahijanian, A. Abate, L. Cardelli, and M. Kwiatkowska, "Formal and efficient synthesis for continuous-time linear stochastic hybrid processes", *IEEE Transactions on Automatic Control*, vol. 66, no. 1, pp. 17–32, 2021. DOI: 10.1109/TAC.2020.2975028.

[76] J. Jackson, L. Laurenti, E. Frew, and M. Lahijanian, "Strategy synthesis for partially-known switched stochastic systems", in *Proceedings of the 24th International Conference on Hybrid Systems: Computation and Control*, 2021, pp. 1–11.

[77] A. Abate, M. Prandini, J. Lygeros, and S. Sastry, "Probabilistic reachability and safety for controlled discrete time stochastic hybrid systems", *Automatica*, vol. 44, no. 11, pp. 2724–2734, 2008.

[78] M. L. Puterman, *Markov decision processes: discrete stochastic dynamic programming*. John Wiley & Sons, 2014.

[79] C. I. Tulcea, "Mesures dans les espaces produits", *Atti Acad. Naz. Lincei Rend. Cl Sci. Fis. Mat. Nat*, vol. 8, no. 7, 1949.

[80] X. Mao, *Stochastic differential equations and applications*. Elsevier, 2007.

[81] R. T. Rockafellar, *Convex analysis*. Princeton university press, 2015.

[82] A. Blaas, A. Patane, L. Laurenti, L. Cardelli, M. Kwiatkowska, and S. Roberts, "Adversarial robustness guarantees for classification with gaussian processes", *arXiv preprint arXiv:1905.11876*, 2019.

[83] M. L. Eaton, "Multivariate statistics: A vector space approach.", *John Wiley & Sons*, 1983.

[84] A. Genz, "Numerical computation of multivariate normal probabilities", *Journal of computational and graphical statistics*, vol. 1, no. 2, pp. 141–149, 1992.

[85] P. Virtanen, R. Gommers, T. E. Oliphant, M. Haberland, T. Reddy, D. Cournapeau, E. Burovski, P. Peterson, W. Weckesser, J. Bright, *et al.*, "Scipy 1.0: Fundamental algorithms for scientific computing in python", *Nature methods*, vol. 17, no. 3, pp. 261–272, 2020.

[86] N. Cauchi, L. Laurenti, M. Lahijanian, A. Abate, M. Kwiatkowska, and L. Cardelli, "Efficiency through uncertainty: Scalable formal synthesis for stochastic hybrid systems", in *Proceedings of the 22nd ACM International Conference on Hybrid Systems: Computation and Control*, 2019, pp. 240–251.

[87] A. Prékopa, "On logarithmic concave measures and functions", *Acta Scientiarum Mathematicarum*, vol. 34, pp. 335–343, 1973.

[88] R. P. Anderson, D. Milutinović, and D. V. Dimarogonas, "Self-triggered sampling for second-moment stability of state-feedback controlled sde systems", *Automatica*, vol. 54, pp. 8–15, 2015.

[89] L. Huang and X. Mao, "On input-to-state stability of stochastic retarded systems with markovian switching", *IEEE Transactions on Automatic Control*, vol. 54, no. 8, pp. 1898–1902, 2009.

[90] B. Oksendal, *Stochastic differential equations: an introduction with applications*. Springer Science & Business Media, 2013.

[91] M. Hertneck and F. Allgöwer, "Robust dynamic self-triggered control for nonlinear systems using hybrid lyapunov functions", *arXiv preprint arXiv:2111.04347*, 2021.

[92] L. Lindemann, D. Maity, J. S. Baras, and D. V. Dimarogonas, "Event-triggered feedback control for signal temporal logic tasks", in *2018 IEEE Conference on Decision and Control (CDC)*, IEEE, 2018, pp. 146–151.

[93] C. Geiß and R. Manthey, "Comparison theorems for stochastic differential equations in finite and infinite dimensions", *Stochastic processes and their applications*, vol. 53, no. 1, pp. 23–35, 1994.

[94] C. Archambeau, D. Cornford, M. Opper, and J. Shawe-Taylor, "Gaussian process approximations of stochastic differential equations", in *Gaussian Processes in Practice*, PMLR, 2007, pp. 1–16.

ACKNOWLEDGEMENTS

First, I would like to thank the PhD committee members for allocating the time to read my work, comment on it, and help me improve it and reflect on several aspects of it.

Moreover, I would like to express my gratitude to my co-promotor Peyman Mohajerin Esfahani, for the fruitful discussions we had and the advice he gave me on several matters.

I owe a lot to my supervisor Manuel Mazo Jr. He has been very helpful in proposing solutions to several technical problems our research was facing. But, he has been much more than the technical expert I needed. He has been very active on my supervision and he had always the time to talk about my concerns. The support and care I got from him during my PhD, especially the tough times, was incredible. He has been a true mentor, guiding me to become a researcher, and teaching me a lot about the nature of research and about scientific ethics. Our research group has been a real pleasure to belong to, precisely because of him being the group's leader. I will never forget how open-minded Manuel has been; we would always argue about politics, philosophy, music, etc., but he would never stop encouraging such discussions within the group. And that is because, I think, he understood that a well-rounded person is a well-rounded researcher and that a well-functioning group is the one whose members have created strong ties beyond work. I could carry on for pages about how grateful I am to him, but he would rightfully say that this would be anti-ecological with all the extra pages, so I will just say this: I could not have imagined of a better supervisor than Manuel.

Next, I would like to acknowledge Luca Laurenti. The last part of this dissertation, which focuses on stochastic systems, is a product of a fruitful collaboration with him. He has taught me lots of things on the field, and he has always been there when I needed guidance on technical problems. However, his contribution does not stop there, as he has provided me with valuable advice on my career.

A special thanks goes to to all members of our research group. I carried out my PhD side-by-side with Gabriel Gleizer, Daniel Jarne Ornia and Cees Verdier. We struggled together, we grew together, and we have become good friends, sharing the shaping experience that is a PhD. All of them have contributed to several parts of this dissertation. Indicatively, but not limited to: Gabriel, working under the same project, has helped me with many discussions on all parts of the work, especially on the ones related to Chapters 3, 4 and 5; Daniel contributed through discussions to certain parts of Section 6.5; Cees contributed to coding the algorithm of Section 3.6 and to the thesis' Dutch summary. Apart from them, I thank Anton Proskurnikov, Khushraj Madnani, Gururaj Maddodi, Alexéy Ilyushkin, Andrea Peruffo and Rudi Coppola for all the nice time we spent together.

I, also, thank the former MSc. students Indeevar Shyam Lanka, Tim Sweering and Stijn Römer for their excellent work on their respective projects. They, definitely, helped me improve my supervising skills, and I hope I paid it back with a good supervision. Moreover, I thank Ivo van Straalen, for the nice collaboration we had on developing ETCetera.

I am grateful to all DCSC staff for making this journey a great experience. A special mention goes to: prof. Tamas Keviczky, whom I assisted as a T.A. in the Control Theory course, from which I gained a lot; Amin Sharifi Kolarijani, for a great collaboration during our common teaching assistant-ship; Twan Keijzer, for our interesting discussions and fun breaks at work; Abhimanyu Gupta for all the tennis and discussions.

Furthermore, I would like to express my gratitude to my former advisors, prof. Kostas J. Kyriakopoulos and prof. Charalampos Bechlioulis. It is largely on them, that I chose control theory; and I haven't regretted it ever since.

I thank all my friends, and especially Spyros, Giannis, Giorgos, Stamatis, Asteris and Dimitris. Their presence in my life has brightened my spare time and helped release all the stress. Also, a special mention to my feline friend, Nori, who has made me a more caring person.

Certainly, if it weren't for my family, I wouldn't be here. They have always been there for me and, to a big extent, they have made me who I am. I owe everything to them.

Finally, I will be eternally grateful to Artemis. Moving to a foreign country; pandemic; PhD. We got through all difficulties, together. Her love and support has been the most valuable weapon in my arsenal, all these years.

Giannis Delimpaltadakis
Delft, March 2022

CURRICULUM VITÆ

Giannis DELIMPALTADAKIS

15-08-1993 Born in Veria, Greece.

EDUCATION

2011–2017 Diploma Electrical and Computer Engineering
National Technical University of Athens
Grade: 8.26/10
Thesis: Decentralized Control with Obstacle Avoidance for Platoons of Car-Like Vehicles with Limited Sensing
Supervisor: Prof. dr. Kostas J. Kyriakopoulos

2018–2022 PhD
Delft University of Technology
Thesis: Grasping the Sampling Behaviour of Event-Triggered Control
Promotor: dr. Manuel Mazo Jr.
Copromotor: dr. ir. Peyman Mohajerin Esfahani

AWARDS AND CERTIFICATES

2012 Nikolaos Kritikos Award

2018–2022 DISC Certificate for Graduate Studies
Dutch Institute of Systems and Control
Grade: 9.5/10

List of Publications

Journal Articles

5. **Giannis Delimpaltadakis**, Charalampos P. Bechlioulis and Kostas J. Kyriakopoulos, *Decentralized Platooning with Obstacle Avoidance for Car-like Vehicles with Limited Sensing*, IEEE Robotics and Automation Letters 3.2 (2018): 835-840.

4. **Giannis Delimpaltadakis** and Manuel Mazo Jr., *Isochronous Partitions for Region-Based Self-Triggered Control*, IEEE Transactions on Automatic Control 66.3 (2020): 1160-1173.

3. **Giannis Delimpaltadakis** and Manuel Mazo Jr., *Abstracting the Traffic of Nonlinear Event-Triggered Control Systems*, arXiv preprint arXiv:2010.12341 (2020), under review.

2. **Giannis Delimpaltadakis** and Manuel Mazo Jr., *Region-Based Self-Triggered Control for Perturbed and Uncertain Nonlinear Systems*, IEEE Transactions on Control of Network Systems 8.2 (2021): 757-768.

1. **Giannis Delimpaltadakis**, Luca Laurenti and Manuel Mazo Jr., *Formal Analysis of the Sampling Behaviour of Stochastic Event-Triggered Control*, arXiv preprint arXiv:2202.10178 (2022), under review.

Conference Papers

3. **Giannis Delimpaltadakis** and Manuel Mazo Jr., *Traffic Abstractions of Nonlinear Homogeneous Event-Triggered Control Systems*, 2020 59th IEEE Conference on Decision and Control (CDC), 2020, pp. 4991-4998.

2. **Giannis Delimpaltadakis**, Luca Laurenti and Manuel Mazo Jr., *Abstracting the sampling behaviour of stochastic linear periodic event-triggered control systems*, 2021 60th IEEE Conference on Decision and Control (CDC), 2021, pp. 1287-1294.

1. **Giannis Delimpaltadakis**, Gabriel de A. Gleizer, Ivo van Straalen and Manuel Mazo Jr., *ETCetera: beyond Event-Triggered Control*, Proceedings of the 25th International Conference on Hybrid Systems: Computation and Control (HSCC), 2022, pp. 1-11.

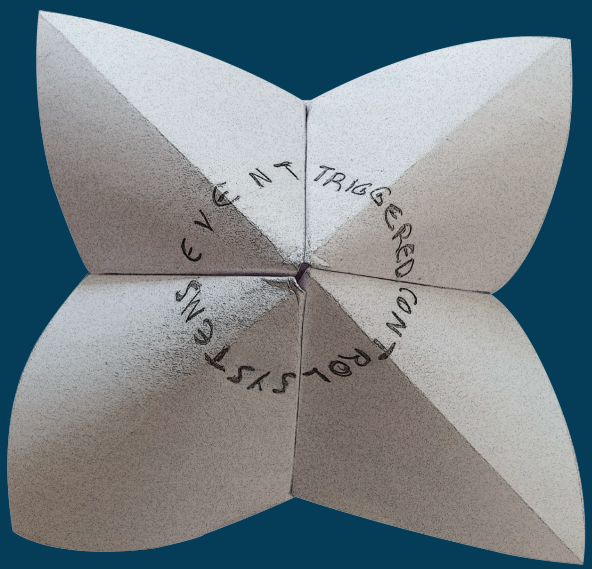

TU Delft Delft University of Technology

ISBN 978-94-6384-346-1